FORCED DISPERSION OF LIQUEFIED NATURAL GAS VAPOR CLOUDS WITH WATER SPRAY CURTAIN APPLICATION

A Dissertation

by

MORSHED ALI RANA

Submitted to the Office of Graduate Studies of
Texas A&M University
in partial fulfillment of the requirements for the degree of

DOCTOR OF PHILOSOPHY

December 2009

Major Subject: Chemical Engineering

FORCED DISPERSION OF LIQUEFIED NATURAL GAS VAPOR CLOUDS WITH WATER SPRAY CURTAIN APPLICATION

A Dissertation

by

MORSHED ALI RANA

Submitted to the Office of Graduate Studies of
Texas A&M University
in partial fulfillment of the requirements for the degree of

DOCTOR OF PHILOSOPHY

Approved by:

Chair of Committee,	M. Sam Mannan
Committee Members,	Mahmoud El-Halwagi
	Charles J. Glover
	Dan Zollinger
Head of Department,	Michael Pishko

December 2009

Major Subject: Chemical Engineering

ABSTRACT

Forced Dispersion of Liquefied Natural Gas Vapor Clouds with Water Spray Curtain Application. (December 2009)

Morshed Ali Rana, B.S., Bangladesh University of Engineering and Technology;
M.S., University of South Alabama

Chair of Advisory Committee: Dr. M. Sam Mannan

There has been, and will continue to be, tremendous growth in the use and distribution of liquefied natural gas (LNG). As LNG poses the hazard of flammable vapor cloud formation from a release, which may result in a massive fire, increased public concerns have been expressed regarding the safety of this fuel. In addition, regulatory authorities in the U.S. as well as all over the world expect the implementation of consequence mitigation measures for LNG spills. For the effective and safer use of any safety measure to prevent and mitigate an accidental release of LNG, it is critical to understand thoroughly the action mechanisms. Water spray curtains are generally used by petro-chemical industries to prevent and mitigate heavier–than-air toxic or flammable vapors. It is also used to cool and protect equipment from heat radiation of fuel fires. Currently, water spray curtains are recognized as one of the economic and promising techniques to enhance the dispersion of the LNG vapor cloud formed from a spill.

Usually, water curtains are considered to absorb, dilute, disperse and warm a heavier-than-air vapor cloud. Dispersion of cryogenic LNG vapor behaves differently from other dense gases because of low molecular weight and extremely low temperature. So the interaction between water curtain and LNG vapor is different than other heavier

vapor clouds. Only two major experimental investigations with water curtains in dispersing LNG vapor clouds were undertaken during the 1970s and 1980s. Studies showed that water spray curtains enhanced LNG vapor dispersion from small spills. However, the dominant phenomena to apply the water curtain most effectively in controlling LNG vapor were not clearly demonstrated.

The main objective of this research is to investigate the effectiveness of water spray curtains in controlling the LNG vapor clouds from outdoor experiments. A research methodology has been developed to study the dispersion phenomena of LNG vapor by the action of different water curtains experimentally. This dissertation details the research and experiment development. Small scale outdoor LNG spill experiments have been performed at the Brayton Fire Training Field at Texas A&M University. Field test results regarding important phenomena are presented and discussed. Results have determined that the water curtains are able to reduce the concentration of the LNG vapor cloud, push the vapor cloud upward and transfer heat to the cloud. These are being identified due to the water curtain mechanisms of entrainment of air, dilution of vapor with entrained air, transfer of momentum and heat to the gas cloud. Some of the dominant actions required to control and disperse LNG vapor cloud are also identified from the experimental tests. The gaps are presented as the future work and recommendation on how to improve the experiments in the future. This will benefit LNG industries to enhance its safety system and to make LNG facilities safer.

DEDICATION

To the memory of my father - who has been my role-model for hard work, persistence and personal sacrifices, who emphasized the importance of education and who instilled in me the inspiration to set high goals and the confidence to achieve them.

To my mother - who made all of this possible with her endless love, sacrifices, patience, encouragement and continuous prayers.

To my wife - who has been proud and supportive of my work and who has shared all the uncertainties and challenges for completing this dissertation.

To my son - who has grown into a wonderful 2 year old in spite of his father spending so much time away from him working.

To my brothers and sisters - who have been my emotional anchors my entire life.

ACKNOWLEDGMENTS

I would like to express my profound gratitude and thanks to my advisor and mentor, Dr. Mannan, for his guidance, instruction and encouragement during the course of this research. I would also like to thank Dr. El-Halwagi, Dr. Glover, and Dr. Zollinger for assisting on my committee and for their constructive suggestions and help.

I would like to thank BP Global Gas SPU for the research funding. Special thanks are extended to Dr. Benedict Ho and Robin Passmore for their continuous attention and valuable guidance throughout the progress of my research. I greatly appreciate Kirk Richardson and his team at Brayton Fire Training Field. I would like to thank Dr. Cormier and Dr. Suardin for their support and contributions to the research. Without them, the field experiments would not be possible. Thanks to Geunwoong Yun, Ruifeng Qi, Dr. Zhang, Dr. Guo and Dr. Ng for their hard work and support.

I am very grateful to all members and staff of the MKOPSC. Valerie Green, Mary Cass, and Donna Startz helped me whenever I needed anything. All the students at the center were like a second family to me. Special thanks to Towanna Arnold for helping me with the administrative matters throughout my involvement at TAMU.

I want to express my sincere gratitude to my mother, brothers, sisters, and my wife and my son for their unconditional support and encouragement during my graduate studies. I would also like to thank Baba and Ma for their encouragement and prayers. Finally, I am grateful to all my friends who make my life here joyful and happy.

NOMENCLATURE

A_d	droplet surface area	m^2
A_m	entrained air molar flow rate	kmol/s
A_{pool}	area of the LNG pool	m^2
A_s	spray (/curtain) area	m^2
C	specific heat capacity	J/kgK
C_D	the drag coefficient	
C_{FD}	gas concentration during forced dispersion	
C_M	momentum coefficient (nozzle)	
C_{ND}	gas concentration during natural dispersion	
C_{p_g}	heat capacity of the gas mixture	J/kgK
$C_{x_{2t1}}$	concentration at x_2 at any time t_1	
$C_{x_{5t_2}}$	concentration at x_5 at time t_2	
$C_{free\_dispersion}$	open field dispersion concentration	
$C_{forced\_dispersion}$	concentration in presence of the water spray	
D	base diameter (eqn 6 and 7)	m
D	droplet diameter (eqn 17)	m
D_F	dilution factor	
D_n	diameter of nozzle	m
DR_m	maximum water spray dilution ratio	
D_w	diameter of solid water jet at the breakup region	m
F	flow number of a nozzle	$m^3s^{-1}kPa^{-0.5}$
F_D	forced dilution	
F_d	the drag force per droplet	N
H_{wo}	height of the water-curtain	m
L	latent heat of vaporization (of the liquid)	J/kg
L_i	characteristics length of the pool	m

M	mass of the pool	kg
MW	molecular weight	kmol/kg
$\dot{N}$	number of droplets falling through the cloud per unit time	s^{-1}
N_d	number of droplets produced from nozzle per unit time	s^{-1}
P and P_w	water pressure (gauge) at the nozzle	kPa
Q	heat flux into the pool	J/s
$\dot{Q}$	rate of heat transfer from the droplets to the cloud	kJ/s
Q_a	volumetric flow of air	m^3/s
Q_{liquid}	average volumetric flow rate of LNG	m^3/s
Q_s	entrainment flow rate	m^3/s
Q_w	volumetric flow rate of water	m^3/s
R	radius of the spray at that level	m
Re	Reynolds number	
R_M	momentum ratio	
T	pool temperature	K
T_a	temperature of ambient air	K
T_b	pool boiling temperature	K
T_g	ambient ground temperature	K
T_{mg} and T_{di}	temperature of gas mixture and water droplet of class i	K
T_L	temperature of the liquid	K
T_s	temperature of the ground	K
$\overline{T}_{water}$	average water temperature during the test day	°C
$T_{reading}$	temperature of the spray region after spray activation	°C
ΔT_{mw}	mean temperature difference between the droplets (water) and the vapor cloud	K
ΔT_{mi}	mean temperature difference between the droplets (ice) and the vapor cloud	K
U	air velocity	m/s

U_{d0}	initial droplet velocity at the nozzle orifice	m/s
U_n	average water velocity from the spray nozzle	m/s
V	entrained air velocity	m/s
V_w	wind speed	m/s
W	vaporization rate	kg/s
Y_{in}	molar fractions of the toxic gas before dilution	
Y_{out}	molar fractions of the toxic gas after dilution	
a_h	average heat transfer coefficient (gas to droplets)	W/m^2K
c_a	heat capacity of ambient air at film conditions	J/kg K
c_{pwater}	specific heat of water	J/gm°C
d_d	diameter of a droplet	m
d_i	diameter of droplet of class i	m
d_w	average droplet diameter	m
f	fraction of liquid LNG flashed	
g	gravity acceleration	m/s^2
h_a	heat transfer coefficient between air and the pool,	W/m^2K
h_{gc}	gas phase enthalpy entering the spray envelop	
h_g, h_v h_s h_a	enthalpy of gas mixture, water vapor, pollutant and air (eqn 14)	
h_w and h_i	convective heat transfer coefficient of water and ice	kJ/s m^2K
k	thermal conductivity of the ground	W/m K
k_a	thermal conductivity of air at film conditions	W/m K
k_s	thermal conductivity of the ground	W/m K
l_{vi}	total volumetric flow rate of water droplet of class i	m^3/s
m_d	average mass of a single droplet	kg
$\dot{m}_a$	mass flow rate of air	kg/s
m_{air}	rate of vapor due to heat transfer from the air	kg/s
m_{evap}	rate of vapor due to evaporation of liquid	kg/s
m_{flash}	rate of vapor due to flashing	kg/s

m_{liquid}	average rate of liquid flow	kg/s
m_{rad}	rate of vapor due to solar radiation above the pool	kg/s
m_{sub}	rate of vapor due to heat transfer from the ground,	kg/s
$\dot{m}$	mass release rate of toxic gas	kg/s
$\dot{m}_{l\mu}$	liquid-flow rate per unit length	kg/m s
$\dot{m}_{mg}$	mass flow rate of gas mixture in the spray	kg/s
$\dot{m}_{gc}$	mass flow rate of gas mixture entering the spray envelop	kg/s
n	number of nozzles per unit length	m^{-1}
q	heat transfer per unit mass of water	J/gm
q_{rad}	radiative heat flux	W/m^2
r	proportionality constant of a the nozzle	$ms^{-2/3}$
t, t_1 and t_2	time	sec
u_a	velocity of entrained air	m/s
u_{a0}	initial entrained air velocity	m/s
u_a^*	dimensionless entrained air velocity	
u_d	velocity of the upward moving droplet	m/s
u_{d0}	initial droplet velocity	m/s
u_d^*	dimensionless drop velocity	
u_{di}	velocity of droplet of class i	m/s
u_r	the relative velocity between the droplet and air	m/s
u_W	average wind speed	m/s
x_2	downwind distance 3.3	m
x_5	downwind distance 11.3	m
x_v and x_s	mass fraction of water vapor and pollutant	
z	vertical direction (z is positive in the upward direction)	m
z^*	dimensionless vertical distance	
α	thermal diffusivity of the ground	m^2/s
α	gravity parameter (eqn 33)	

β	viscous-interaction parameter (eqn 34)	
γ	geometric parameter (eqn 35)	
ξ	alternative gravity parameter (eqn 36)	
μ_a	viscosity of ambient air at film condition	kg/ms
λ_f	latent heat of freezing	kJ/kg
v_a	kinematic viscosity of air	m^2/s
ρ_a	density of ambient air density at film condition	kg/m^3
ρ_c	cloud density	kg/m^3
ρ_{dw}	water droplet density	kg/m^3
ρ_l	liquid density	kg/m^3
ρ_{LNG}	density of liquid LNG	kg/m^3
ρ_w	density of water	kg/m^3
θ	spray angle	(degree)
θ_w *and* θ_i	residence time of droplet (w: water, i: ice)	s

TABLE OF CONTENTS

Page

Page

LIST OF FIGURES

Page

Page

Page

Page

Page

LIST OF TABLES

1 INTRODUCTION

1.1 Liquefied Natural Gas

Liquefied Natural Gas (LNG) refers to natural gas converted into liquid state by super cooling to 111K (-162.2°C/-260°F) at ambient pressure. LNG commonly consists of 85%-98% methane with the remainder as a combination of nitrogen, carbon dioxide, ethane, propane, and other heavier, less volatile hydrocarbon gases. At normal temperature and pressure, the density of natural gas is 0.667 kg/m^3. When it is cooled to 111 K at 1 atmosphere, the liquid density becomes 425-450 kg/m^3; that is the gas volume reduce by a factor of about 640-670 (CLNG, 2008; Raj, 2007). This large reduction in volume has made the transportation and storage of natural gas more economic and easier. LNG is usually stored at 111K and atmospheric pressure in heavily insulated tanks. Properties of LNG at the storage conditions are given in Table 1. The change of density of methane vapor and air at different temperatures is demonstrated in Fig. 1.

This dissertation follows the style of *Journal of Loss Prevention in the Process Industries*.

Table 1. LNG properties and storage conditions in LNG tanks (MKOPSC, 2008).

Property	Value	Units
Molecular weight	16.043	kmol/kg
Critical temperature	190.6	K
Critical pressure	4.64E+06	Pa
Freezing temperature	111.6	K
Liquid density at boiling point (for pure methane)	422.6	kg/m^3
Liquid density at boiling point (Commercial LNG)	450.0	kg/m^3
Vapor density at boiling point	1.82	kg/m^3
Density of gas at NTP (1 atm, 20 ^oC)	0.651	kg/m^3
Heat of vaporization	510	kJ/kg
Heat of combustion (lower) - LHC	50.0	MJ/kg
Heat of combustion (higher) - HHC	55.5	MJ/kg
Specific heat of vapor @ constant pressure	2200	J/kg K
Ratio of specific heats	1.30815	
Stoichiometric air-fuel mass ratio	17.17	
Stoichiometric methane vapor concentration in air (volumetric)	9.5	%
Upper flammability limit (UFL) in air (volumetric concentration)	15	%
Lower flammability limit (LFL) in air (volumetric concentration)	5	%

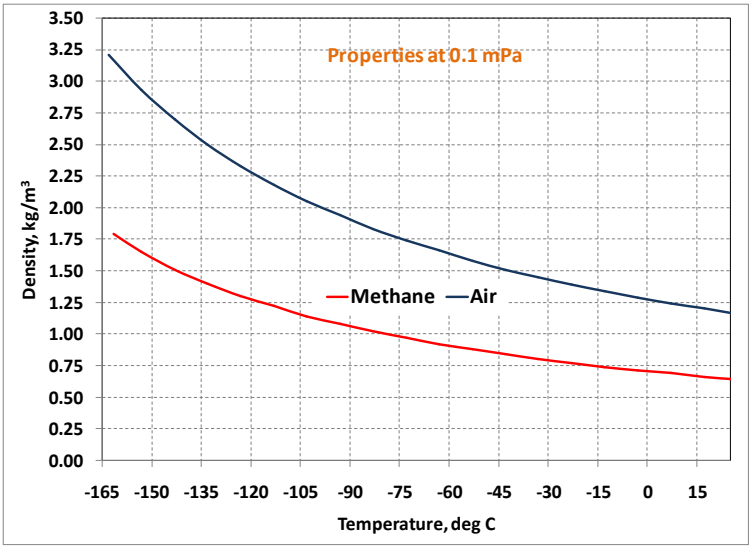

Fig. 1. Densities of methane (vapor) and air at different temperatures. Modified from CMS (1962).

1.2 LNG Demand

Natural gas has been used as an industrial and residential fuel for heating and other purposes for over a century (Raj, 2007). The natural gas energy consumption in the United States (US) is about 25% of the overall energy. As forecasted by the U.S. Department of Energy, demand for natural gas in the US is increasing by 20% over the next 25 years because of its clean-burning characteristics (FERC, 2008). Due to this increasing demand for natural gas, LNG has been considered as an alternate fuel that can meet the demand because of its low production cost and practicability in transportation and storage. Thus LNG has become an important energy source as well as a vital industrial feedstock in the economy of the United States. Several active LNG facilities are operating across the US, including marine terminals, operating and storage facilities for use during periods of peak natural gas demand ("peak shaving") or as a base load source of natural gas. Table 2 includes the list LNG facilities currently (as of October, 2008) active in the U.S. More LNG receiving terminals are under construction and several more are proposed to be constructed in the US.

Table 2. U.S. LNG facilities (CLNG, 2008; FERC, 2008).

LNG Facilities
113 active LNG facilities
58 facilities to liquefy and store natural gas
39 used for LNG storage only
5 facilities receive imported gas and regasify for domestic use
1 export terminal

1.3 LNG Concerns

The density of methane at normal temperature and pressure is lighter than air. However, methane at its boiling point (111 K) is significantly denser (factor of 1.5) than the ambient air. The cryogenic liquid, LNG, when released on land or water vaporizes by boiling or evaporation due to heat transfer from the substrate and environment and forms a heavier-than-air vapor cloud at atmospheric conditions (Ivings et al., 2007; Raj, 2007). Temperature and specific gravity of methane cloud can be realized from Fig. 2.

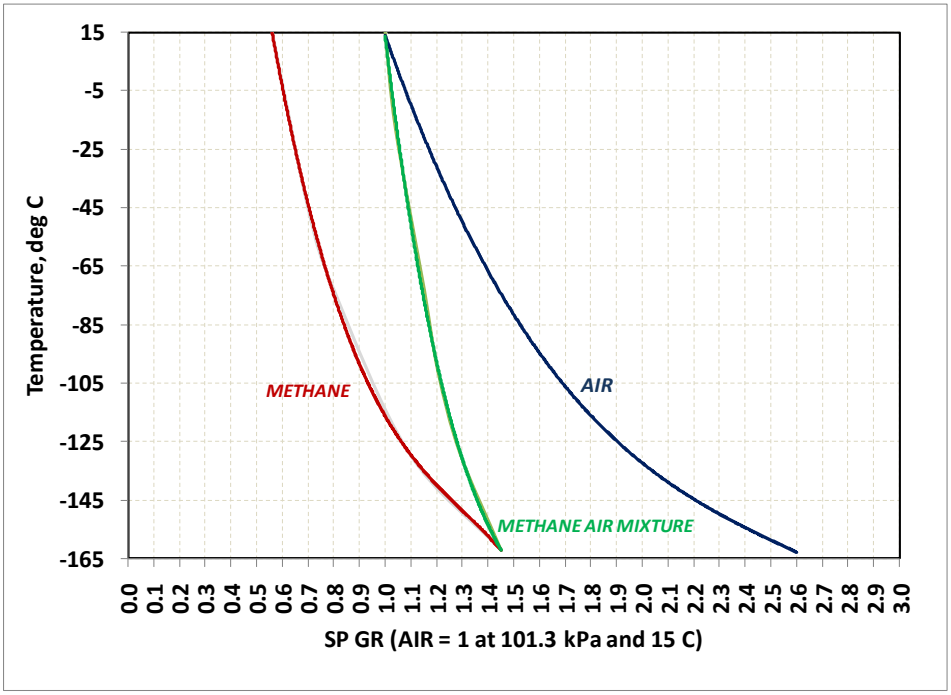

Fig. 2. Temperature and specific gravity of methane, air and methane-air mixture at atmospheric pressure. Modified from CMS (1962).

The very cold, methane rich and heavy vapor cloud formed from an LNG spill as disperses in the prevailing wind direction, becomes warmer, diluted and lighter due the heat transfer from surroundings and other effects. When the methane concentrations are between the lower and upper flammability limits (LFL and UFL), 5% and 15% by volume in air, the vapor cloud becomes flammable. The massive volume of LNG storage tanks therefore poses fire and explosion hazards due to its highly flammable feature.

1.4 Hazards of LNG

Several potential hazards can arise from an uncontrolled LNG spill. The following potential hazards of an LNG spill are of major concern for the LNG industries.

1.4.1 Cryogenic Hazards

LNG is stored and transported at very low temperature, around 111 K. Cryogenic hazards include extreme thermal effects associated with freezing of living tissue as a result of direct contact with very cold liquid. Cryogenic fluids may cause the embrittlement and subsequent failure of containment materials and structure. For instance, carbon steel loses ductility and impact strength (ability to withstand an impact force) at cryogenic temperature. Thus, careful selection of materials for equipment involved in the process (e.g., tank, pipe, pump, gas detector, valve, flow meter, etc.) is critical for the LNG industry.

1.4.2 Flash Fire

LNG will vaporize upon release and the vapor generated by this boiling liquid will start to mix with the surrounding air and will be carried downwind with the air creating a heavier-than-air, cold vapor. As the cold vapor cloud continues to be carried downwind, it will mix with additional air and be further diluted. However, some portion of the vapor cloud will be within the flammable limits (between 4.4-16.5% volumetric concentration mixtures with air). If this flammable portion comes in contact with an ignition source, the vapor cloud may ignite. The flame might then propagate through the cloud, back to the source of the vapor, particularly if the flammable portion of the cloud is continuous. This simple burn-back of an unconfined vapor cloud can cause secondary fires by igniting materials in the path of the flame and can cause severe burns to persons caught within the cloud. Damage to equipment will generally be limited since the time of exposure to the fire will be relatively short (West & Mannan, 2001; Qiao, West & Mannan, 2005).

1.4.3 Pool Fire

LNG may accumulate as liquid on the ground from an accidental release if the spill is of sufficient size. If any ignition source is encountered, a pool fire can occur. Ignition can occur at the pool location (either immediately or delayed), or the pool can be ignited by a vapor cloud fire. The pool fire will continue if the spill expands from its source and continues evaporating. Compared to a vapor cloud fire, the effects are more localized, but of longer duration (Qiao, West & Mannan, 2005; Zinn, 2005).

1.4.4 Jet Fire

When a flammable liquid is accidentally released from pressurized containment, the leak may form a spray of liquid droplets and vapor. If ignited, the resulting fire is termed jet fire. Such a fire also can result from a pressurized vapor leak. Jet fires present the same types of hazards as pool fires, i.e., direct flame contact and radiant heat. However, the radiant heat from a jet fire is often greater than that from a pool fire of similar size.

1.4.5 Rapid Phase Transition (RPT)

The phenomenon of rapid vapor formation with loud "bangs" has been observed when LNG is released under water. This non-flaming physical interaction is referred to as "rapid phase transition" or "flameless explosion" (Qiao, West & Mannan, 2005; Zinn, 2005).

1.4.6 Rollover

The addition of LNG with different densities to partially filled LNG tanks or the preferable evaporation of nitrogen has been known to lead to the formation of stratified layers. The density difference may be due to different sources of LNG or the weathering of LNG in the tank. Due to heat and mass transfer, the densities of the two layers approach each other. Eventually, these two layers mix resulting in a sudden increase in the vapor evolution and sometimes tank pressure. Rollover may result in excessive loss

of valuable fuel at best, or lead to an incident under extreme conditions (Qiao, West & Mannan, 2005; Zinn, 2005).

1.5 Motivation

The development of LNG terminals requires a thorough evaluation of potential release consequence associated with the installations. Usually an LNG terminal is composed of an off loading deck, storage tanks, control room and re-gasification unit. Fig. 3 shows a typical configuration of an LNG base-load terminal. The off loading deck is where the LNG tanker is anchored and then loading arms are used to transfer the LNG from the ship to the storage tanks. The storage tanks may be located near off-shore or inland (Cormier, 2008). Safety barriers such as dikes or impounding walls are usually designed and built around the LNG storage tanks for holding accidentally spilled LNG to protect adjacent properties.

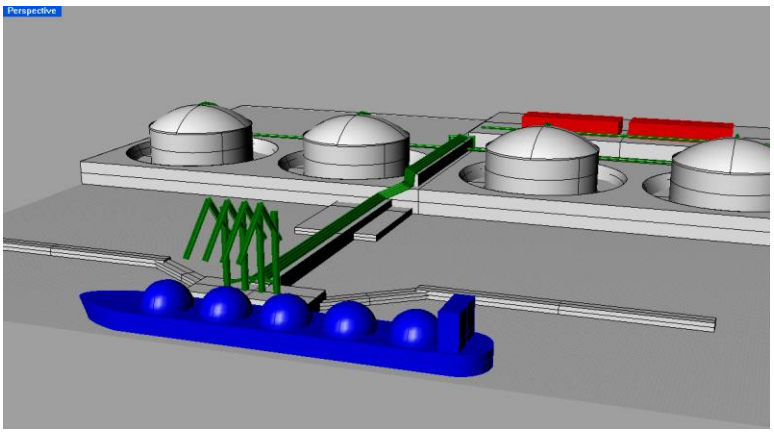

Fig. 3. Typical representation of an LNG base load terminal. Adopted from Cormier (2008).

Safety standards require LNG facilities to have a “dispersion exclusion zone” so that flammable vapor cloud from an accidental release will not propagate beyond the plant boundaries (FERC, 2008). This exclusion zone is defined from the LNG spill source to the predicted distance at which the average vapor concentration is one-half of the LFL, i.e. 2.5% volume in air. This distance is estimated with various dispersion modeling techniques incorporating appropriate control and mitigation measures. Effective control and mitigation measures are required to reduce the size of the flammable vapor cloud, created by liquefied gas spills, by enhancing the dispersion of vapors.

1.6 Water Spray Curtain

Water spray curtains have been considered by industry to be a valuable tool for mitigating toxic and flammable vapor hazards because of its availability and simplicity, efficiency and adaptability in gas dispersion, absorption, and fire inhibition (Uzanski & Buchlin, 1998; Hald et al., 2005). Water sprays are also reliable and inexpensive and their installation can be either fixed or mobile. A water spray curtain is composed of a line of spray nozzles which creates a curtain of water droplets in the path of a naturally moving gas cloud or to the radiant heat from a fire. It has been demonstrated that water spray curtains significantly reduce the gas cloud concentration or fire heat radiation through several physical actions. The performance of water spray curtain depends on its own characteristics and extrinsic parameters. The types and application methods also vary widely. Generally, water sprays can be classified as full cone, full square cone,

hollow cone and flat-fan type nozzles characterized by water droplet size is a function of both pressure and flow rate. The spray can be directed downward and upward, vertically or inclined.

Water curtain has also been considered as one of the most economic and promising techniques to reduce flammable LNG vapor concentration. The ability of water curtain to show different effects initiated an interest in the utilization of water curtain as a potential LNG vapor cloud mitigation measure in the late 70's (Atallah, Guzman & Shah, 1988). The effectiveness of water curtain in controlling LNG vapor depends on: (a) parameters of its own characteristics: water droplet distribution, nozzle type and size, direction, width and height, water pressure etc.; and (b) external parameters: vapor cloud features, LNG properties, wind speed, atmospheric stability etc.

1.7 Statement of Problem and Significance

Fixed water spray curtains are being installed to a limited extent at some LNG storage facilities for the purpose of dissipating the vapor cloud that may be generated during an accidental release. So far no definitive engineering guideline has been developed to design a water curtain system to control LNG vapor cloud effectively. This is because the interaction between an LNG vapor cloud (methane and air mixture) and water droplet of a water curtain is a sophisticated phenomenon to predict and model. Development of comprehensive and authentic design guidelines for water curtain to mitigate LNG release thus still requires a thorough understanding of the underlying physical phenomena through a reasonable amount of experimental works. Because of

many uncertainties present in the water curtain – LNG vapor interaction, representative water curtain types need to be studied experimentally with real LNG spills under simulated conditions before installation for specific applications.

1.8 Research Objective

Development of comprehensive and authentic design guidelines for water curtain to mitigate LNG release requires a thorough understanding of the underlying physical phenomena through a reasonable amount of experimental and theoretical works. This research has been developed to investigate the interaction of representative types of water curtains with LNG vapor clouds. The main purpose is to experimentally study the effect of water curtain parameters on the interaction phenomena during a LNG spill. Overall, the extent of LNG vapor concentration reduction and temperature increase downwind of a curtain and effect of significant parameters of various water curtains will be studied from experiments. Finally, this work will identify the effectiveness of water curtain in controlling LNG vapor mainly from LNG spill experiments.

1.9 Organization of the Dissertation

This dissertation presents the research on the application of different water spray curtains on controlling LNG vapor dispersion. Therefore, this dissertation is arranged to meet its objectives.

Section 1 provides the introduction of this research. Background information regarding LNG and its associated hazards, and water curtain applications are described

in this section. In addition, the frameworks of the research are also explained by the problem statement and research significance and objectives.

Section 2 describes the background knowledge of water curtain application, its action phenomena as well as LNG dispersion characteristics. Action of water curtain on LNG vapor dispersion and identification of pertinent parameters that affects its performances is crucial to understand. This section also provides the literature review of previous work by other researchers to support the significance of this research. Previous studies and experiments are explained and compared with the pertinent parameters. This is to identify the gaps and to ensure this research is part of an attempt to fill the identified-gaps.

Once the research gaps are recognized, a detailed experiment plan was developed to meet the research objectives. Section 3 illustrates the experiment development. Each of the experiment was conducted in sequence with improvement in between one experiment to another. Equipment and sensors played important roles in this research. Thus, all equipments, data acquisition system, and its setup are illustrated in Section 3.

Section 4 describes the simple theoretical model used in the research to study two mechanisms of spray action. This section also includes parametric studies conducted with a computer program, developed to solve the model numerically.

Section 5 discusses the detailed experiment results related as well as some theoretical calculations and summarizes the findings. This dissertation is completed by Section 6 where all conclusions, limitation, and recommendations, and future researches are presented.

2 WATER SPRAY CURTAIN MECHANISM AND DISPERSION OF LNG – REVIEW*

2.1 Background

The mitigation of accidental releases of flammable LNG has been a great concern in the LNG industry. Theoretically, water curtains will enhance LNG vapor cloud dispersion and reduce the "vapor cloud exclusion zone" effectively, if properly designed (Atallah, Guzman & Shah, 1988). However, their effectiveness for the control of a specific hazard requires careful evaluation of credible release scenario, chemical characteristics, action mechanisms and spray hydrodynamics (or characteristics). The variables which can affect the efficiency of a water-spray curtain for the case of LNG release are described in the section. This section also summarizes previous research on water spray curtain application to disperse LNG vapor cloud.

---

* Part of this section is reprinted with permission from "Development of Design and Safety Specifications for LNG Facilities Based on Experimental and Theoretical Research" by Cormier, B, R., Suardin, J, A., Rana, M. A., Zhang, Y. and Mannan, M. S., 2009. *OPEC, Oil Prices and LNG*, 12, 295-424, Copyright [2009] by Nova Science Publishers Inc.

2.2 Phenomenology of LNG Vapor Cloud

LNG is stored at the boiling temperature of methane (111 K) at atmospheric pressure. Therefore a breach in LNG-pipe or LNG tank may results in a boiling liquid pool. LNG will vaporize immediately and form a cold, denser-than-air, flammable gas cloud if it escapes from its containment (Ivings et al., 2007). This cold vapor cloud will condense the water content in the air (humidity) and create a visible white condensate cloud, which may or may not represent the actual methane cloud. If the cloud is not ignited immediately, it will entrain in the atmospheric air and disperse downwind at wind speed. These complicated processes of vapor cloud formation and dispersion can be divided into: (1) the source term and (2) the vapor dispersion. The source term includes the physical process of the LNG pool to transform into the gas phase and is mainly characterized by vaporization and spreading of the pool. The vapor dispersion includes the physical process of the entrainment of the vapor cloud into the air and dilution. Understanding those two mechanisms is important for the effective application of any LNG vapor control and mitigation device. The mechanisms are as follows.

2.2.1 Vaporization of LNG

The generation of flammable LNG vapor cloud crucially depends on the area of the liquid pool and its rate of vaporization. Generally vaporization of LNG pool depends on the temperature of the pool, the heat transfer to the pool from the surroundings, and heat removal from the liquid to provide the heat of vaporization (Webber et al., 2009). The rate of vaporization can be slow or very rapid depending on the circumstances of the

release scenario as well as on the surface where the release occurs. Sometimes these circumstances can be described as evaporation or boiling. If the vaporization occurs well below the boiling point, where the vapor pressure is much lower than atmospheric pressure, then it is refers as evaporation. Whereas the vaporization at, or very close, to the boiling point, where the vapor pressure is atmospheric, or very close to it, is recognized as boiling. Usually evaporation occurs from the upper surface of a pool and boiling often occurs primarily at nucleation sites on an adjacent solid surface, or on the underside of a liquid undergoing film boiling (Webber et al., 2009). However the overall physical processes involved are the same but cause and effect in this process can appear differently in different situations. The heat balance for the entire pool can be written as (Ivings et al., 2007):

$$MC\frac{dT}{dt} = Q - LW \tag{1}$$

Upon release, initially the LNG pool will boil very rapidly, and the vaporization rate is the controlled mainly by the heat flux into the pool from the ground. If the pool is confined, the surface beneath it will cool down and the heat flux form the surface will diminish with time, leaving a still very hazardous pool though vaporizing more slowly. If the pool is unconfined then it will be able to spread on to new warm surface and rapid boiling may continue. The rate of production of flammable vapor also increases with increasing surface area of the pool. The heat transfer to a circular confined pool on ground can be estimated by assuming perfect thermal contact between pool and ground, and only vertical temperature gradients in the ground. The conduction is thus modeled by the one-dimensional simple Fourier conduction equation in the ground, with an initial

state where the ground is uniformly at ambient temperature and an initially singular boundary condition whereby its top surface is held at the boiling point of the pool (Briscoe & Shaw, 1980). The simple governing equations and boundary conditions are:

$$\frac{\partial T}{\partial t} = \alpha \frac{\partial^2 T}{\partial z^2} \tag{2}$$

$$T\,(0, z) = T_g \quad ; z > 0$$

$$T\,(t, 0) = T_b \quad ; t \geq 0$$

The solutions for temperature and heat flux are:

$$T(t, z) = T_g + (T_b - T_g) erfc\left(\frac{z}{\sqrt{4\alpha t}}\right) \tag{3}$$

$$Q = -k\frac{\partial T}{\partial z} = (T_b - T_g)\frac{k\sqrt{\pi}}{4\sqrt{\alpha t}} \exp\left(-\frac{z^2}{4\alpha t}\right) \tag{4}$$

where, at the surface (z=0), thermal conductivity, *k* is inversely proportional to the square root of time.

2.2.2 Natural Dispersion of LNG Vapor

Usually LNG is composed of methane, which is lighter than air. However LNG vapor is heavier-than-air because of its high gas density at a cold temperature. A heavy cloud usually forms above the liquid pool after any LNG release because of vaporization and very cold temperature of LNG. This heavy cloud will then slump and progress towards the prevailing wind direction. This natural transport of the vapor cloud is called the natural dispersion. During this downwind progression of the cloud, two dilution

mechanisms might occur: (1) heat transfer from the surroundings may warm and then expand the vapors to the point that the cloud start to lift off, and/or (2) wind entrainment may dilute the concentration. Other factors like the ground roughness, obstacles, wind and weather conditions, heat flux from ground and atmosphere, etc. affect the natural dispersion of LNG. The dispersing cloud approaches air density asymptotically from above, just as it approaches ambient temperature from below, as it dilutes and warms (Ivings et al., 2007). Understanding of this natural dispersion for the development of an effective safety measure to prevent and mitigate accidental releases of LNG is critical.

2.2.3 Forced Dispersion of LNG Vapor Cloud

Like any other vapor suppression devices, the water curtain is used to enhance the dispersion process. If any external force is applied to the naturally dispersed LNG vapor cloud to enhance the entrainment and heat transfer, then the dispersion is referred as the forced dispersion. The physical processes involved in using a water curtain to reduce the concentration of any vapor cloud include (1) dilution effects of mixing the gas cloud with entrained air; (2) mechanical effects of creating a barrier to the passage of a gas cloud, imparting momentum to the gas cloud to disperse it upwards, downwards or sideways; (3) thermal effects between the gas cloud, water, and entrained air; and (4) mass transfer effects of absorbing gases with or without chemical reaction (Dusserre, Dandrieux & Thomas, 2003; Hald et al., 2005). The actions of a water spray in mitigating a vapor cloud may consist of all or any combination of these mechanisms (McQuaid & Fitzpatrick, 1981; McQuaid & Fitzpatrick, 1983; Moodie, 1985; Moore &

Rees, 1981). However to enhance LNG vapor cloud dispersion, any combination of the first three mechanisms are considered as water curtain actions. As the solubility of CH_4 in water is minimal, the mass transfer effects can be ignored (Rojey, Jaffret & Marshall, 1997). Because of low molecular weight (methane) and extremely low temperature, LNG vapor cloud dispersion behaves differently from other dense gases (Raj, 2007). The physical mechanisms involved in the LNG vapor and water curtain action are described in the following.

2.3 Physical Phenomena of Water Curtain Action

There is substantial literature on modeling momentum transfer, air entrainment, and mass transfer processes within a single water droplet or whole spray region. These models, derived for evaluating the effectiveness of water sprays in mitigating accidental releases, fall into two broad categories: macroscopic and microscopic. Macroscopic models are usually based on semi-empirical formulations (Moore & Rees, 1981; Buchlin, 1994) and describe the interaction between the two phases, gas and liquid phases. However, microscopic models are based on fluid dynamics and reproduce the movement and mass transfer between the liquid phase and the gas phase (Buchlin & Alessandri, 1997). The microscopic models, generally, only specify the mitigation ability of the water curtain without assessing downwind concentration which is essential for assessing the effectiveness of water spray for an accidental release of LNG. Neither macroscopic nor microscopic models have been widely used in the process industry because of the unavailability, unfamiliarity or lack of full validation (Hald et al., 2003;

2005). Most of the work in the publically available literature focuses on mitigation of Cl_2, CO_2, NH_3 or HF release. The published works on the effective use of water curtain in mitigating LNG vapor releases is, however, very limited. Some of the main research on general water curtain applications are as follows.

2.3.1 Air Entrainment into the Spray and Dilution

The use of water spray curtains for the dispersion of hazardous vapor clouds mainly applies the feature of air entrainment into the spray. Water spray can dilute a gas cloud by mixing it with the entrained air. When the spray is activated, mixing and dilution result from momentum transfer between the air and water droplets. The mixing of the entrained air and the gas cloud reduces the gas concentration in the downstream region of the water spray. According to the design requirements, it is necessary to deliver air not only in sufficient quantity, but also at a sufficient velocity to ensure dilution. It should also be noted that the turbulence induced by the spray may aggravate the intensity of combustion if the vapors are flammable and are somehow ignited (Fthenakis, 1991).

Air entrainment is a strong function of spray configuration, droplet size, droplet velocity, and spray arrangements. Large droplets entrain less air than smaller droplets but induce better mixing and dispersion. Although smaller droplets entrain more air, they have smaller terminal velocities which are almost constant and cause poor mixing and dilution due to less turbulence (CCPS, 1997; Fthenakis, 1991).

The fluid mechanics of liquid sprays into a gas phase received substantial attention in the past. Measurements of air velocities and entrainment rates were reported in literature (Bennat & Eisenklam, 1969; Binark & Ranz, 1958; Briffa & Dombrowski, 1966; Gluckert, 1962; Ito, 1970; Nakakuki, 1973; Rabash & Stark, 1962). Two theoretical studies of air entrainment into liquid sprays were first reported by Briffa and Dombrowski (1966), and Bennet and Eisenklam (1969). The first one treated a flat fan spray theoretically and the second one proposed a theory for hollow cone sprays. Neither of these theories incorporated momentum exchange between the liquid drops and entrained air, the dominant mechanism for considered in this research. The works conducted by Heskestad et al. (1981) and Rothe and Block (1977) presented similar entrainment models incorporating momentum exchange.

An approach for the design and application of a water spray to entrain air into a gas cloud were presented by McQuaid (1977) who developed a correlation between air entrainment rates and water flow rates using experimental data assuming that adequate mixing requires an induced air velocity of 6 m/s (McQuaid, 1977; McQuaid & Fitzpatrick, 1983). With his correlation, McQuaid described a design methodology for a water spray system depending upon the entrainment rate and the assumed air velocity. To ensure necessary airflow, the author considered five parameters as the design requirement, two of which are fixed and three adjustable (McQuaid, 1977). The fixed parameters are gas flow rate and water pressure. The adjustable parameters are water flow rate, nozzle type, and number of spray nozzles. A single parameter, called the

"Flow Number", was incorporated to demonstrate the influence of the nozzle type on the rate of air entrainment. Flow number was defined as:

$$F = \frac{Q_w}{\sqrt{P_w}} \tag{5}$$

"Flow number" was also considered as a constant discharge coefficient for a given nozzle provided the flow rate is large enough to ensure a turbulent flow in the nozzle. The relationship among the flow rate of air, the air velocity V at the base of the spray cone, and the base diameter was simply expressed by the following:

$$D = \sqrt{\frac{4Q_a}{\pi V}} \tag{6}$$

McQuaid finally obtained a correlation of the ratio of the volumetric air rate to volumetric water rate as function of flow number. The equations are shown below and represented in Fig. 4.

$$\frac{Q_a}{Q_w} = f\left(\sqrt{\rho_w}\,\frac{F}{D^2}\right) = A\left(\frac{D^2}{F}\right) \tag{7}$$

here, $$A = \frac{\pi V}{4\sqrt{P_w}} \tag{8}$$

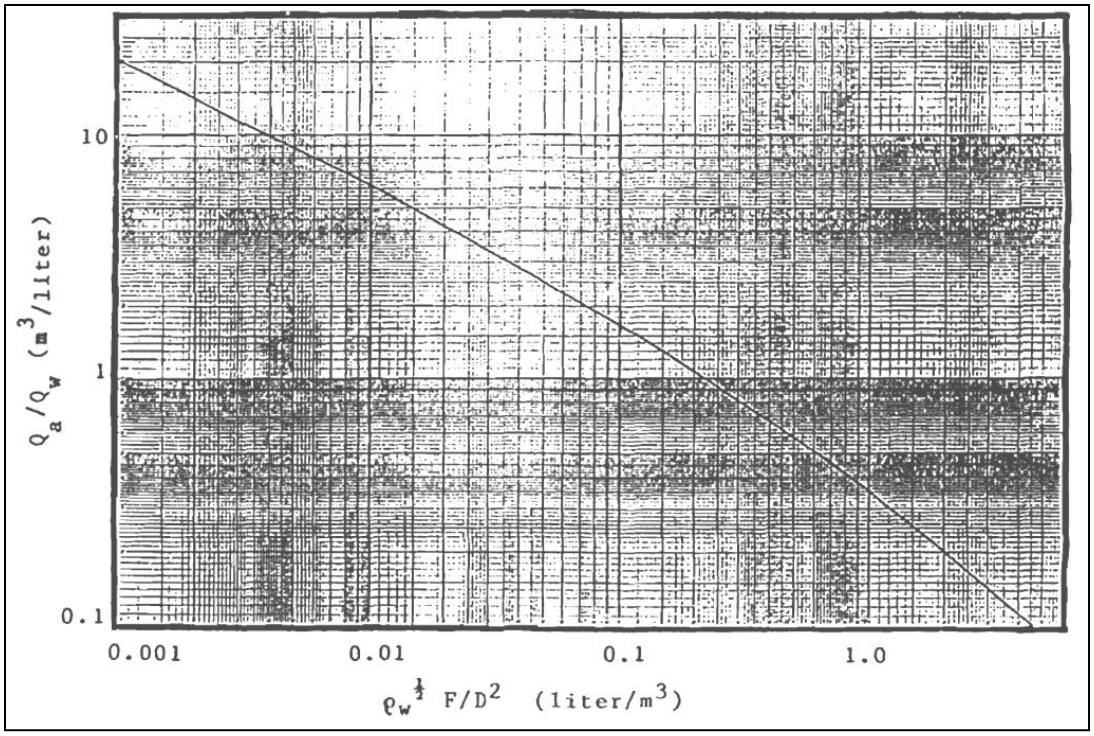

Fig. 4. Air entrainment for a water spray. Adopted from Atallah et al. (1988).

McQuaid recommended a ratio of Q_a/Q_w to measure the efficiency of the spray as well as a design parameter. It was given as a function of the water pressure and flow number. There is some range in the choice of the number of nozzles, since this does not affect the ratio of Q_a/Q_w. As the number of nozzles increase, the required flow number of each nozzle decreases and each nozzle must be mounted closer to the leak source to provide the required velocity. To obtain the high efficiency in terms of Q_a/Q_w, either the water pressure or the design air velocity is allowed to vary and then F/D^2 value should be low. Nozzles with low F values produce fine sprays and require high pressure at a constant flow rate. To get a large base diameter, the air velocity has to be low.

The effectiveness of a water spray in diluting a gas also can be determined from the "air entrainment ratio," expressed as the volume of entrained air per unit volume of water sprayed (m^3 air/m^3 water). Heskestad et al (1976, 1981) carried out experiments and theoretical studies to establish methods for predicting air entrainment rates into water spray systems. In these experiments, water was sprayed vertically downwards into an uninterrupted enclosed space. A simple theoretical model (eqn 9) was also developed for determining the entrainment flow rate.

$$Q_s = 2\pi \int_0^n URdR - 2\pi U_n \int_0^n \left(\frac{U}{U_n} \right) RdR \qquad (9)$$

This equation was used to determine the air entrainment rate across any level of a single spray. It was integrated numerically by curve fitting from the plots of the measured U/U_n versus R. A comparison of the theoretical entrainment flow values with the experimental results showed that the agreement was within 17% for a single nozzle and 11% for multiple nozzles. The models were capable of predicting air entrainment for single sprays and water curtains, provided the spray boundary was known. The experimentally determined air entrainment flow rates and efficiencies for single nozzle are given in Fig. 5. The figure is plotted from experimental data from Heskestad et al. (1981) for a single Rockwood T-4 ¼ inch nozzle. In the figure the solid lines represent entrainment flow and dotted lines represented entrainment ratio.

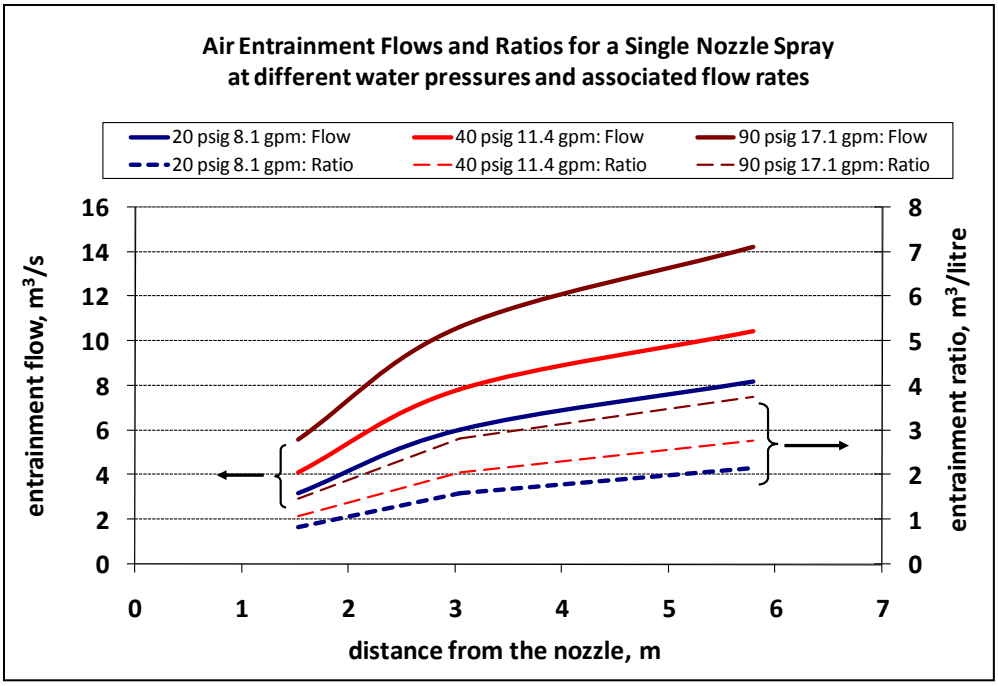

Fig. 5. Air entrainment flows and ratios for a single nozzle spray. Reprinted with permission from "Development of Design and Safety Specifications for LNG Facilities Based on Experimental and Theoretical Research" by Cormier, B, R., Suardin, J, A., Rana, M. A., Zhang, Y. and Mannan, M. S., 2009. *OPEC, Oil Prices and LNG, 12*, 295-424, Copyright [2009] by Nova Science Publishers Inc.

Fthenakis and Zakkay (1990) derived an equation to assess the dilution provided by a water spray. Under the assumption that only gas free ambient air is entrained by the spray and it "perfectly mixes" with the gas, maximum water spray dilution ratio was estimated from the gas mass balance (Fthenakis, 1991):

$$DR_m = \left(\frac{Y_{in}}{Y_{out}}\right) = \frac{\left(\left(\frac{\dot{m}}{MW}\right) + Y_{in}A_m\right)}{\left(\frac{\dot{m}}{MW}\right)} \qquad (10)$$

2.3.2 Forced Dispersion

Hald, et al. (2003, 2005) proposed a research methodology to quantify the forced dispersion factor provided by a water curtain with respect to its configuration. An engineering code CASIMIRE was developed to design water curtains for the chemical industry. This code can evaluate the mitigation efficiency for different water curtain configurations (type of nozzles, nozzle spacing, operation, pressure, height) by predicting the dilution factor. This code uses information on spray hydro-dynamics and physical and chemical properties of gases. In this work, dispersion of CO_2 and Cl_2 has been studied in field and wind gallery tests, as well as CFD simulation.

In the CFD simulation of forced dispersion of a heavy cloud like Cl_2 by water spray curtain, behavior of the gas phase is modeled by the averaged Navier-Stokes equations coupled with the RNG k-ε model for the turbulence. The droplet phase is described by a Lagrangian approach where single droplet injections model the particulate flow at the nozzle exit. The droplet velocity is calculated by solving the motion equations. The Rosin-Rammler droplet size distribution models the poly-dispersed nature of the spray.

The dilution factor is defined as the ratio of the ground concentration with and without sprays. The momentum ratio is defined as ratio of the momentum of the water curtain to a representative momentum of the gas cloud (Hald, et al., 2003; 2005):

$$D_F = \frac{C_{free\_dispersion}}{C_{forced\_dispersion}} \tag{11}$$

$$R_M = \frac{\dot{m}_{l\mu}}{\rho_c V_w^{\,2}} \frac{U_{do}}{H_{wo}} \tag{12}$$

Plots of dilution factor versus momentum ratio, based on results from both experimental tests and simulation analysis, indicated D_F as a good gauge for potency of water curtain. If the curtain-to-cloud height ratio is sufficiently large, an R_M value of 10 should lead to a D_F value of 10. At low momentum ratio, the gas cloud goes through the curtain without noticeable change in concentration. As R_M increases, the strength of the curtain with respect to the wind intensifies, and at high R_M values, typically 10, the water spray curtain has a significant effect and behaves as an active obstacle for the gas cloud.

The effect of the curtain-to-cloud height ratio, H_{wc}/H_c, on the dispersion factor also has been investigated by Hald et al. (2003, 2005). The height of the gas cloud considered is the cloud thickness at the curtain location during free dispersion experiment. Typical results are plotted in Fig. 6. The effect of the height ratio on the dispersion factor becomes more significant as R_M increases. However, at high R_M the trend tends to saturate as shown by the dashed curve ($\Delta D_F/D_F$) plotted in Fig. 6. As a practical rule, a water spray with more than twice the height of the gas cloud is recommended.

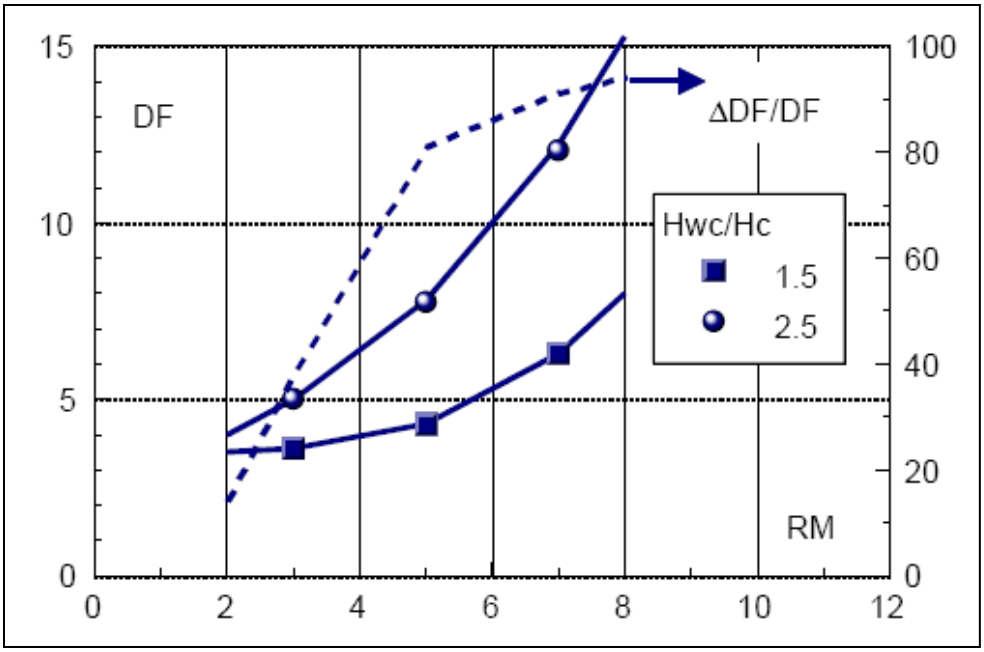

Fig. 6. Effect of curtain-to-cloud height on the forced dispersion factor. Reprinted with permission from "Development of Design and Safety Specifications for LNG Facilities Based on Experimental and Theoretical Research" by Cormier, B, R., Suardin, J, A., Rana, M. A., Zhang, Y. and Mannan, M. S., 2009. *OPEC, Oil Prices and LNG, 12*, 295-424, Copyright [2009] by Nova Science Publishers Inc.

Moore and Rees (1981) tried to find the most effective way of increasing natural dispersion of an explosive or toxic gas following an accidental release. They mainly concentrated on forced dispersion, which is the dilution of gas caused by entrainment of air with gas, entrainment of gas with air, momentum, turbulence and speed of the gas. They derived a "semi-empirical" model, built on Bosanquet's equation of air entrainment (Bosanquet, 1957), for the forced dispersion of gases by water or steam curtains and then applied that model in eight experiments to dilute dense gas plumes.

The authors extended the pioneering work of McQuaid (1977) by concentrating on the central question of mixing. One of the key parameters controlling the effectiveness of forced dispersion is the ratio of the air velocity to the wind speed. They developed new theories on the assumption that the mixing of gas with air could be described by empirical entrainment parameters which made the results semi-empirical. Three different spray configurations were considered to give three different relationships: (1) theory A: downward pointing spray and gas cloud from a point source; (2) theory B: upward pointing spray and gas cloud from a point source; and (3) theory C: upward pointing spray and gas cloud from a line source.

Moore and Rees (1981) used water and steam curtains to mitigate a vapor release. The effectiveness of water and steam curtains was defined as the ratio of gas concentration during natural and forced dispersion. The defined relationship was as follows:

$$F_D = \frac{C_{ND}}{C_{FD}} \tag{13}$$

Moore and Rees also described field trials conducted to validate their models using water spray and steam curtains. The trials included a continuous release of propane gas at 2 kg/min, a spill of 60 kg of liquid propane and a continuous release of liquid propane at 10 kg/min. The barrier was generally located 1 meter downwind of the source. The concentration was measured at 15 meters downwind. Other experiments were conducted with argon and sulfur hexafluoride at much lower flows and different downwind measurement distances. For downward pointing nozzles, the F_D factors were

in the range of 1.1-3.3, and for upward pointing nozzles, they were in the range of 2.5-6.3. The upward pointing nozzles were more effective. The experimental data and models showed that forced dispersion works best for small leaks, low wind speeds, and over short distances.

2.3.3 Heat Transfer

Heat transfer between water droplets and cold vapor also has been thought to play an important role in dissipating cold clouds by enhancing their buoyancy. However, very little literature dealt with this complex phenomenon of heat transfer by water sprays. St.-Georges and Buchlin (1995) presented a simple one-dimensional spray model to evaluate the heat transfer action by water curtain. The model was based on macroscopic mass and heat transfer balances and was developed considering three-fold spray actions: (1) gas (air and pollutant) entrainment and gas mixing; (2) absorption of pollutant in water droplets; (3) aerosol evaporation and dispersion enhancement by spray heating. It was also considered that (1) heat transfer between the phases to be induced by conduction and convection in the gaseous and liquid boundary layers, (2) temperature gradients inside the droplets to be small and constant, and (3) mass transfer between the phases to be induced by convection and diffusion. The final enthalpy balance for the spray envelope and single spray was derived as the following equation.

$$\dot{m}_{mg} C_{pg} \frac{dT_{mg}}{dz} = \frac{d\dot{m}_{gc}}{dz}\left(h_{gc} - h_g\right) - \dot{m}_{mg}\left(\left(h_v - h_a\right)\frac{dx_v}{dz} + \left(h_s - h_a\right)\frac{dx_s}{dz}\right) - \sum_{n_d}\left(\rho_l\left(h_v\big|_{Tdi} - h_g\right)\frac{dl_{vi}}{dz} + \frac{6a_h l_{vi}}{d_i u_{di}}\left(T_{mg} - T_{di}\right)\right) \tag{14}$$

Simulations were performed with two full cone sprays with chlorine clouds, and the results concluded that the heat transfer could be high enough to make the cloud buoyant and greatly increase the dispersion. The pollutant cloud temperature was increased by several degrees during the simulation. The authors also found that spray with smaller droplets gave higher heat transfer rates, but induced less momentum and was more affected by wind. The spray height must be higher than cloud height to gain more mechanical mixing with fresh air.

Alessandri et al. (1996) presented a mixed Lagrangian-Eulerian model of a water curtain where heat, mass and momentum processes were modeled in a Lagrangian framework for the dispersion phase and in an Eulerian framework for the carrier phase. Simulation and tests of full cone spray curtains with nitrogen-air mixture were performed. Both upward and downward pointing sprays were simulated to identify the gas and droplet temperature in the spray region with the consideration of simultaneous mass transfer. The water curtain performance in changing the gas cloud height also was studied. Results indicated that the downward pointing nozzle configuration was preferable to the upward pointing one, when both heat and mass transfer processes were considered. There were indications of droplets freezing by premixing the cold gas with the entrained air, before interacting with the spray droplets for the case of upward pointing nozzles. In the simulations, the downward nozzles actually increased the cloud height significantly as compared to the upward nozzles.

2.3.4 Mass Transfer and Chemical Reaction

Some research indicates that water spray can more effectively control unconfined releases of gases which are highly soluble in water. However, there is limited information on the effectiveness of this control option with less soluble gases. Prugh (1987) has quantitatively assessed the effectiveness of water sprays on several gases, based on differences in the Henry's law constant. According to his findings, water spray is effective for highly soluble chemicals such as many acid vapors; however, total absorption should not be expected. Water sprays are marginally effective in reducing the hazard of vapors with limited solubility in water (Prugh, 1987; Prugh & Johnson, 1988). Prugh (1985, 1986) also has presented mass balance to relate the theoretical effectiveness of water sprays/curtains with the water and gas flow rates, the initial gas concentration and the Henry's law constants. Although useful for the estimation of the maximum effectiveness, these equations do not consider the influences of several other parameters, e.g., droplet size, spray pattern, gas and liquid mass-transfer coefficients, which are important in the design of an effective system (Fthenakis, 1991).

2.4 Effects of Spray Parameters on Physical Phenomena

The sprays produced by a nozzle can be categorized by their shapes as conical, fans, or fogs. The spray pattern that will be used is highly dependent on the planned application. Conical sprays can be further broken down into either full-cone or hollow-cone sprays. In the hollow cone pattern all of the spray is located at the surface of the cone produced by the nozzle and none of it is inside the cone. In the full cone pattern the

liquid being sprayed fills the cone pattern produced by the nozzle. Conical sprays produce medium size droplets. Nozzles that spray water as a sheet of liquid produce a pattern known as a fan. The droplet sizes produced by fan nozzles are usually coarse. The fog nozzles atomize the liquid stream into a mass of very fine droplets (CCPS, 1997).

Water spray curtains are mainly curtains of water droplets. Information of the size of the droplets produced by a spray nozzle is essential as it affects the action mechanisms. The droplet size of a certain type of curtain provides a certain surface area. When a water curtain control a vapor cloud by diluting it, then the volume of the droplets (i.e., its momentum) is important. A spray nozzle actually produces a range of droplet sizes. The simplest approach is to define a representative droplet diameter in terms of mean or median. The Sauter Mean Diameter (SMD) defines a droplet with mean surface area and volume for the whole spray. It is calculated from the sum of the droplet volumes in a given spray divided by the sum of their surface areas. Another commonly used representative diameter is the Volume Median Diameter. Half of the droplets in a spray have diameters greater than this value and half of the droplets smaller (CCPS, 1997; Gant, 2006). Fig. 7 illustrates the effects of drop size on water curtain mechanism.

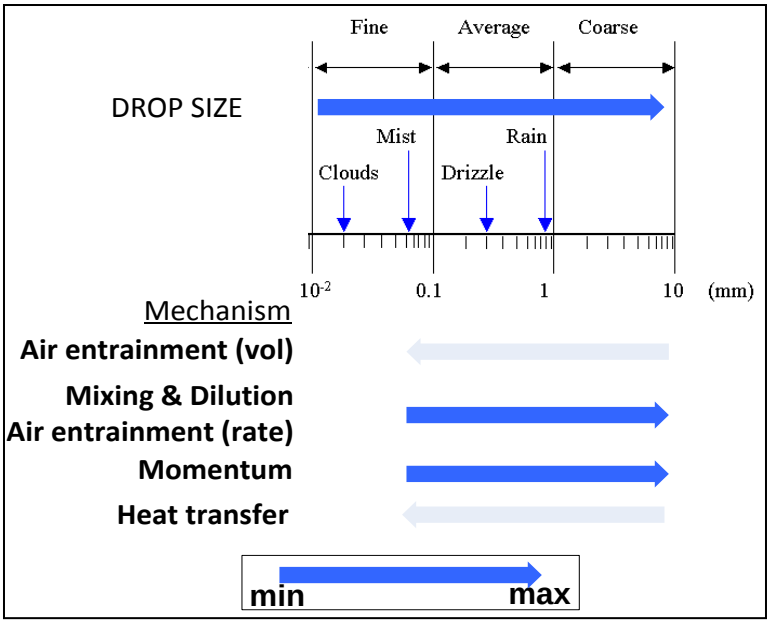

Fig. 7. Effect of water droplet size on water curtain action mechanism.

The spray flow direction is another important factor to consider when dealing with a vapor cloud of specific nature. The primary purpose of a water curtain to control a flammable gas release is the attainment of a suitable dilution of the released gas, so that the cloud reach lower flammability limit rapidly before dispersing too far. When dealing with toxic cloud water curtains are used to ensure a partial abatement of the released compound by chemico-physical absorption, in addition to the dilution phenomenon. Usually downward water curtains are used for heavier than air flammable and toxic gases to contain the gas cloud in an area. Downward curtains create a barrier to the gas cloud by the air vortex created by the spray and force the gas downwards (Palazzi et al., 2004). In the LNG industry, upward-pointing water curtains should be used to facilitate LNG dispersion. Though LNG is a heavier than air vapor cloud, it becomes lighter when

gets diluted and warmer. For this water curtains with an upward flow should show better effectiveness to control LNG than those with a downward flow (Atallah, Guzman, & Shah, 1988). The momentum from an upward spray can enhance air entrainment through the lower surface of the LNG cloud and influences the mixing between the LNG cloud and entrained air. Thus a better dilution could be achieved. The upward momentum imparted to the LNG cloud, also pushes it from the bottom and facilitates the cloud's dispersion upward. However care should be given to prevent water entering the LNG pool, as it will increase vaporization rate.

2.5 Research on the Application of Water Curtain to Disperse LNG Vapor Cloud

2.5.1 Effectiveness in Reducing Concentration

It is a complex problem to predict downwind concentration or quantify the effectiveness of water sprays in mitigating accidental releases of toxics. Both theoretical and experimental work has been carried out to capture the underlying mechanisms and the parameters in the use of water spray. However, a very limited number of these published works are on the use of water curtains to control LNG vapor clouds. Experiments on using water curtains for small LNG spills by University Engineers for the US Coast Guard in the mid- 1970's, and modeling, wind tunnel and small scale spill tests by Factory Mutual Research Corporation for Gas Research Institute in the early 1980's are the major published works to date. The former conducted experiments to

simulate spills on LNG ships and used fan-shaped sprays; the later one developed models as well as performed tests considering a spill contained in a dike and used solid and flat sprays, to determine the effectiveness of water spray curtain.

Martinsen and Muhenkamp (1977), and Brown, Martinsen and Cornwell (1983) summarized the small scale experiments by the U.S. Coast Guard in 1976. Those small-scale experiments were performed to determine the effectiveness of water sprays to disperse LNG vapors using spray nozzles, available aboard LNG ships. The type of nozzle used in the tests were fan shaped sprays and produced a wide angle, flat spray pattern in the shape of a circular segment with a radius of 2.44 to 3.05 m and an arc of 150 to 160 degrees. The spray pattern created by these nozzles was a sheet of water for the first few inches of spray and then the remaining spray consisted of water drops. To study a spill which can occur on a ship, a 3.05 m diameter pan was used to test 15.24 cm of LNG dispersion. Ten catalytic bead-type combustible gas detectors were used to measure the gas concentration downwind of the pan 2.13 m (7 feet) and 0.61 m (2 feet) above the ground. Fig. 8 shows the gas sensors layout for the test.

During the experiments, the numbers of nozzles as well as water flow rates were varied in twelve different runs. The nozzles were located about 0.46 m (1.5 feet) below the edge of the LNG container. The closest nozzle was placed about 1.68 m (5.5 feet) downwind from the leading edge of the pool and the second and third nozzles were 25.4 cm (10 inches) and 50.8 cm (20 inches) downwind of the first nozzle, respectively. The wind speed during that day was 4 m/s (9 mph) with gusts up to 7.6 m/s (17-mph).

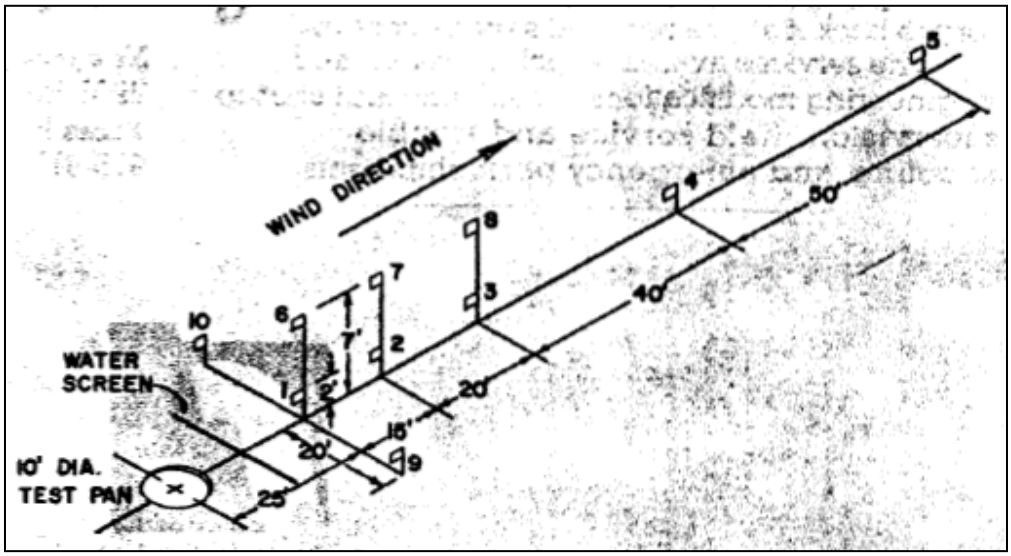

Fig. 8. Gas detectors placements. In FPS unit system. Reprinted from Martinsen & Muhenkamp (1977) with permission from the authors.

Gas concentrations were measured first with no water spray, then with one, then two and finally with three nozzles. The readings were time-averaged over 5 or 10-minutes period by graphical integration because of fluctuations of methane concentration caused by wind gustiness' crosswind turbulence. Due to some sensors' failure during the test, 33 data points of 48 tests were reliable. Twelve of these data were gathered without water spray. Fig. 9 and Fig. 10 show the results:

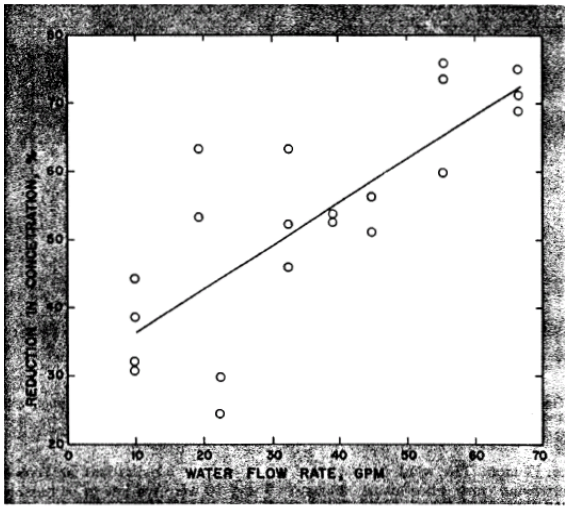

Fig. 9. Effects of water spray conditions on methane concentration downwind of the LNG pool. x axis: water flow rate (gpm), y axis: reduction in concentration (%); correlation coefficient = 0.802 and standard error of estimate = 0.0963. In FPS unit system. Reprinted from Martinsen & Muhenkamp (1977) with permission from the authors.

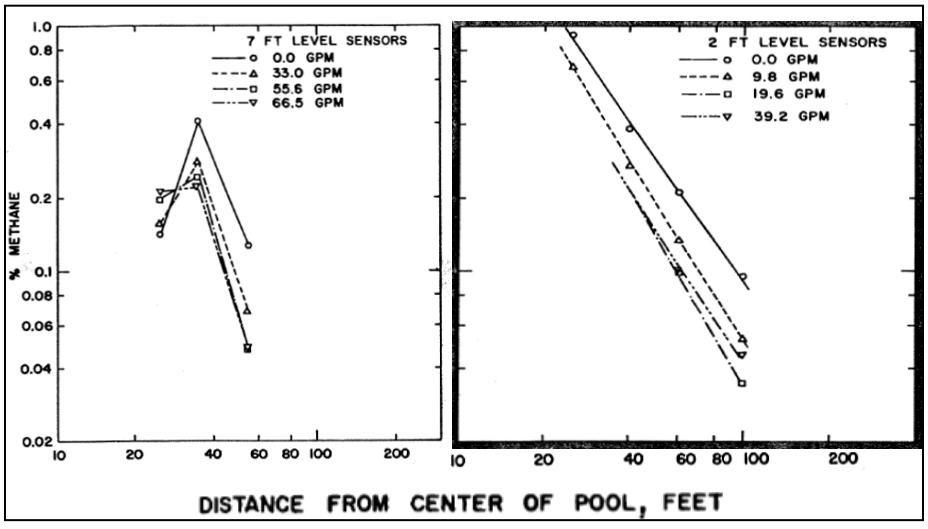

Fig. 10. Methane concentrations downwind of the LNG pool, with and without water spray. In FPS unit system. Reprinted from Martinsen & Muhenkamp (1977) with permission from the authors.

Fig. 9 summarizes the data to determine the percentage reduction in gas concentration for the various water flow rates conditions. The best-fit straight line was drawn by linear regression. Fig. 10 shows gas concentration at 2.13 m (7 feet) and 0.61 m (2 feet) levels downwind of the LNG pool. From the 2.13 m (7-feet) high sensors, the readings of sensor 6 and 7, before and after water spray, shows increase in plume height. Fig. 11 shows the effects of water sprays in dispersing LNG vapor cloud.

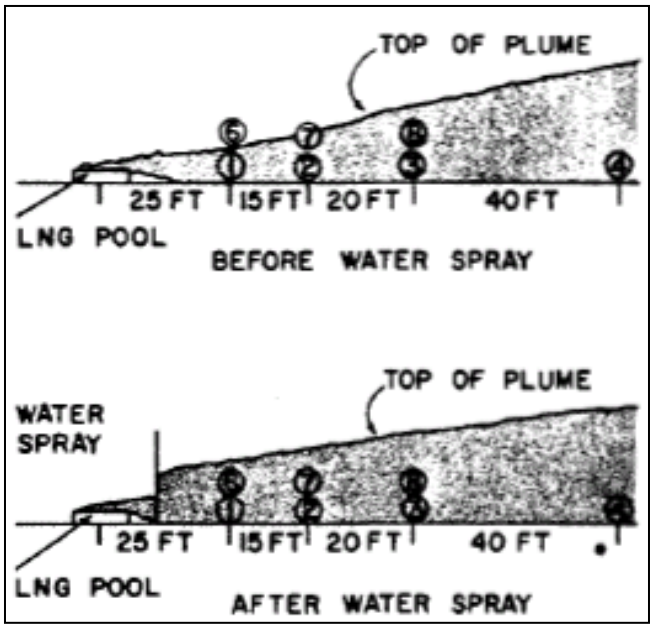

Fig. 11. Illustration of mixing effect of water spray. Reprinted from Martinsen & Muhenkamp (1977) with permission from the authors.

Only a few tests were performed to observe water spray dispersion of LNG vapor, but no theoretical model was suggested in this research. The experimental results proved that methane concentration reduction did occur with the water spray. However,

the authors neither gave any precise method of designing an effective water spray system for vapor concentration reduction, nor gave any information about the materials of the pan where LNG was spilled. The material of construction of the pan is important as it affects the vaporization rate. Their experiments were not concerned with the vapor concentration in front of the spray nozzles. They also made conclusions about two mechanisms that caused the concentration reduction. Between the two mechanisms, the increase in mechanical turbulence caused by the decrease in the concentration was clearly indicated from the results. However, as the heating of the vapor plume was not measured, the effect of heating on vapor dispersion was not clearly identifiable from the experiments.

Heskestad et al. (1981, 1983) summarized the three-phase research program to develop engineering design guidelines for the use of water spray curtains to disperse LNG vapor cloud. The Gas Research Institute contracted with Factory Mutual Research Corporation (FMRC) to develop this research program. In this program, theoretical models were developed according to the previous calculations of air entrainment rate by spray nozzles. To understand LNG vapor dispersion, a design methodology for water spray curtains was formulated and small-scale experiments were then designed based on this model. The experimental results were summarized later several articles.

In the earlier phase of the work, a theoretical steady-state model of the interaction of a line spray with a vapor cloud driven by atmospheric wind was formulated. Interaction and downwind vapor dispersion calculations to determine the state of the diluted gas leaving the interaction region were performed with the FMRC

computer code, SPRAY. In order to develop engineering design guidelines for water spray systems based on these theories, small-scale experiments were designed. These experiments were guided by a simple entrainment theory for spray discharging vertically downward in quiescent air (Heskestad, Kung & Todtenkopf, 1976; 1981).

To formulate and calculate the interaction of spray and vapor, droplet evaporation, drag, mass, momentum and energy were considered. Two-dimensional flow field was assumed by ignoring all the variations in the third dimension (perpendicular to the wind and parallel to the ground). This is an inherent limitation of the two-dimensional flow approximation. To theoretically analyze the effectiveness of a water curtain in dispersing LNG vapor, a hypothetical large diked LNG spill was assumed. A spray-vapor-wind interaction was calculated for the cited LNG spill from the derived model. The assumptions for formulating the interaction model were: (1) methane layer approached from the dike and mixes with ambient air; (2) the concentration of methane in the layer is close to 100%; (3) in the spray-vapor layer interaction region the mixing was adiabatic and flow was two-dimensional; and (4) water condensed from the ambient air due to layer heating.

The calculated results for a 2-m thick vapor cloud and a variety of spray configurations and wind speeds clearly indicate that for a given spray configuration, effective dilution and heating occurs at lower wind speed (Heskestad, Meroney & Kothari, 1983). For standard downward spray configuration, a 65% reduction in methane mass fraction occurs at the lowest wind speed of 1 m/s, but at the highest considered

wind speed of 4 m/s, the decrease is only 18% and the highest cloud temperature at the layer is 275 K for the lowest wind speed.

The calculated results at the downwind end of the spray-vapor-wind interaction regions were used as inputs for downwind plume dispersion calculations. These calculations were performed to determine the significance of spray dilution and heating of the LNG vapor cloud in reducing the size of the dispersion exclusion zone. Fig. 12 and Fig. 13 show the calculated ground-level methane vapor mass fractions calculated with neutrally buoyant plume and positive buoyant dispersion models for the spray and no-spray situations.

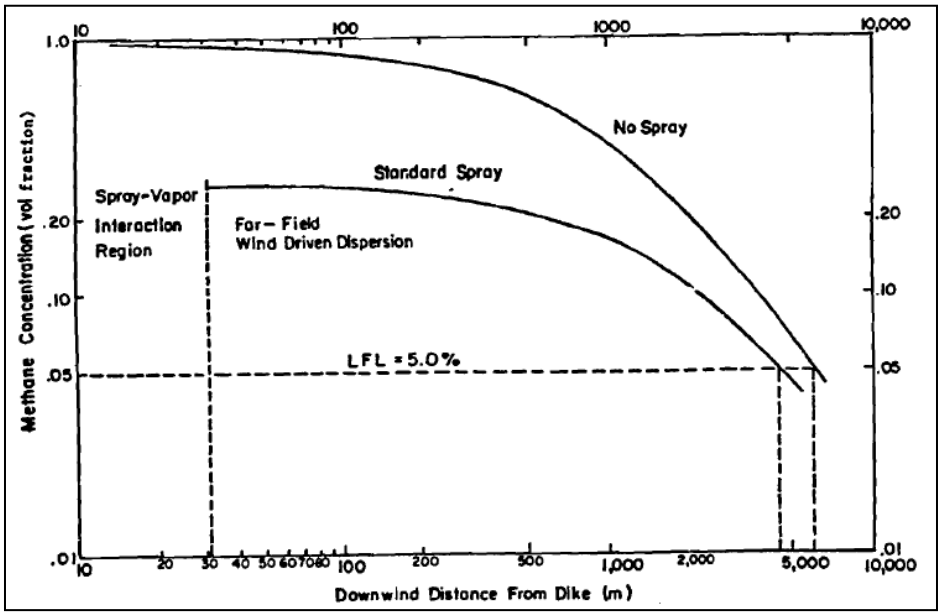

Fig. 12. Calculated ground level methane concentrations with and without water spray (neutrally buoyant plume model). Reprinted with permission from "Dispersal of LNG Vapor Clouds with Water Spray Curtains," Report No GRI-80/0107 by Gas Research Institute.

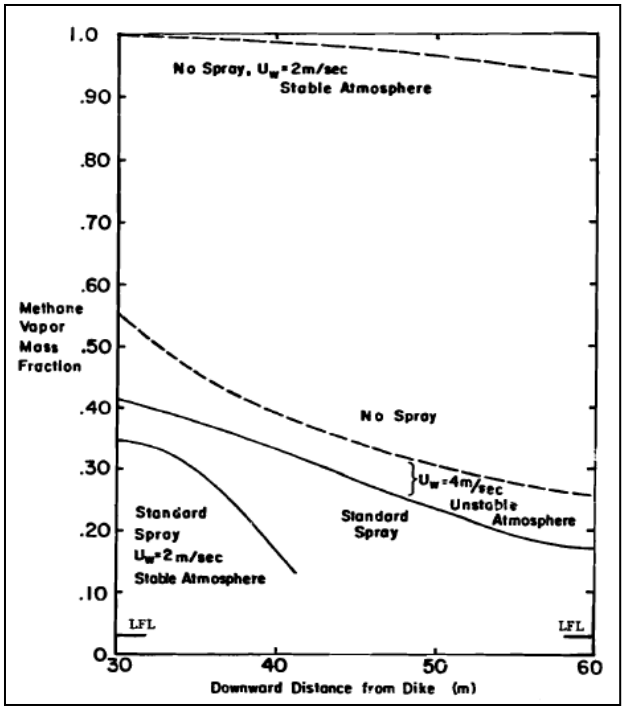

Fig. 13. Calculated ground level methane concentrations with and without water spray (positive buoyant dispersion model). Reprinted with permission from "Dispersal of LNG Vapor Clouds with Water Spray Curtains," Report No GRI-80/0107 by Gas Research Institute.

Theoretical results of the study concluded that water sprays can provide significantly enhanced dispersion at a low wind speed, but the usefulness of water curtain decreases as wind speed increases beyond 4 m/s. The figure also indicates that water curtain causes the downwind zone of high vapor concentration to be substantially smaller at low speed than at high wind speeds (>4 m/s). The formulated results were used afterwards to design small-scale outdoor experiments, as well as model experiments based on wind tunnel simulations. The experiments were guided by a simple entrainment theory for conical sprays discharging vertically downward in

quiescent air. The average entrained-air velocity in the spray was determined by the theory as a function of vertical distance below the spray nozzle for given water pressure, nozzle diameter and spray cone angle. For the downward pointing spray, the effect of atmospheric wind on the air entrainment and any additional entrainment that could occur in the ground jets were ignored for the sake of simple design calculations. It was assumed that air entrainment rate is some multiple of the spill rate in order to make the spray system capable of entraining surrounding air and mixing it with the vapor flow.

Heskestad, et al. (1983) also presented the results from initial experiments to study the effectiveness of water spray curtains in dispersing LNG vapor. The tests consisted of outdoor experiments with LNG spills into a 3 m by 3 m diked area, as well as reduced scale, model experiments in a wind tunnel simulating massive spills of LNG into a 60 m by 60 m diked area, both surrounded by water spray nozzles. For the outdoor tests, LNG was spilled into a 3 m by 3 m pit. The LNG entered through an insulated 1.5 inch stainless steel pipe that was welded to a 6 inches diameter discharge elbow. As the expansion in the pipe reduced the velocity of any vapor in the flow, the elbow discharged on a 1 m by 1 m evaporator pad consisting of a stainless steel embossed plate heat exchanger carrying high flow rates of water covered by a stone layer approximately 0.05 m thick which was framed by bricks. The LNG discharge rate measured to be about 0.45 kg/s and considered equivalent to the evaporation rate at steady state.

In the outdoor tests, infrared type gas sensors were used to monitor gas concentration. Twenty-four nozzle sites were chosen to use “swirl” type nozzle of 4 mm diameter, which produced “full cone” sprays. For downward spray, the nozzles were

installed at an elevation of 0.99 m, which produced a spray impact diameter of 0.49 m at the test pressure (84 psig). Fig. 14 shows the layout of gas sensors, wind station, spray nozzles and a meteorological station for the outdoor tests. Among the 33 regular experiments performed, 11 were analyzed. Upward pointing spray configurations were also studied.

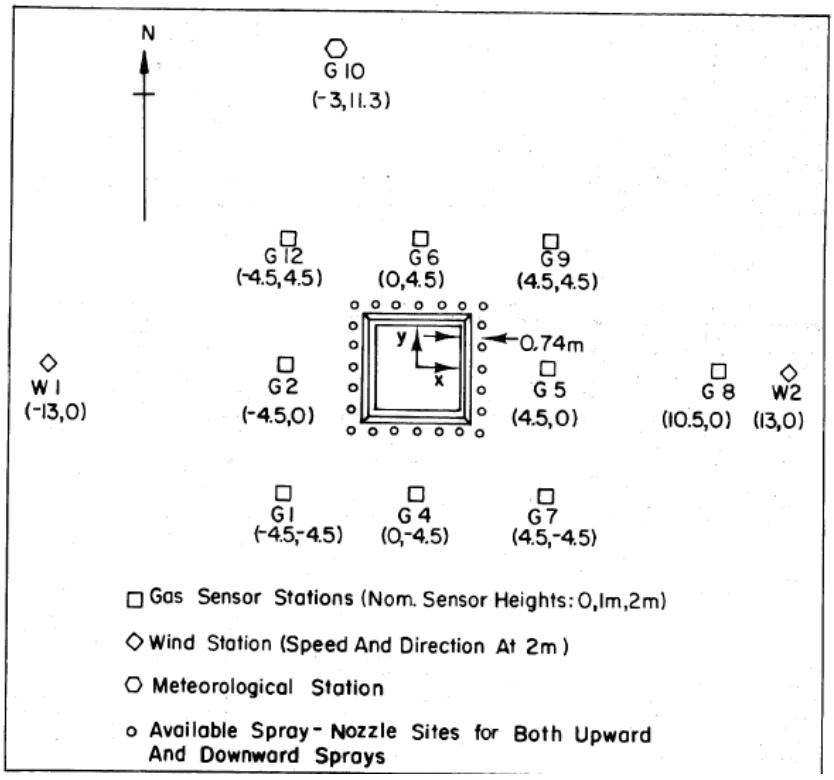

Fig. 14. Layout of test pit area. Reprinted with permission from "Dispersal of LNG Vapor Clouds with Water Spray Curtains," Report No GRI-80/0107 by Gas Research Institute.

From the outdoor test results, the authors only analyze three runs for downward spray, which was not sufficient for validating the theoretical calculations (Gas Research Institute, 1982). The placement of sprays was very close to the pit, which might spray water into the pool and increase the boil-off rate and the concentration in the air. The results did not suggest any precise method of designing an effective water spray for a small spill on the ground. Based on the model and theoretical calculations, it was expected that for a ground entrained air velocity of 6 m/s, twelve vertical downward sprays would reduce the downwind vapor concentrations to near 5% by volume (spill rate 0.45 kg/s and 87.4 % methane in LNG). The expectation was met although the pre-spray concentrations were already very low. This configuration diluted the vapor concentration to the anticipated level from the ratio of the LNG-vapor rate versus the theoretical entrainment rate in quiescent air. Results show that twelve and twenty-four upward sprays dilute the concentrations to about 2% and 1%, respectively. The vapor plume was lofted above the diked area by the sprays, producing a low ground level concentration downwind with some vapor potentially escaping between adjacent sprays. The associated water rates were somewhat higher than the minimum estimated theoretically.

The main part of this study was carried out on 1:100 model scales in a wind tunnel, simulating massive spills of LNG into a 60 m by 60 m diked area. At room-temperature, CO_2 was used to simulate LNG-vapor. Experiments with vertical downward and vertical upward sprays showed disappointing results because of poor mixing between entrained air and ground level vapor. However, the downward sprays

inclined 45° toward the dike wall and increased water pressure improved the dilution performance of water per unit flow rate of water. For the vertical upward spray, high water pressure also enhanced the dilution performance per unit flow rate of water. Other wind tunnel experiments in the same available literature indicated that storage tanks and increased dike heights had little effect on the dilution performance of the downward inclined and vertical upward spray curtains. Regarding the nozzle diameter in case of upward sprays, substituting a larger spray nozzle at a decreased water pressure theoretically having a similar entrainment rate and entrained air velocity in quiescent surroundings compared to the original pressure and nozzle size, resulted in similar dilution performance. However, for reasons unknown, downward inclined sprays resulted in inferior performance (Gas Research Institute, 1982).

2.5.2 Study of Heat Transfer

A rigorous heat transfer analysis was carried out by Atallah et al. (1988) to determine the required amount of water and droplet size for warming a cold LNG vapor cloud, from its boiling temperature (110 K) to the neutral buoyancy temperature (165 K). The authors derived an equation based on the consideration and assumption that: (1) downward water spray was located above the LNG vapor cloud; (2) droplets had a uniform and spherical diameter d; and (3) water spray produced $\dot{N}$ droplets per second. The rate of heat transfer between the droplets and the cloud was given by the equation:

$$\dot{Q} = \dot{N}\left[\left(\frac{\pi d_w^3}{6}\right)\rho_{d\,w}\lambda_f + \pi d_w{}^2 h_w \Delta T_{mw}\theta_w + \pi d_w{}^2 h_i \Delta T_{mi}\theta_i\right] \qquad (15)$$

The water flow rate in the spray barrier was derived as (in kg/s):

$$\dot{m} = \dot{N}\left[\left(\frac{\pi d_w^3}{6}\right)\rho_w\right] \tag{16}$$

A parametric study was carried out for four droplet sizes (0.3, 0.5, 1.0 and 1.3 mm) and two assumed cloud heights (1 and 2 meters). They found that droplet sizes required to warm up an LNG cloud to the point of its neutral buoyancy were achievable by commercial spray nozzles operating at reasonable pressures of 4 to 7 bar. In addition, the droplets must be as small as feasible and applied as close as possible to the LNG source as per their calculations. Fig. 15 shows the results of the parametric study conducted by Atallah et al. (1988).

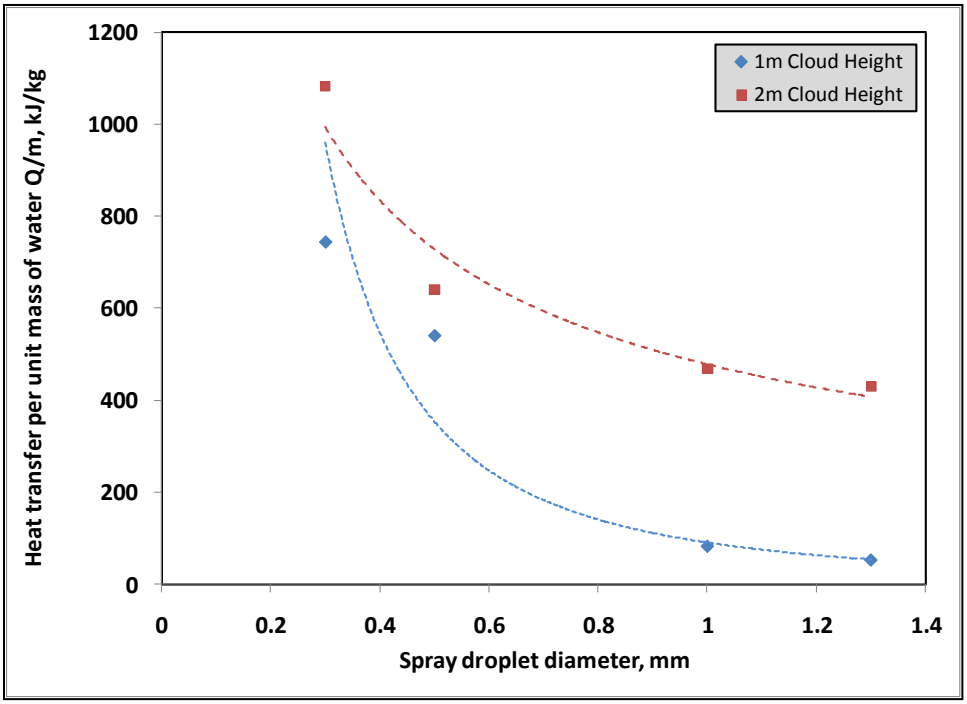

Fig. 15. Effect of water drop size on heat transfer by water spray.

Arthur D. Little, Inc. (1974) evaluated several LNG vapor control methods and considered upward water curtains as one of those methods. The upward spray was evaluated with regard to warming LNG vapor clouds. A gross heat balance was the basis for the evaluation. They determined that to bring an LNG vapor cloud, vaporized from 104 to 15x104 gpm LNG spilled in a soil floored 91.44 m by 91.44 m (300 ft by 300 ft) dike with 6.3 m (20.6 ft) wall, to neutral buoyancy point (165 K), a water curtain must transfer 30,000 to 50,000 Btu/s heat. Then, the corresponding water requirement would be 1300 to 2200 gpm, assuming all of the water would transfer heat to the cloud. This result was fully dependent upon other heat balance assumptions. Also, they determined the optimal water droplet size to be in the range of 0.3 to 0.4 mm in diameter, for which the upward spray would only reach 0.9 to 1.2 m.

2.5.3 Research Gaps

Previous work has confirmed that the water curtain represents one promising technique to mitigate the hazards of an accidental LNG release. However, it is not clear from such work how to design an effective water curtain. It is also true that at this time there is no simple set of optimum parameters, rather there will be a specific set of design parameters for the water curtain to be effective for each particular type of circumstances (Harris, 1981). As there are wide differences in nozzle and design variables, some researchers believe that for each orientation, a unique combination of nozzle type, spacing, orientation and water pressure can provide equally effective performance. The effectiveness of water curtains can also be affected by the LNG source and wind

velocity. The rate of LNG vaporization also will increase if water droplets are deposited on the LNG spill; thus, the effectiveness of the water curtain may be affected. Minimizing water consumption and draining water are another two factors in designing a water curtain system. So, more studies are needed to determine the main controlling factors in designing an effective water curtain for the purpose of controlling LNG vapor clouds.

3 EXPERIMENTAL DEVELOPMENT*

3.1 Introduction

The effectiveness of water curtain to disperse any vapor cloud depends on its own characteristics, unique properties of the vapor cloud as well as on the environment. Therefore development of comprehensive and authentic design guidelines for water curtain to mitigate LNG release require a thorough understanding of the underlying physical phenomena from a reasonable amount of research especially experimental works. The purposes of this research are to (i) study the interaction of representative types of water curtains with real vapor clouds produced from LNG spills, and (ii) determine the effectiveness of the water curtains in controlling the LNG cloud. The research plan includes multiple sets of outdoor field experiments with different types of upward water curtains and LNG release. The overall experimental methodology is developed according to the basic scientific investigation procedure which follows 4

---

* Parts of this section are reprinted with permissions from (1) "Experimental Study of Effective Water Spray Curtain Application in Dispersing Liquefied Natural Gas Vapor Clouds" by Rana, M. A., Cormier, B. R., Suardin, J. A., Zhang, Y. and Mannan, M. S., 2008. *Process Safety Progress*, 27 (4), 345-353, Copyright [2008] by John Wiley & Sons, Inc., and (2) "Use of Water Spray Curtain to Disperse LNG Vapor Clouds" by Rana, M. A., Guo, Y. and Mannan, M. S., 2009. *Journal of Loss Prevention in the Process Industries*, 22, 707-718, Copyright [2009] by Elsevier Ltd.

steps: (1) identification of the variables; (2) design of the experiments; (3) careful observation and measurements; and (4) interpretation of experimental data. The experiments for this research are designed based on the previous experiments, experiences and preliminary calculations.

3.2 Experiment Facility

Outdoor experiments are designed to spill LNG onto confined land and water. The individually or combined use of different types of water spray curtains to control the LNG vapor cloud are tested. Experiments are carried out in the LNG test facility at the Brayton Fire Training Field (BFTF) of Texas Engineering Extension (TEEX) Service at Texas A&M University, College Station. Located adjacent to the Texas A&M University campus, the 120-acre training field is the largest live-fueled, firefighter training facility in the world and provides realistic, large-scale and hands-on emergency response and fire training. The field is equipped with 132 props or training stations and 21 live-fire props (TEEX, 2009). A liquefied natural gas (LNG) emergency response training facility has been constructed in the training school to conduct hands-on spill control and fire suppression training to personnel involved in LNG production, transportation, storage, and response activities.

The Mary Kay O'Connor Process Safety Center of Texas A&M University has been involved in research on LNG safety and mitigation system since 2005. One of the main focuses of the research is to study water curtain application to suppress LNG vapor. The Mary Kay O’ Connor Process Safety Center is using the LNG training

facility of BFTF as well as the help of the experienced training personnel to conduct LNG spill experiments. The LNG training facility has three concrete containment-pits, and one L-trench, described as below:

i. Two 1.22 m (4ft) deep pits below the ground with areas of 3m x 3m (10ft x10ft) and 10m x 6.7m (33ftx22 ft), called Small Pit (Pit 1) and Large Pit (Pit 2) respectively

ii. One L-shaped trench (L-trench) used to simulate the trenches whose purpose is to divert any LNG spills into the containment pits

iii. One 2.44 m (8ft) deep pit (1.22 m below and 1.22 m above the ground) with an area of 6.7 m x 6.7 m (22 ft x 22 ft) called Marine Pit (Pit 3). This pit includes a high dike wall, typical of the containment facilities used during LNG offloading

The flat ground of the LNG facility is also made of concrete. Photographs of the LNG training facility area are shown in Fig. 16 and Fig. 17.

1. Small Pit (Pit 1): 3.05m×3.05m×1.22m
2. Large Pit (Pit 2): 10.06m×6.71m×1.22m
3. L Trench
4. Marine Pit (Pit 3): 6.71m×6.71m×2.44m

Fig. 16. Aerial view of the LNG training facility. Adopted from Suardin (2008).

Fig. 17. North side view of the LNG training facility.

To ensure safety within the facility, a series of water curtains are installed around the LNG training site to control the dispersion of spilled LNG. Three water monitors (or hydrants) are also installed in three corners of the LNG props. The Brayton Field LNG facility is equipped with a 20.3cm (8") water pipe loop. Sufficient water supply is available during an LNG training workshop or a spill test, from the city water supply, with the aid of a pump powered by a pumper truck. Additional use of the pumper truck confirms adequate water supply to operate multiple water curtain heads and water monitors simultaneously when necessary. Fig. 18 shows a detailed diagram of the facility layout.

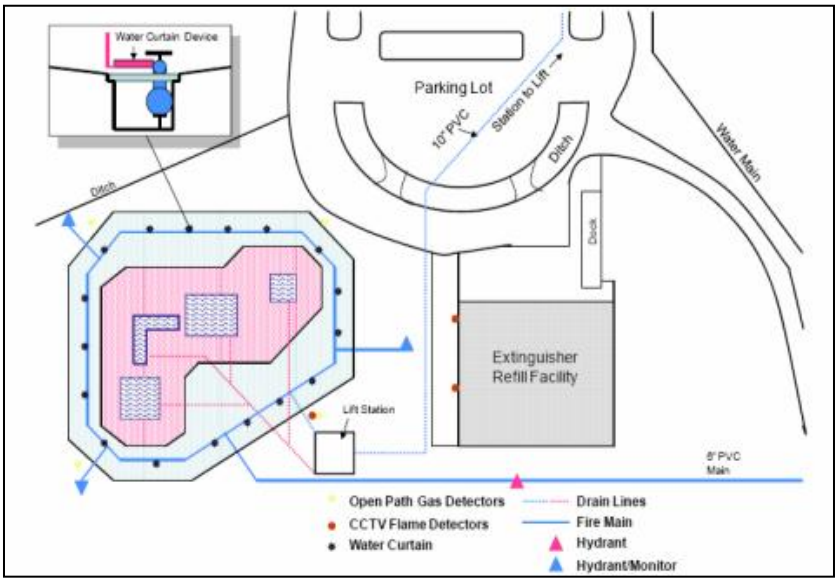

Fig. 18. LNG training facility layout. Courtesy of Brayton Fire Training Field.

Four open path detectors are permanently installed around the LNG training facility to detect any methane cloud dispersed outside the perimeter. These four "Searchline Excel IR" open path detectors are installed on four separate fixed concrete poles (South, East, North and West) in four corners of the field. Each open path detector is constituted of two parts, sender and receiver. The sender part of one detector mounted on one pole sends a laser beam to a receiver installed on another pole. Because of laser beam, the detectors need to be fixed on poles. Any hydrocarbon gas cloud crossing the path of laser beam changes the intensity of the laser beam and this change in intensity is used to estimate the linear concentration of the cloud along the open beam path. The measurement unit of these open path detectors is "% LFL (/LEL) per meter" of methane. Fig. 19 shows photographs of a open path detector.

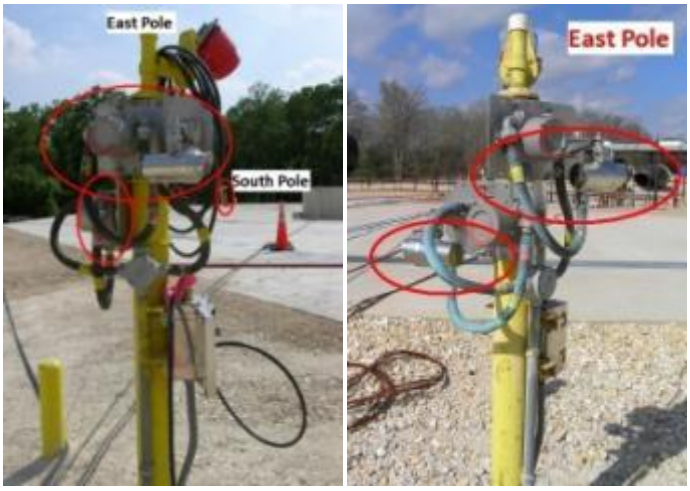

Fig. 19. Searchline Excel IR open path gas detector.

A 53 meters long insulated cryogenic pipe line is installed near the LNG training field. During a spill an LNG tanker truck is usually connected to the end of the pipe line which is far away from the field boundary. LNG flow rate in the pipe line is controlled by the valve of the LNG tanker and the flow from the tanker through the line is gravity pressure driven. Normal practice is to add a few psi pressures inside the truck to speed up the process of discharge. The added pressure is obtained by boiling LNG inside the tanker. There is no system to pre-cool the delivery pipe line prior to a spill.

3.3 Field Experiments

A total of four sets of LNG spill experiments have been conducted so far from the year 2006 until 2009 to determine the effectiveness of different water curtains in dispersing LNG vapor. All of the tests were conducted in the LNG fire fighting training facility at BFTF in presence of real medium scale LNG spills. In each experiment LNG was spilled on confined area of either concrete land or water. Thus LNG vapor was produced due to the vaporization phenomena. In the LNG industry, upward-pointing water curtains are mainly used to facilitate LNG dispersion. So in the experiments upward water curtains were considered and placed downwind of the LNG release location. The extent of LNG vapor concentration and temperature change by a water curtain are studied to determine the effectiveness. The experiments also focused on the effects of significant parameters, such as size, location, terminal height and width of a certain type of water curtain on the dispersion of LNG vapor cloud. Table 3 shows list of the field experiments.

Table 3. Summary of LNG spill experiments with water curtains.

Field Expt.	Spill Location	Spill Surface	Water Curtain			Measurement
			Type	Nozzles	Tests	
April 2006	Marine Pit (Pit 3)	Water	Flat Fan (upward)	3	1	LNG flow Gas conc. Weather
November 2007	Flat Ground	Concrete	Full Cone (upward)	7	2	LNG flow Water flow Water pressure Gas conc. Gas temp. Water (curtain) temp. Weather
			Flat Fan (upward)	1	2	
March 2008	Box	Concrete	Full Cone (upward)	8	1	LNG flow Water flow Water pressure Gas conc. Gas temp. Water (curtain) temp. Concrete temp. Weather
			Flat Fan (upward)	1	1	
March 2009	Pit 1	Water	Full Cone (upward)	8	1	LNG flow Water flow Water pressure Gas conc. Gas temp. Water (curtain) temp. Water (spill) temp. Weather
			Flat Fan (upward)	1	1	
			Full cone Mist (downward)	6	1	
			Combined	15	1	

3.3.1 Experiment: April 2006

3.3.1.1 General Description

On April 20, 2006, LNG spill tests was conducted by spilling LNG onto water surface to test LNG vapor dispersion (natural) and then effectiveness of water curtain and foam to disperse LNG vapor. The test was conducted in the Marine Pit (Pit 3 in Fig. 16 and Fig. 17) by filling it with water up to the top (2.3 m deep water pool). LNG was delivered on the top of the water surface in the middle of the water pool. Fig. 20 shows a photograph of the marine pit used during the test.

Fig. 20. LNG spill location in 2006 experiment (marine pit).

This experiment was considered to be unconfined LNG spill on water, because the pit geometry did not constrain the vapor cloud migration. The experiment consisted of three phases:

1. Phase (a) when LNG was continuously spilled on water and no mitigation measures were applied to control the vapor dispersion;
2. Phase (b) when LNG was continuously spilled on water and water curtains were used to control the downwind vapor dispersion; and
3. Phase (c) when LNG was continuously spilled on water and hi-expansion foam were applied on LNG pool to suppress the vapor dispersion.

This research only focuses on the phase (b) of the experiment as it is the main interest of the research. In phase (b) the effectiveness of current methods for LNG spill mitigations such as water curtains were studied. Three spray nozzles already installed in the south-west side of the LNG training field, were used in the. These spray nozzle heads produce flat fan patterned water spray. They are called “Hydoshield HSC” and are manufactured by Angus (Fig. 21).

Fig. 21. Angus Hydroshield HSC water spray head.

3.3.1.2 Setup

The effect of the mitigation systems in changing the methane concentration in the cloud (%LFL levels) were studied by detecting the gas concentrations downwind of the cloud before and after the activation of the mitigation system. Sixteen "Searchpoint Optima Plus" hydrocarbon point gas detectors were used for the gas detection purpose. Eight tripod poles were used to mount the detectors and on each pole, two detectors were mounted at 0.3m (1ft) and 1.2m (4ft) elevations. The poles were arranged at different downwind distance from the spill area during the experiment. The measurement range of these point gas detectors is 0-100 %LFL of LNG (/methane) concentration. Two additional hydrocarbon point gas detectors were placed at a higher elevation above the water surface. The experimental setup for this phase is shown in Fig. 22 and Table 4 shows the gas detector identification number (ID) on each tripod pole.

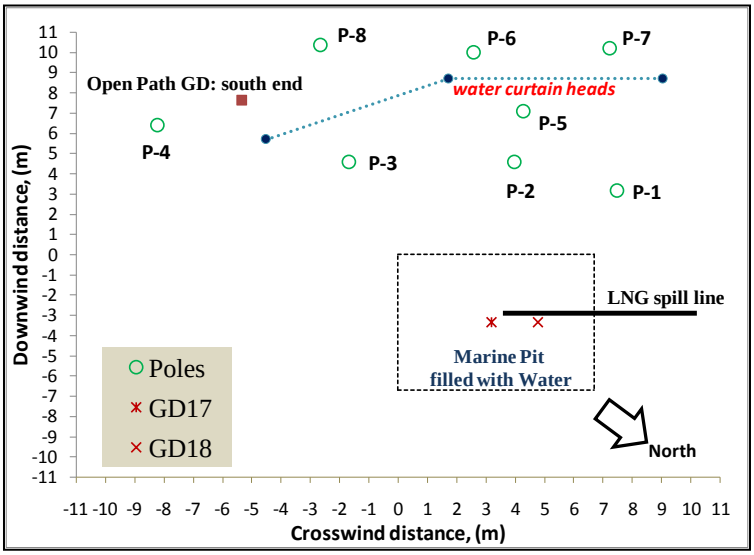

Fig. 22. Setup of 2006 experiment.

Table 4. Location of gas detectors on poles: 2006 experiment.

Pole ID	Gas Detector (GD) ID	
	Elevation =0.3m	Elevation =1.2m
1	15	16
2	14	13
3	6	5
4	2	1
5	12	11
6	8	7
7	10	9
8	4	3

The fixed open path gas detectors installed in the LNG field were also used in the experiment. Fig. 23 below shows the location of the fixed open path gas detectors in the field.

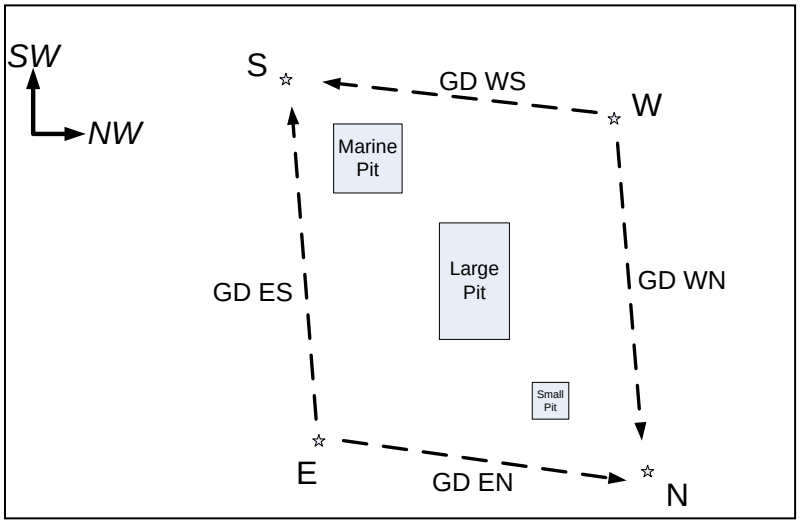

Fig. 23. Location and ID of the four open path gas detectors (E, N, W and S).

3.3.1.3 Procedure

In the experiment, LNG was spilled on water surface at low flow rate and vapor cloud concentrations were measured in both upwind and downwind locations of the water curtain region, without and with spray activation. Other than gas concentration, LNG pool temperature and weather data were also recorded. A weather station, provided by Texas Mesonet at TAMU, was used to measure wind direction and wind speed at two heights of 2 and 10 meters. The weather station was mounted on the south-east side of the LNG test facility boundary. Humidity and atmospheric pressure data were collected as well. The weather data were collected and stored every three seconds.

3.3.2 Experiments: November 2007 and March 2008

3.3.2.1 General Description

Two sets of similar outdoor spill experiments were conducted on November 16, 2007 and March 25, 2008. Both of the experimental sets were conducted on the flat concrete ground of the north-east side of the Marine Pit, by spilling LNG on concrete. In each set of experiments multiple tests were conducted. The scenario of continuous LNG flow through a pipe on the concrete ground was simulated in both the experiments by supplying LNG continuously from a tanker truck to the spill location with a flexible discharge hose connected to the insulated, fixed Aluminium pipe line. One cryogenic volumetric flow meter was installed close to the truck to measure LNG flow rate. Fig. 24 shows the location of these tests.

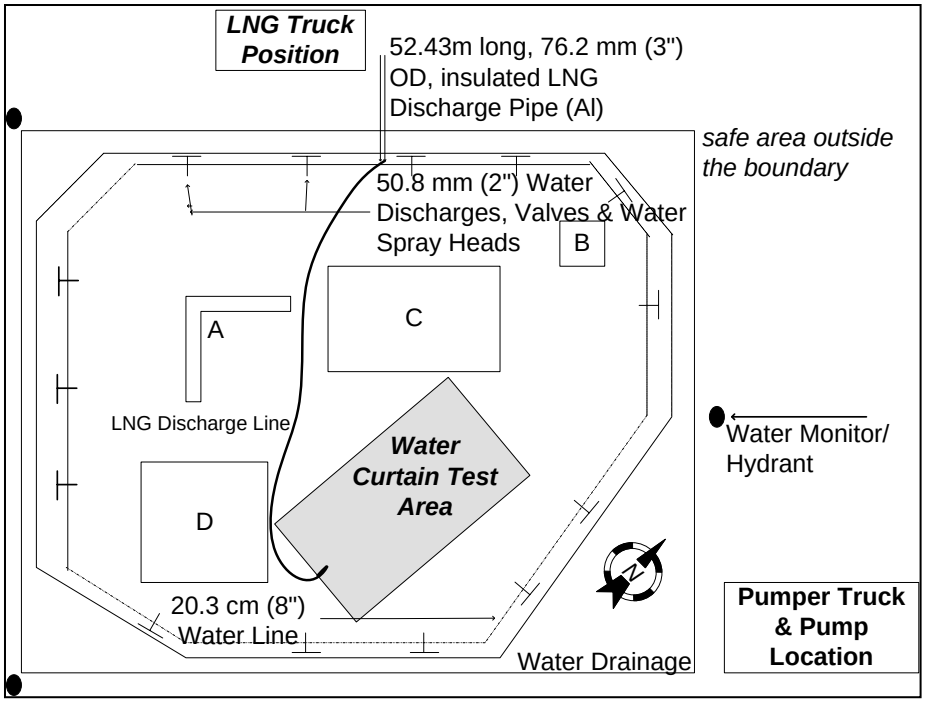

Fig. 24. Location of 2007 and 2008 experiments. Reprinted from Rana et al. (2008).

Two types of portable upward directed spray curtains were employed in both the experiments. One was constructed with several 60º full cone, spiral, (1-inch) nozzles installed on a carbon steel pipe. These nozzles are manufactured by BETE Fog Nozzles. The other one was Angus Hydroshield HSC 180º flat fan spray head. This portable water curtain device is available through the Brayton Fire School. During the experiments, the water curtains were placed at specific downwind distances from the LNG spill, allowing some free area between the spill location and the water curtain. Water was supplied from the water line to the water spray curtain with 64 mm (2.5 inch) OD fire hoses. Flow meters and pressure gages were connected at the exit of the fire hose to measure the volumetric flow rate and pressure of water at the inlet of the curtain during the tests.

Water flow was turned on and off with ball valves connected to the water supply line. Fig. 25 shows the photographs of the water curtains used the experiments.

Fig. 25. Photographs of water spray nozzles used in 2007 and 2008. Left: full cone spray nozzle, right: flat fan spray nozzle. Reprinted from Rana et al. (2009).

In 2007, the LNG spill area was enclosed with 1.52m × 1.52m (5ft × 5ft) inner and 1.83m × 1.83m (6ft × 6ft) outer wooden frames. The space between the frames was filled with wet sand during the tests. The intention of using wet sand was that when LNG contacted wet sand it would freeze immediately and stop liquid LNG flow out of the spill area through the gaps. LNG was discharged at the spill location with a flexible discharge hose (15.2 m long, 7.6 cm OD), connected to the 52.4 m long pipe line from the tanker truck. Fig. 26 shows the photograph of the enclosed spill area.

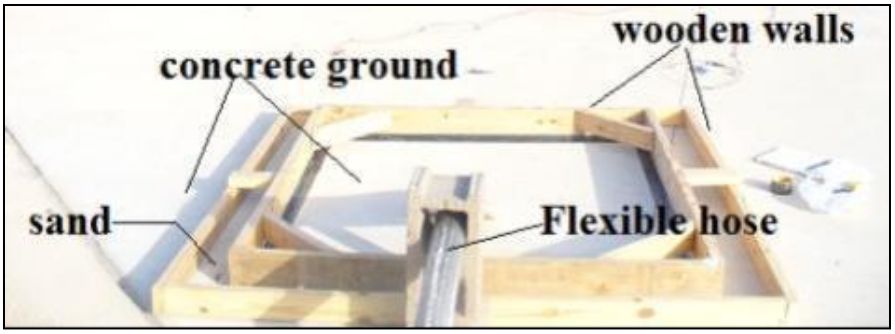

Fig. 26. Enclosed spill area in 2007 experiment.

In 2008, LNG spill location area was changed to a square shaped enclosed box. The spill box was a 1.52m × 1.52m × 0.152m (5ft × 5ft × 6in) box with 1.52m × 0.152m wooden frames as the side walls and 2 inch thick concrete as the base. In this test, LNG was discharged inside the spill box with an insulated L-shaped discharge pipe (18 cm ID 2.1 m long) connected to the Aluminium pipe line (52.4 m long and 10.16 cm OD). Fig. 27 shows a photograph of the enclosed spill area for 2008 experiment.

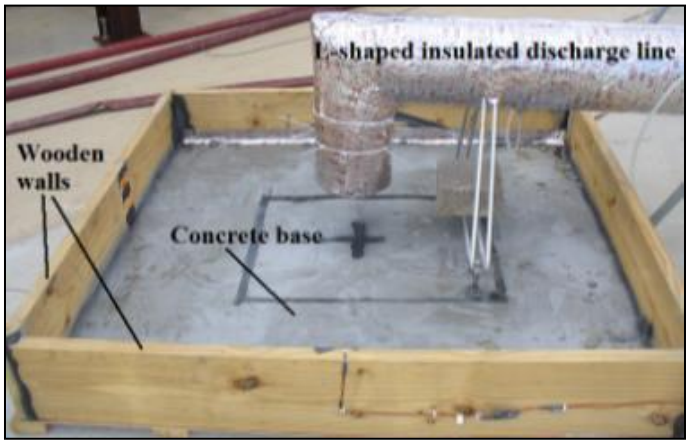

Fig. 27. Enclosed spill area in 2008 experiment.

3.3.2.2 Setup

The effect of the mitigation systems in changing the methane concentration (% v/v) and temperature in the cloud were studied by detecting the concentrations and temperature downwind of the cloud before and after the activation of the water curtains. In 2007, 34 IR point gas detectors and 32 type K thermocouples were used and installed on 14 tripods at different heights to measure the methane gas concentration at 0.5 m, 1.2 m and 2.1 m elevations and temperature of air-methane mixture at 0.5 m, 1.0 m and 2.0 m elevations. The sensor placement heights were chosen on the basis of prior simulation and previous research. During the tests, the tripods were placed at different downwind and crosswind distances from the LNG spill area to measure the concentration and temperature both up and downstream of the water curtain. The instruments were placed according to the predicted wind direction of the experiment day. The water curtain was positioned downwind from the spill area and the location was identified considering the flow pattern of full cone nozzles to avoid any water spillage onto the LNG spill area during tests. One cryogenic turbine meter, two flow sensors, two pressure transducers and three weather stations were the other major equipment used in tests. Fig. 28 shows tripod and water curtain placements during the 2007 tests.

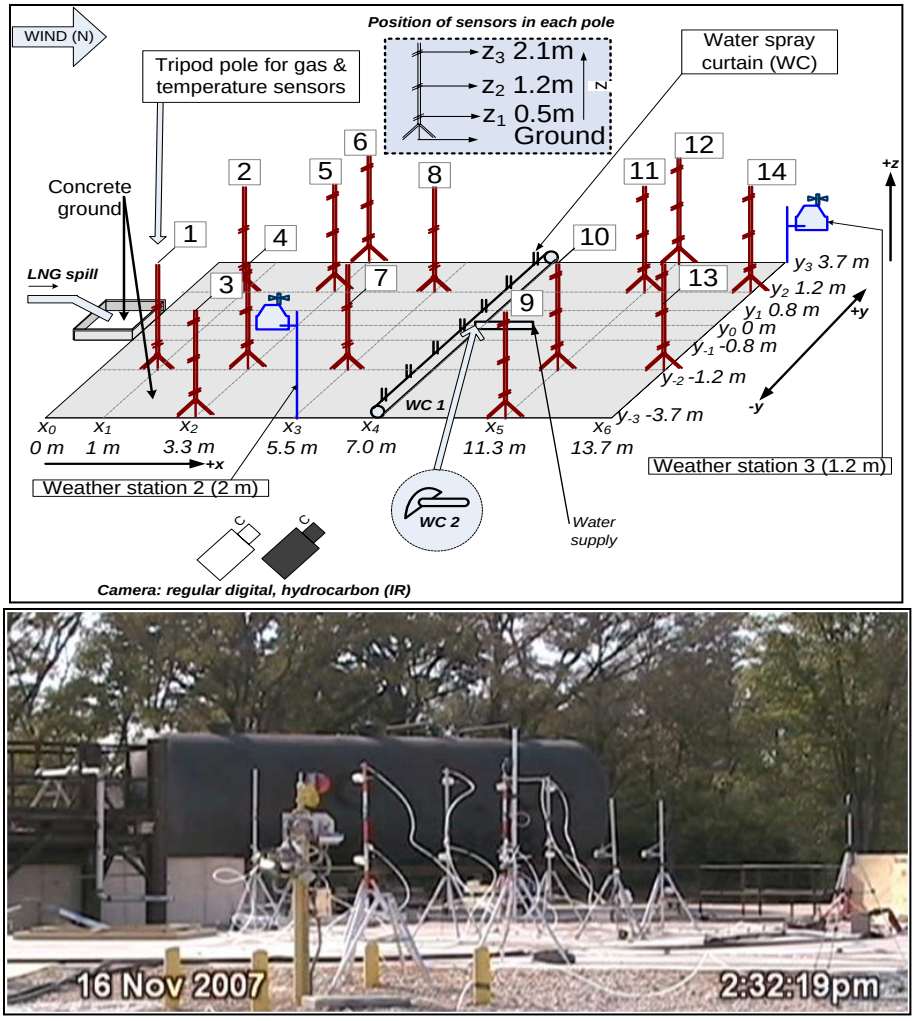

Fig. 28. Overall setup of 2007 experiment. Top: schematic, bottom: photograph. Reprinted from Rana et al. (2009).

The wind velocity, direction, temperature, humidity and heat index were measured in 2007 with three weather stations. Two stations were placed in two separate positions, 2.1m above ground-level and the third was installed around 15.2 m east of the test ground at 9.1 m height. Hydrocarbon and IR cameras were used to observe the actual dispersion of invisible flammable hydrocarbons (mainly methane). The cameras

were positioned at 90º to each other, so that they can capture the whole dispersion process during the tests.

The detectors were not physically installed on the tripods, but were installed in a wooden vacuum chamber. Teflon tubes were used for the purpose of flowing methane from the field to the detectors. One end of each tube was connected to a gas detector and the other end was placed on the tripod pole. A vacuum pump was used to pull LNG vapors at 0.3 l/min to the detector through the tubes and then released to the environment. Table 5 shows the position of tripod poles and gas detectors and temperature sensors on those poles.

Experiment of 2008 experiment was a repetition of previous experiment with some modification in the spill location, LNG discharge pipe and water curtain pipe design. In 2008, 40 IR point gas detectors and 43 type K thermocouples were used and installed on 14 tripods at different heights to measure the methane gas concentration and temperature of air-methane mixture at 0.5m, 1.2m, 2.1m and 3.4m above ground. Like the previous year's experiments, the detectors were not actually installed on the tripods. Gas detectors were placed in a steel cabinet in 2008 experiments instead of a wooden chamber.

Table 5. Location of tripod poles and positions of gas detectors and thermocouples on poles: 2007 experiment.

Pole no.	Downwind position, x (m)	Crosswind position, y (m)	Gas Detector ID (GD #)			Thermocouple ID (TG #)		
			Elevation, z (m)			Elevation, z (m)		
			0.5	1.2	2.1	0.5	1.2	2.1
1	1	-1.2	22	21	---	3	4	---
2		1.2	24	23	---	1	2	---
3	3.3	-3.7	25	26	36	5	6	7
4		-1.2	27	28	35	8	9	10
5		1.2	30	29	39	11	12	13
6		3.7	38	37	40	14	15	16
7	5.5	-1.2	---	---	---	29	30	---
8		1.2	---	---	---	31	32	---
9	11.3	-3.7	13	12	11	17	18	19
10		-1.2	01	15	07	20	21	22
11		1.2	19	18	17	23	24	25
12		3.7	20	02	10	26	27	28
13	13.7	-1.2	06	34	04	---	---	---
14		1.2	08	32	31	---	---	---

Fig. 29 shows the experimental set up and the sensors, detectors and water curtain placements for 2008 experiment. The figure is followed by Table 6, which shows the position of tripod poles and gas detectors and temperature sensors heights on the poles.

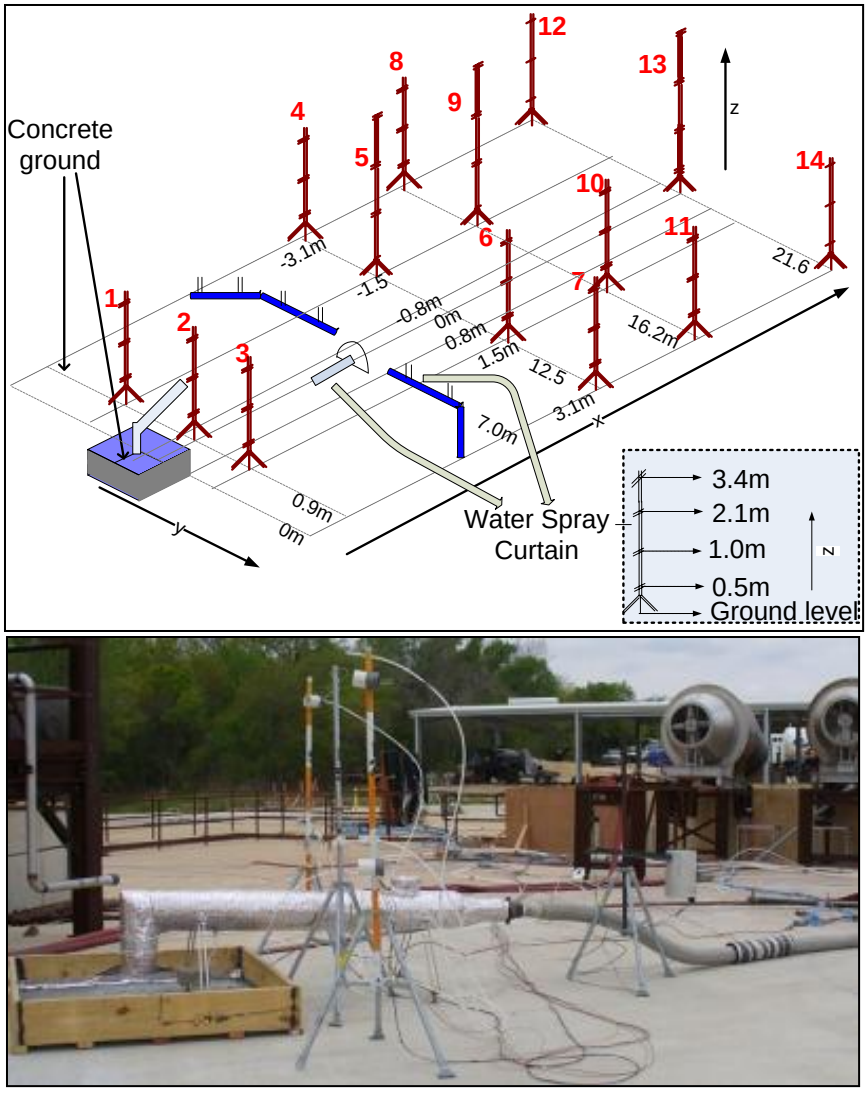

Fig. 29. Overall setup of 2008 experiment. Top: schematic, bottom: photograph.

Table 6. Location of tripod poles and positions of gas detectors and thermocouples on poles: 2008 experiment.

Pole no	Downwind position, x (m)	Crosswind position, y (m)	Thermocouple ID (TG #)				Gas Detector ID (GD #)			
			Elevation, z (m)				Elevation=z (m)			
			3.4	2.1	1.0	0.5	3.4	2.1	1.0	0.5
1	0.9	-1.5	-	38	39	40	-	2	4	3
2		0	-	42	43	41	-	-	-	-
3		1.5	-	37	36	35	-	8	7	9
4	12.5	-3.1	-	10	9	8	-	6	10	5
5		-1.5	1	34	33	-	27	28	29	-
6		1.5	-	25	27	26	-	16	14	15
7		3.1	-	19	21	20	-	11	12	13
8	16.2	-3.1	-	6	7	5	-	22	26	25
9		-1.5	3	4	2	-	20	19	1	-
10		1.5	-	24	23	22	-	24	21	23
11		3.1	-	30	28	29	-	18	17	30
12	21.6	-1.5	-	32	31	14	-	31	33	32
13		0	15	13	11	18	34	40	37	36
14		1.5	-	17	16	12	-	38	35	39

To measure the evaporation of LNG, five N-type thermocouples were installed in the spill area (box) inside the concrete, in 2008. Fig. 30 shows the thermocouple set up diagram.

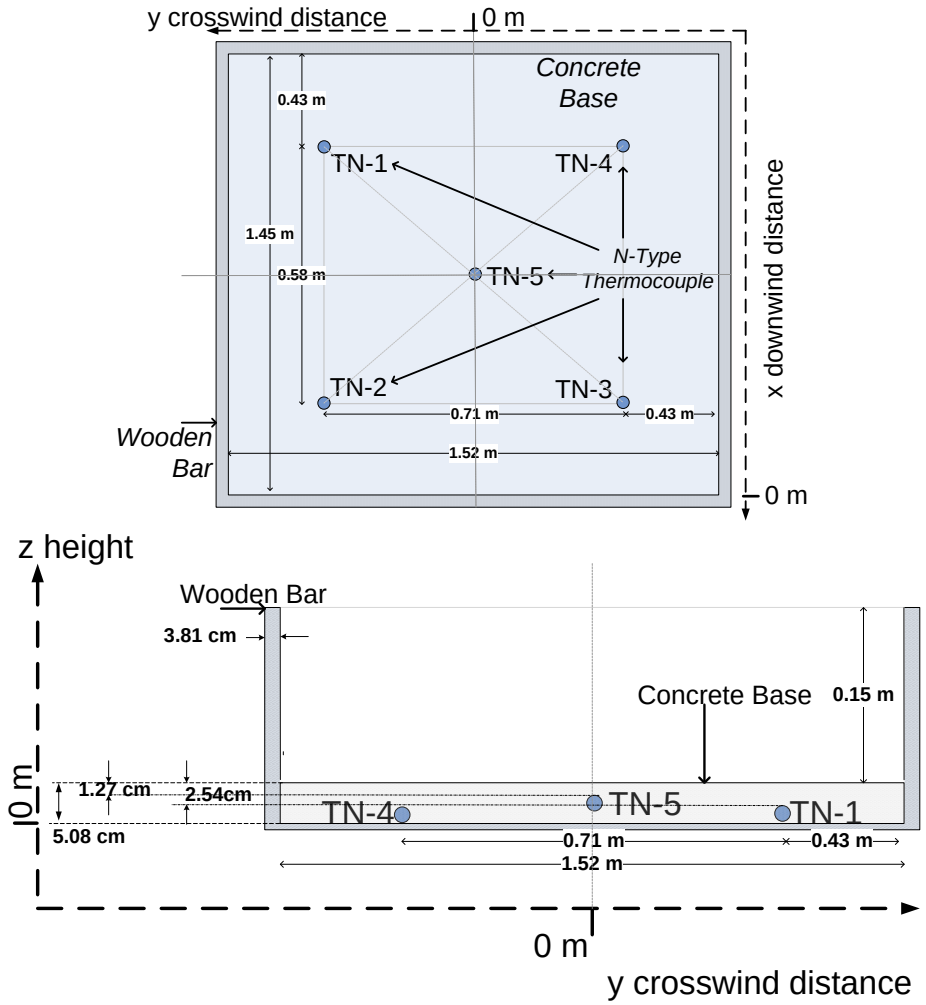

Fig. 30. Thermocouple placement inside the concrete base for 2008 experiment. Top: top view, bottom: side view.

3.3.2.3 Procedure

Four similar spill tests were conducted in 2007 to evaluate the effectiveness of two types of water spray curtains in controlling an LNG vapor cloud. Each curtain was tested twice with a separate spill. The first two tests were conducted with a full cone

spray curtain. Then it was replaced with the Hydro-Shield flat fan spray and two more similar tests were conducted.

Each test started with continuous release of liquid LNG onto the enclosed spill area. Initially only LNG vapor started to emerge from the hose and within a couple of minutes liquid stared to flow from the hose. As soon as the liquid touched the concrete ground it vaporized and dispersed naturally towards the prevailing wind direction. Several minutes after start of the LNG release, the water spray curtain was turned on to disperse the cloud forcefully. The flow of LNG was also continued for a few minutes during forced dispersion. When the LNG pool reached about 5 cm to 8 cm (2" to 3") height, the LNG flow was turned off while continuing the water curtain operation. The curtain was kept on until the visible white cloud disappeared.

In 2008, experiments started with continuous release of liquid LNG onto the enclosed spill area (box). Spill was continued for several minutes and when there was a liquid pool in the spill area, the LNG release discontinued. Natural dispersion data were collected during the whole time. In this natural dispersion test none of the water curtains were used. After the natural dispersion test, tests with the full cone water curtains started. LNG was again spilled in the spill box and several minutes after the start of the LNG release, the full cone water spray curtain was turned on to disperse the cloud. The flow of LNG was also continued for a few minutes during the forced dispersion by water curtain. The LNG flow was turned off after several minutes while continuing the water curtain operation. The curtain was kept on until the visible white cloud disappeared. The last test was with the fan type curtain and the procedure was similar to the second test.

3.3.3 Experiment: March 2009

3.3.3.1 General Description

The fourth LNG spill experiment was performed on March 5, 2009. This time the Pit 1 (3.05 m × 3.05 m × 1.22 m) was filled with water up to 1.2 m and LNG was spilled on top of the water surface. LNG was spilled on water to create steadier vapor flow from the spill area. To confine the LNG spill to a smaller area, four wooden frames were used to make an enclosed area of dimension 1.52 m × 1.52 m × 0.31 m on the water. LNG was discharged at the spill location with the similar pipe line configuration used in 2008 experiment. The two sides of LNG spill area and LNG vapor path were blocked with 1.2 m high wooden walls to guide the vapor straight to the water curtain by preventing LNG vapor to drift crosswind. Fig. 31 shows the photographs of the enclosed spill area.

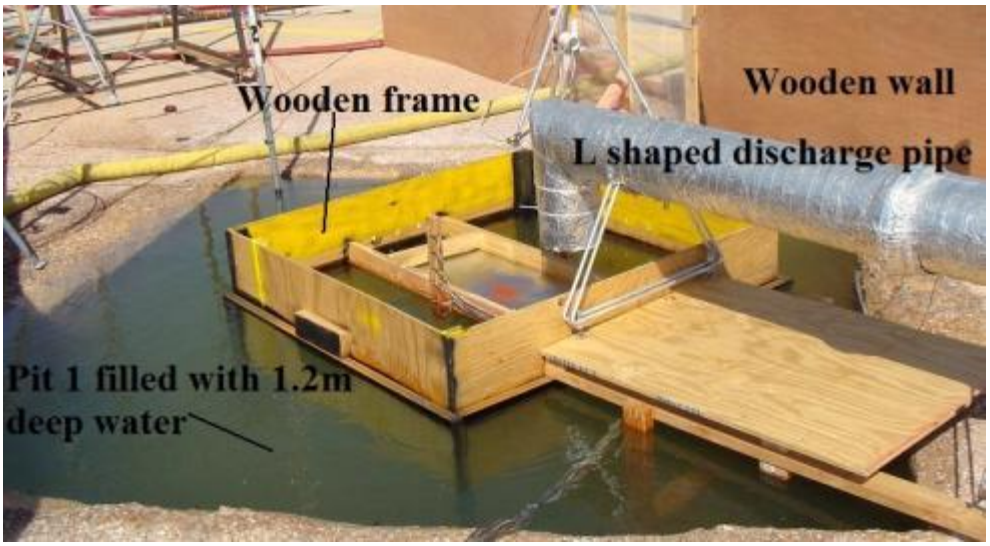

Fig. 31. Spill area of 2009 experiment.

Three types of portable spray curtains were employed. Two of them were the similar upward directed water curtains used in previous experiment of 2008 and the third one was a downward spray which produces much smaller droplets. The downward spray was constructed with six spray nozzles (½-inch TF 24 NN BETE Fog Nozzles) installed at 3.05 m height. Each of these nozzles produces 60º full cone type spray and its working pressure and flow rate were much lower than the other two types. So the nozzles of this water curtain are named here mist full cone nozzles.

3.3.3.2 Setup

36 IR point gas detectors were used and installed on several tripods at different heights to measure the methane gas concentration at 0.5 m, 1.0 m and 2.0 m above ground. Four portable LFL gas meters were also used to identify LFL distance far downwind from the spill area. The heights were chosen based on the previous research. Six type-K thermocouples were installed to measure the water curtain temperature at three different heights. Fig. 32 shows the experimental set up of 2009 experiment.

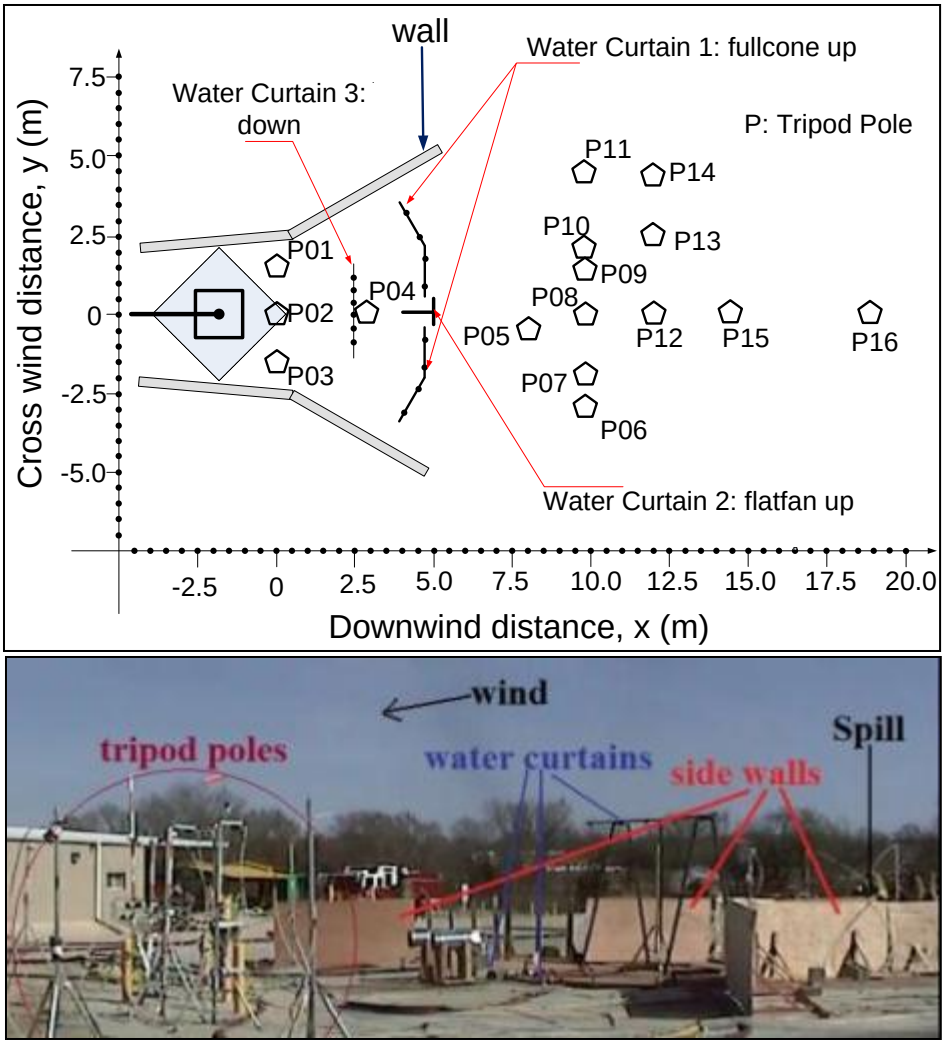

Fig. 32. Overall setup of 2009 experiment. Top: schematic, bottom: photograph.

Table 7 shows the positions of tripod poles and gas detectors and temperature sensors' locations on the tripod poles. Table 8 shows the position of the water curtains.

Table 7. Location of tripod poles and positions of gas detectors and thermocouples on poles: 2009 experiment.

Pole no.	Downwind position, x (m)	Crosswind position, y (m)	Gas Detector ID (GD #)			Thermocouple ID (TG #)		
			Elevation, z (m)			Elevation, z (m)		
			0.5	1.2	2.1	0.5	1.2	2.1
1	0	1.5	1	2	3	--	--	--
2		0	11	8	7	--	--	--
3		-1.5	14	12	13	--	--	--
4	2.6	0	--	--	--	1	2	3
5	8	-0.5	33	--	32	31	32	33
6	9.7	-3	37	34	35	--	--	--
7		-2	16	36	4	--	--	--
8		0	22	24	23	--	--	--
9		1.3	39	26	29	--	--	--
10		2	40	25	10	--	--	--
11		4.4	28	31	9	--	--	--
12	12	0	17	--	18	--	--	--
13		2.5	19	--	30	--	--	--
14		4.4	20	38	27	--	--	--
15	14.4	0	Port* 02	Port 03	Port 04	--	--	--
16	18.7	0	Port0 1	--	--	--	--	--

*Port #: portable gas detector (LFL meters) identification number.

Table 8. Location of the water curtains: 2009 experiment.

Water Curtain	Downwind distance , x (m)
Full cone upward water curtain	4.75
Flat fan upward water curtain	5
Mist type full cone downward water curtain	2.5

Twelve K-type thermocouples were installed in the spill area in two bars to measure the evaporation rate of LNG. Each bar contained six thermocouples and

distance between two adjacent thermocouples was 3.175 cm (1.25 in). These thermocouples were installed to cover both under and above the water surface temperature. Fig. 33 shows the thermocouple set up diagram.

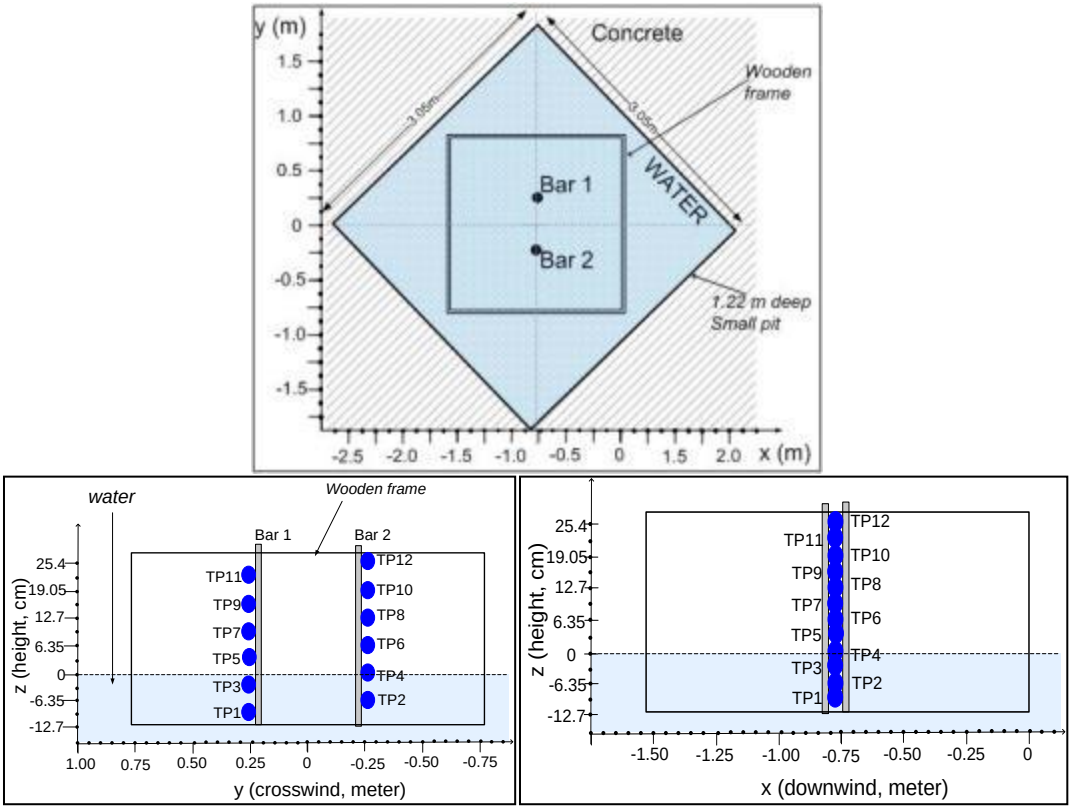

Fig. 33. Thermocouple placement inside the spill area for 2009 experiment. Top: top view, bottom: side views.

3.3.3.3 Procedure

Test started with continuous release of liquid LNG onto the water surface. Spill was continued for several minutes and natural dispersion data were collected during this time. As no water curtains were used in the first test, it is called natural dispersion test.

Continuing the natural dispersion test for several minutes the tests with the water curtains started. The water curtain tested first was the full cone water curtain. The water curtain test procedure was similar to previous years' tests: at first LNG was released continuously, then after several minutes the water curtain was turned on. Full cone curtain test was followed by two more tests with flat fan and mist cone water sprays with similar procedure. After testing the mist cone spray, a final test was conducted by activating all of the curtains altogether. The intention of this test was to observe the effects of the combined curtains on LNG vapor cloud. During the whole test period LNG spill was turned on and off to maintain a steady flow from the pool.

3.4 Equipment and Data Acquisition

Gas concentration, gas, water curtain and spill surface temperature, LNG and water flow rate and water pressure were measured in the experiments with multiple gas detectors, K and N type thermocouples, cryogenic and regular flow sensors and pressure transducers. Table 9 shows the list of equipment used in the experiments.

Table 9. Types of equipment used in the experiments.

Measurement	Equipment	Experiment
Gas concentration	Gas detector (%LFL/m) Gas detector (%LFL) Gas detector (% v/v) Port detector (%LFL)	2006 2006 2007-2009 2009
Gas temperature	Type K-thermocouple	2007-2009
Water curtain temperature	Type K-thermocouple	2007-2009
Spill surface temperature	Type K-thermocouple Type N-thermocouple	2009 2008
LNG flow	Cryogenic flow meter (volumetric)	2007-2009
Water flow	Regular flow sensor (volumetric)	2007-2009
Water pressure	Pressure transducer	2007-2009
Weather	Weather station Anemometer	2006-2009 2007-2009

3.4.1 Gas Detection

Four different types of gas detectors were used to measure methane gas concentration in the air in different experiment. The detectors are IR open path detectors, IR point gas detectors (%LEL), IR point gas detectors (% v/v) and portable gas detectors. The IR open path detectors were only used in 2006 experiment and information about the detectors are already provided in section 3.2. The IR point gas detectors (%LEL) and (% v/v) are actually similar type detectors only deference is in their measurement range. In 2006 experiment the measurement unit of % LEL (methane) was used and in rest of the experiments, multiple IR point gas detectors in the measurement unit of 0-100% v/v (methane) were used. These detectors are “Searchpoint Optima Plus Infrared Pint Gas detector” by Honeywell Analytic. They are designed for use in potentially hazardous areas where it provides gas and vapor detection which is free from poisoning and independent of the presence of oxygen. Searchpoint optima plus

is a micro-processor controlled, infrared gas detector with comprehensive built-in self diagnostic and fault finding facilities. It produces output signal of 4 – 20 mA with power requirement of 5 watts per detector (Honeywell, 2005).

The “Searchpoint Optima Plus” is originally designed for industrial application where detecting methane leak and its concentration in the range of 0% volume by volume (v/v) to 5% v/v (Low flammability level, LFL) is important. Since the experiment is to measure the methane concentration up to 100 % v/v, “Searchpoint Optima Plus” was be modified to measure 0% v/v to 100% v/v methane concentration. The application of this modified point gas detectors required the suction of methane gas sample by using vacuum into the detector gas cell. This cell is able to measure high concentration methane gas. While it is possible to install them directly at the field for the experiment, this configuration is not very flexible due to the size and the weight of detectors. Again as LNG vapor dispersion movement is very dynamic depending the wind speed and direction, the detector set up needs to be flexible to relocate easily depending on the wind direction during an experiment. So it is recommended to gather all “Searchpoint Optima Plus” in one place and then pull the measurement gas from different location with tubes into the detectors (Suardin, 2008). To reduce the uncertainty, each “Searchpoint Optima Plus” should be connected with the same type and length of tubing. That is why, though the detectors were placed in the gas cloud in the 2006 experiment, the detectors were not physically placed in the gas cloud in other experiments. They were installed in a wooden vacuum chamber (in 2007) or metal cabinet away from the gas cloud. Teflon tubes were used for the purpose of flowing

methane from the field to the detectors. One end of each tube was connected to a gas detector and the other end was placed on the tripod pole in the field. A vacuum pump was used to draw LNG vapors at 0.3 l/min to the detector through the tubes and then released to the environment. Fig. 34 and Fig. 35 show the gas detector connection and photograph of detector chambers.

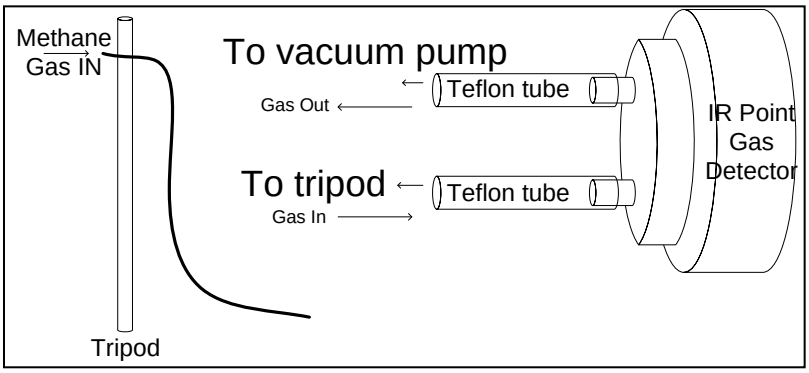

Fig. 34. IR gas detector-Teflon tube connection.

Fig. 35. Gas detector installation in chambers. Left: 2007 experiment, right: 2008 & 2009 experiments.

Four portable gas detectors (MiniMax X4) manufactured by Honeywell Analytics were also used in 2009 experiments. The application of these detectors is to measure gas concentration at a certain point where the point gas detectors are not available as well as for the safety of the person conducting the experiment. MiniMax X4 has the capability to store data using a regular memory card and the data can be retrieved later. These detectors measure methane concentration in 0-5% v/v level (% LEL).

3.4.2 Temperature Measurement

Temperature measurement was conducted by using K and N type thermocouples. The type-K thermocouples, manufactured by Omega Engineering, were used to measure gas temperature. These thermocouples are capable of measuring temperature as low as 173K (-100ºC) up to 373K (100ºC). Gas temperature measurement also required the protection of the thermocouples from the surrounding, e.g. heat from the sun, wind, etc. Thus, partial enclosure was provided around the thermocouples installed in the tripod pole. N type thermocouples, also manufactured by Omega Engineering, were used to measure cryogenic temperature as this type of thermocouple is more stable at extreme temperature. The application includes the measurement of LNG pool spreading on water.

3.4.3 Flow and Pressure Measurement

Two types of flow meters were used in the experiments to measure volumetric flow rate. The LNG flow rate was continuously measured with a cryogenic flow meter connected between the pipe line and the discharge hose during the tests. The cryogenic

flow meter used was a 3-inch FTB-911 turbine meter with male NPT end fittings. It is recommended that the meter should be placed at the beginning of the discharge pipeline. As some of the LNG release from the truck might flash at the end of the pipe and produced two phase flow, installing it at the end of the pipe may cause the measurement of both liquid and vapor thus giving incorrect reading.

Water was supplied from the water line to the water spray curtain with 6.4 cm (2½") OD fire hose. For the measurement of non-cryogenic liquid, e.g. water supply for water curtains, non-cryogenic volumetric flow meters, FP-2540 stainless steel flow-meter was used. DPG1000 series pressure was used for the purpose of measuring water pressure. Both FP-2540 and DPG1000 produce 4-20 mA output. Flow meters and pressure transducers were connected at the exit of the fire hose to measure the water flow rate and water pressure at the inlet of the curtain during the tests. Water flow was turned on and off with the ball valve already connected to the water supply line.

3.4.4 Weather Monitor

The meteorological conditions were measured with multiple weather stations. Purpose of these stations was to measure the wind velocity, direction, temperature, humidity and heat index. Weather stations manufactured by Davis Instruments were used in 2007 to 2009 experiments. The wind speed at the test field was measured with commercially available three axis cup and vane anemometers. This product is also manufactured by available at Davis Instruments or at Campbell Science Inc. This type of

anemometer measures the wind speed directly without any signal conditioning. Signal is then sent to computer using cable or built in wireless system.

3.4.5 Imaging

Hydrocarbon (H/C), IR and regular digital cameras were used in 2007, 208 and 2009 experiments to capture the experiments. The hydrocarbon and IR cameras were used to observe the actual dispersion of invisible flammable hydrocarbons (mainly methane). All of the cameras were placed away at a safer location from the visible cloud region. Two H/C cameras were positioned at 90º to each other, so that they can capture the whole dispersion process during the tests.

3.4.6 Data Acquisition

Gas detector, temperature sensor, flow meter and pressure gauge data were acquired at an interval of 1 second with an Ethernet based data acquisition system and recorded simultaneously in computers. The experiments form 2007-2009 utilized one data acquisition system (DAS) with the exception of the weather station and hydrocarbon imaging cameras. DaqScan 2005 data acquisition system, manufactured by IOTECH was used. This data acquisition system is able to handle up to 896 thermocouple channels or up to 256 channels when used with other cards. As the computer was placed at safe location, far away from DAS and sensor, the chosen DAS was able to send data to computer from a long distance. The weather stations have built-

in data record system, which could save data for three days. The weather data were transferred to computers after the experiments.

3.5 Spray Nozzle Specification

Water curtains are mainly curtains of water droplets produced from spray nozzles at higher pressure. The sprays produced by a nozzle can be categorized by their shapes as conical, fans, or fogs. Conical sprays can be further broken down into either full-cone or hollow-cone sprays. In the hollow cone pattern all of the spray is located at the surface of the cone produced by the nozzle and none of it is inside the cone. In the full cone pattern the liquid being sprayed fills the cone pattern produced by the nozzle. Nozzles that spray water as a sheet of liquid produce a pattern known as a fan. The fog nozzles atomize the liquid stream into a mass of very fine droplets (CCPS, 1997).

Three types of portable curtains were used in the experiments. The first one was the flat fan spray head where water flows out through a pipe (2 inch ID) of half circular end, and hits a half circular flat metallic plate at the exit (Fig. 21) . Because of the obstacle created by the flat plate, the spray head produces 180° flat fan shaped spray pattern. This nozzle is called “Angus Hydroshield HSC”. The second one was constructed of seven or eight 1-inch 60° full cone spiral nozzles installed in a carbon pipe (2 inch ID). These nozzles are named TF 48 NN by BETE Fog Nozzles. Both of the above water curtains are vertically upward directed spray (Fig. 25). The third one was made with six ½ inch 60° full cone spiral nozzles installed in a pipe to flow downward. These are TF 24 NN nozzles by BETE Fog Nozzles. In this report these nozzles are

addresses as mist-full cone nozzles. Table 3 provides information on the types of water curtains used in the experiments.

Some of the key parameters, like (i) the flow-rate-versus-pressure characteristics of a nozzle, (ii) the droplet size produced from a nozzle, (iii) the droplet distribution in the spray area, and (iv) the coverage of the spray are very important to understand in detail the role of a spray nozzle. The volume of liquid flowing through a nozzle depends primarily on the difference in fluid pressure upstream of its orifice and the pressure into which the nozzle discharges (normally the atmosphere). Usually nozzle manufacturers provide this information as catalog flow rate table. The following equation is also used to calculate the flow rates for different pressure.

$$Flow\ rate = K\sqrt{Pressure} \tag{16}$$

Here, the factor *K* depends on the nozzle. Fig. 36 shows the flow rate versus pressure specification of each nozzle used in the experiments (Angus, 2005; BETE Fog Nozzles, 2007).

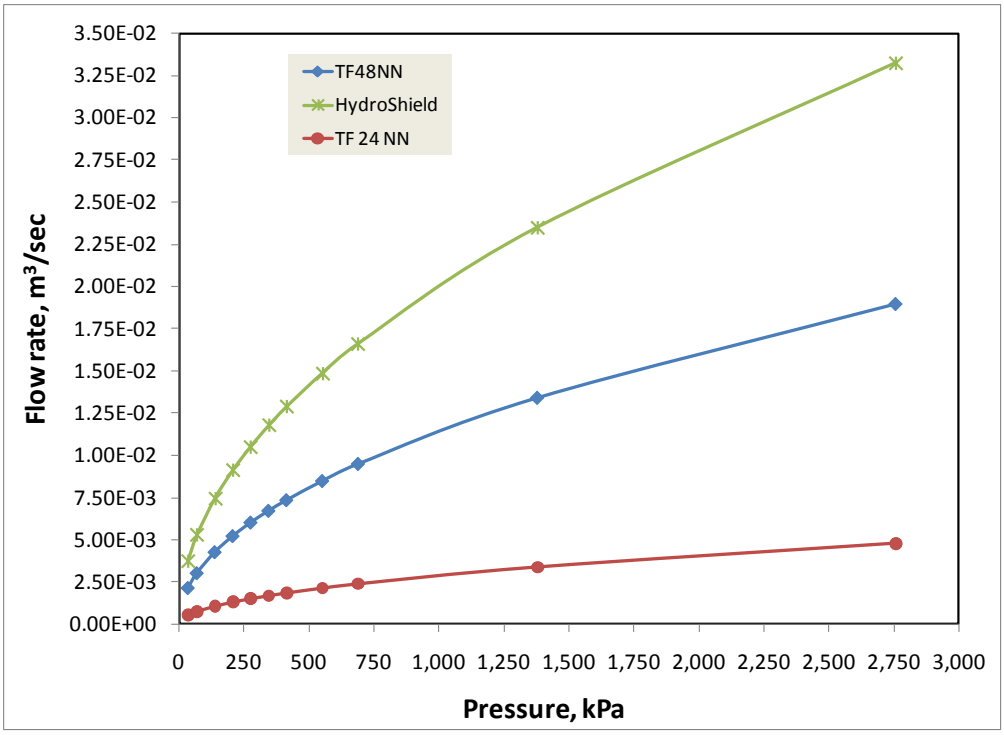

Fig. 36. Flow rate- pressure relationship of the nozzles.

The droplet size of a certain type of curtain provides a certain surface area. So the information of the size of the droplets produced by a spray nozzle is essential as it affects the action mechanisms. Usually conical sprays produce small to medium size droplets and the size of droplet produced by fan nozzles are usually coarse. The full cone nozzles (TF 48) used in the experiments can create smaller droplets of sauter mean diameter (SMD or D_{32}) of 580 microns. This SMD value is based on vendors' information which was calculated at 0 m/s wind speed and 690 kPa absolute pressure. Simulated SMD value of the mist-full cone nozzles (TF 24) is approximately 361.5 microns at 690 kPa. A nozzle actually produces a range of droplet sizes from the solid liquid stream. Since it is inconvenience to list all the sizes produced, droplet size (in

micron) is usually expressed by a mean or mean diameter. SMD or D_{32} is the diameter of a droplet whose ratio of volume to surface area is equal to that of the complete spray sample (BETE Fog Nozzles, 2007). It was observed that the drops of the flat fan spray nozzle are almost two to two and half times larger than the full cone nozzle. So in the research it is considered that the mean drop size of the flat fan nozzle is two and half time larger than the mean drop size of full cone (TF 48) nozzles. The actual drop size was not measured in the tests because of unavailability of appropriate measuring device which could be used safely outdoor conditions in the presence of a flammable vapor cloud. As the drop size depends based on pressure, the effect of a change in pressure (P) on the drop size (D) can be predicted with following equation (BETE Fog Nozzles, 2007).

$$\frac{D_2}{D_1} = \left(\frac{P_2}{P_1}\right)^{-.3} \tag{17}$$

Based on the above equation and drop size information from vendors and observation, Fig. 37 was developed to realize the effect of pressure on drop size (SMD).

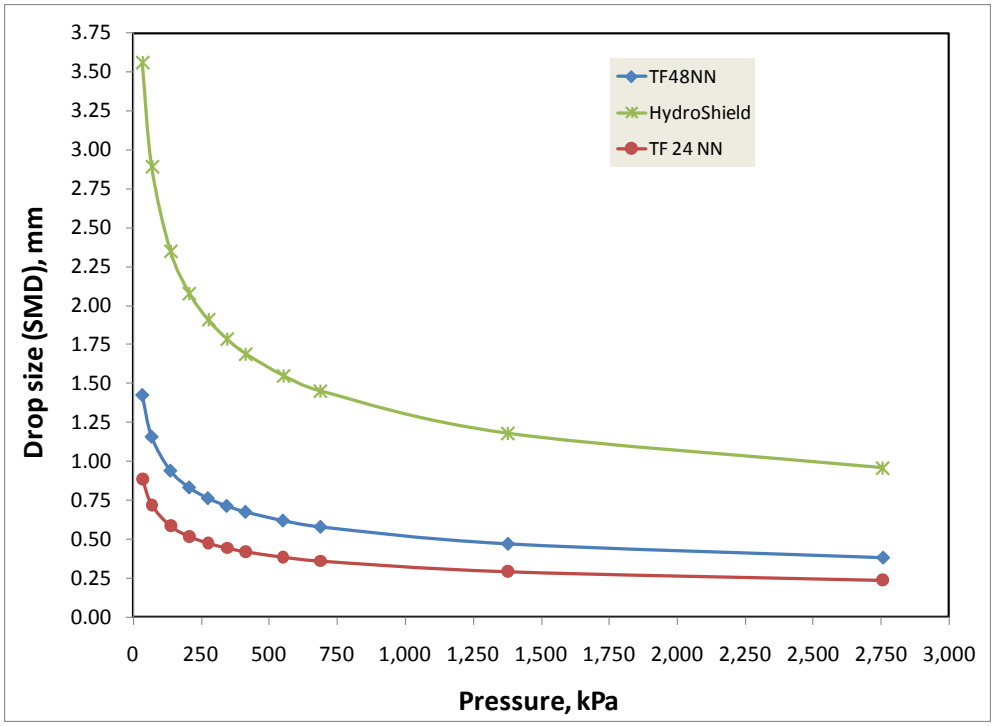

Fig. 37. Drop size (SMD) versus pressure characteristics of the nozzles.

Important information on the distribution of water density in the space and change in droplet size along the height for the used curtains cannot be determined in this research due to the unavailability of exact information. Again experimental determination of those parameters was also impossible in the tests due to the lack of appropriate measurement devices and many limitations when dealing with LNG vapor out door.

In this research, the water curtains mainly considered was upward. So the heights these water curtains covered is important to know their total coverage capability. Each of the full cone nozzles (TF 48) creates 60° flow pattern and it is capable to flow water upward as high as 4.9 m (16 ft) at 690 kPa (100 psi) and 0 m/s wind speed. In the

experiment of 2007, the water curtain created with seven TF 48 nozzles actually covered around 7 m (23 ft) wide, 2.9 m (9.5 ft) high. However in 2008 and 2009 tests eight TF 48 nozzles were used and divided into two pipes (4 on each) to get more pressure in each nozzle. This modification helped the water curtain to reach up to 3.35 m (11 ft) in 2008 and 4.57 m (15 ft) in 2009. Fig. 38 shows the simulated coverage of the full cone nozzle at 0 m/s wind speed and 690 kPa pressure.

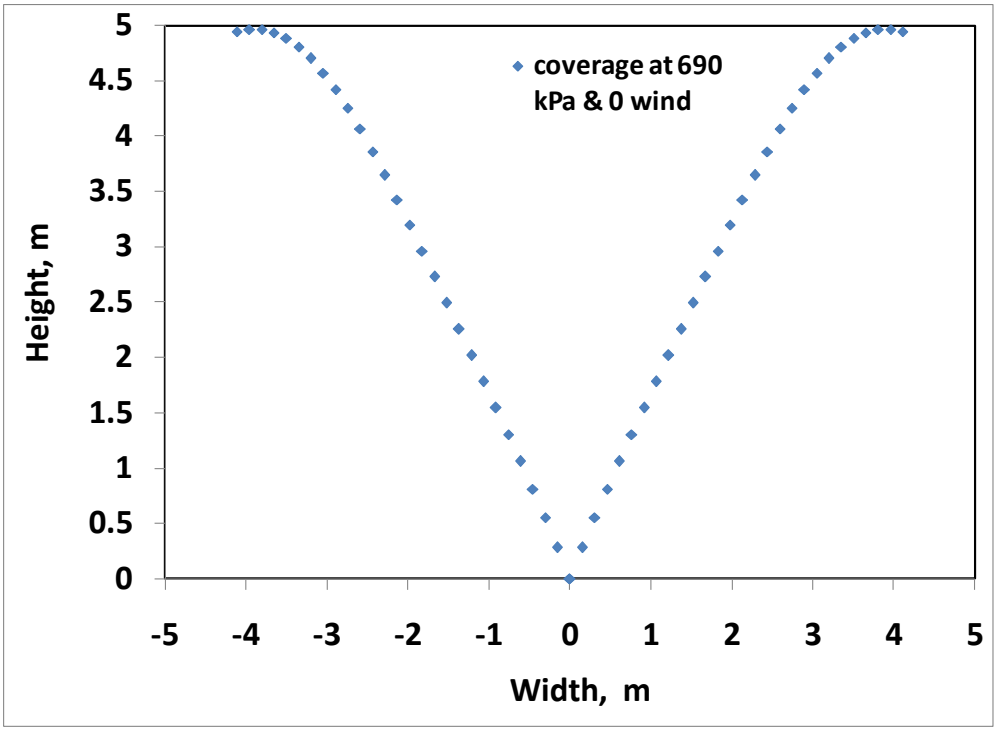

Fig. 38. Coverage of the full cone nozzle at 690 kPa pressure. Reprinted from Rana et al. (2009).

The fan nozzle creates 180° flat flow pattern. According to product specification this device is capable of projecting a fan shaped water curtain covering about 22 m

crosswind distance and 6 m height at 600 kPa (Angus, 2005). Basically it forms sheets of water and produces 0.5-1.5 m wide curtain which does not vary that much with height at low wind speed. So its width can be considered as flat rectangular shape. Note that the water curtain actually produced around 15.2 m (50ft) crosswind and 6.0 m (20 ft) high coverage in the experiments. Fig. 39 shows the simulated coverage of the flat fan nozzle at two different pressures.

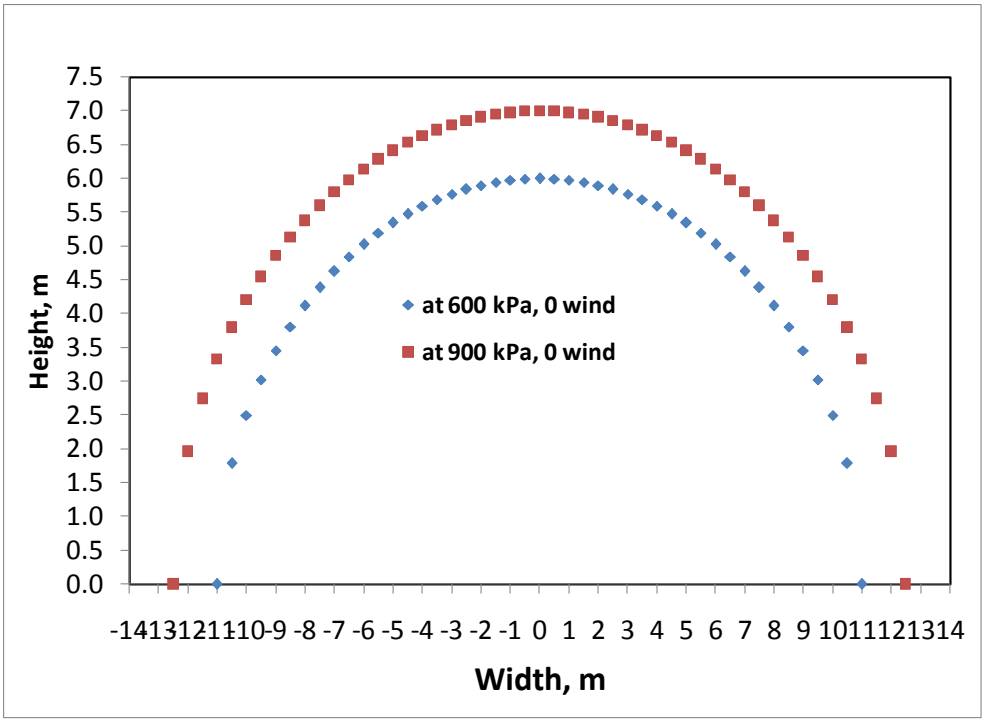

Fig. 39. Coverage of flat fan nozzle at two pressures.

Upward momentum at each of the nozzle tip was calculated from the nozzle flow rate versus pressure information, to understand the spray effects. Fig. 40 shows the

calculated momentum at the nozzle tips for two upward nozzles. As these curves are represents momentum at the nozzle tip (z=0), the momentum along the vertical axis would decrease with the decrease of droplet velocity. The figure also indicates that the flat fan spray is capable of imparting more momentum to any cloud than the full cone spray.

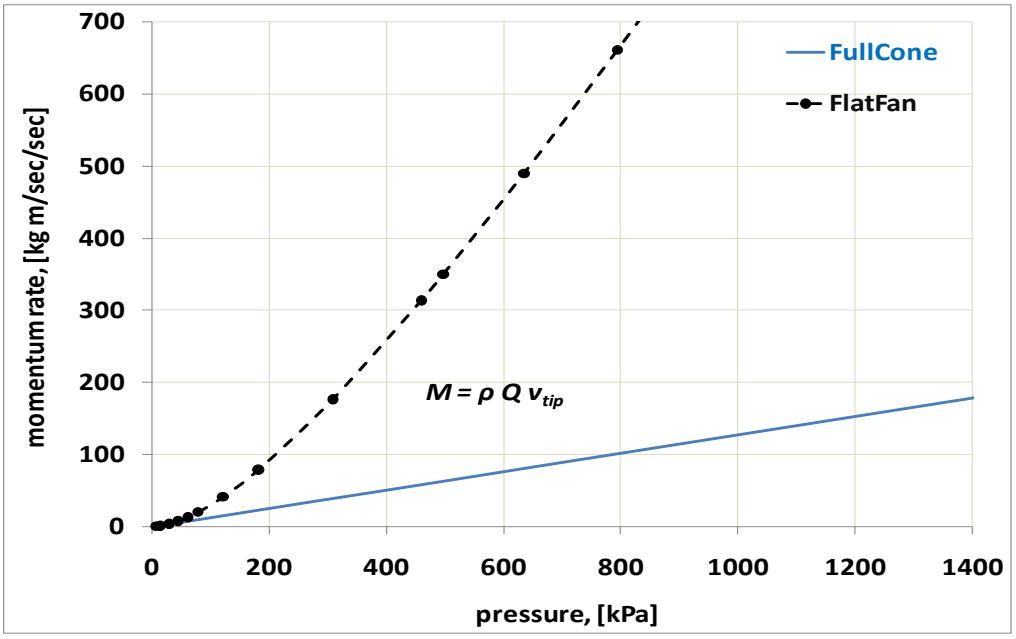

Fig. 40. Rate of momentum calculated at the nozzle tip. Reprinted from Rana et al. (2009).

3.6 Summary

Three representative water curtains were studied with real LNG spills in four sets of out-door experiments, conducted in consecutive four years, from the year 200. All of the experiments were conducted in the LNG training facility at Brayton Fire Training Field. In the experiments, LNG was released either on concrete or water surface to simulate spill from pipe and the water curtain and LNG vapor interaction phenomena was evaluated. Each experiment consists of LNG source, water curtain, placements of the measurement devices and meteorological measurements. The procedure was to create natural and forced dispersion of LNG to evaluate the effectiveness of the water spray curtain in terms of concentration and temperature change. Multiple numbers of gas detectors, thermocouples, cryogenic flow meters, regular flow meters weather stations were employed in each experiment to gather data. The types of water curtain used were: (i) upward water curtain of single/multiple 180° flat fan spray head(s) (ii) upward water curtain of multiple 60° full cone spray nozzles, and (iii) downward water curtain of 60° full cone spray nozzles. The nozzles used to make three water curtains were 2-inch Hydroshield HSC, 1-inch TF48NN spiral, and ½-inch TF24NN spiral nozzles respectively.

In 2006 experiment, LNG was spilled on large water surface to simulate LNG release on unconfined water and multiple flat fan water curtains were used to control the vapor cloud. In 2007 and 2008 experiments, LNG was spilled on concrete to simulate LNG release from pipe on ground, and fan and upward cone type water curtains were tested. The 2009 experiment evaluated all of three types of water curtains individually

and all together. LNG was spilled on confined water surface to simulate LNG spill from pipe and to produce steadier vapor cloud.

The water curtains represent three main classes of water curtains used in the industries. The ranges of water droplets generated by the nozzles are different at same gage pressure. Drop size of the upward cone spray is considered small to medium where the upward fan spray is considered to be coarse. The downward cone spray produces smaller droplets and considered as mist type drops. The coverage and imparted momentum by the two upward sprays are also different. The conical spray gives large width (downwind coverage) than the fan spray. Again the fan spray is able to impart more momentum to any cloud as because it operates at higher pressure. Thus the effects of these sprays in controlling LNG vapor clouds are expected to be different in terms of the action mechanisms.

4 STUDY OF AIR ENTRAINMENT INTO SPRAYS

4.1 Introduction

The feature of air entrainment into a water spray is considered as the major and most dominating physical action to control and disperse a hazardous vapor cloud. When water comes out from a pressurized spray nozzle, it breaks down to water droplets and thus creates a curtain of water drops. Air entrainment takes place into the spray region as a result of momentum transfer from the water droplets to the ambient air. Vapor cloud can get diluted by mixing with the entrained air when comes inside a spray. Thus entrained air, flowing inside the spray, interacting with the cloud can reduce the gas cloud concentration downstream region of the water spray (Van Doorn, 1981). Overall the mixing and dilution can result from the momentum transfer between the air, gas and water droplets.

Air entrainment is a strong function of spray configuration, droplet size, droplet velocity, and spray arrangements. Large droplets entrain less air than smaller droplets but induce better mixing and dispersion. Although smaller droplets entrain more air, they have smaller terminal velocities which are almost constant and cause poor mixing and dilution due to less turbulence. According to the design requirements, it is necessary to deliver air not only in sufficient quantity, but also at a sufficient velocity to ensure dilution (CCPS, 1997; Fthenakis, 1991).

Study of entrainment into water sprays has received much attention by the researchers. Though most of the works were focused on experimental measurements as

well as theoretical study of different types of water sprays, those were mainly for downward spray configuration. Usually downward water sprays, used for heavier than air flammable and toxic gases to contain the gas cloud in an area, stand as a barrier to a drifting gas cloud by the air vortex created by the spray and force the gas downwards (Palazzi et al., 2004). LNG vapor is initially a heavier than air vapor cloud and becomes lighter when gets diluted and warmer. For this water curtains with an upward flow might show better effectiveness to control LNG than those with a downward flow. However neither detail experimental studies nor simple entrainment models could be identified to characterize air entrainment into upward water sprays.

This study includes development of a simple air entrainment theory and theoretical estimation of entrainment velocity and volumetric entrainment rates for the upward spray nozzles used in the experiments. The basis of this theoretical study is the research reported by Heskestad et al. (1976, 1981), in which a simple physical model of air entrainment into downward conical spray in quiescent, surrounding air condition has been developed. So this study uses the similar model of Heskestad by modifying it for the upward flow. The numerical calculation procedure is developed with Visual C plus program by using 4^{th} order Ranga-Kutta method.

4.2 Simple Air Entrainment Theory

In this study estimates of air entrainment flow rate inside a spray can be obtained by examining in detail, the momentum exchange between the droplet and the surrounding air. A simple air entrainment model can be derived for a vertically upward

pointing spray by assuming: (1) one dimensional flow and air flow is incompressible, (2) spherical drop size and spray droplet size distribution is uniform, (3) aerodynamic drag on a drop is not influence by its neighboring droplets, (4) air flow in a spray cross-section is uniform; and (5) the frequency of coalescence of droplets in the spray volume is negligible. A force balance on a single drop of mass, m_d can be expressed as:

$$m_d \frac{du_d}{dt} = -m_d g - F_d \tag{18}$$

Since at steady state the velocity of the drops crossing a particular observation point does not vary in time, i.e. at fixed vertical position from the drop source (z), $u_d = u_d(z)$. Then eqn (18) can be written:

$$m_d u_d \frac{du_d}{dz} = -m_d g - F_d$$

$$\Rightarrow \frac{du_d}{dz} = -\frac{g}{u_d} - \frac{F_d}{m_d u_d} \tag{19}$$

In the air phase, the cross-sectional flux of momentum increases along the spray axis because of a steady force exerted by the droplets, generated through a nozzle. If $\dot{m}_a$ is the mass flow rate of air in any cross sectional area (A_s) of the spray, u_a is the velocity of entrained air and N_d represents the number of droplet generated per unit time at the drop source, then force exerted by the water drops:

$$\frac{d(\dot{m}_a u_a)}{dt} = F_d N_d$$

$$\Rightarrow \frac{d(\rho_a u_a^2 A_s)}{dz} = \frac{F_d N_d}{u_d} \tag{20}$$

Note that at fixed vertical position from the drop source (*z*), the local cross sectional area of spray, $A_s = A_s(z)$. In the equation the drop generation rate, N_d can be determined from the following equation:

$$N_d = \frac{Q_w \rho_w}{m_d} \tag{21}$$

The drag force per each drop can be expressed:

$$F_d = C_D A_d \left(\frac{\rho_a u_r^2}{2} \right) \tag{22}$$

In the eqn (22) A_d is the frontal area of the droplet ($A_d = \pi \frac{d_d^2}{4}$), u_r represents relative velocity ($u_r = u_d - u_a$), and C_D is the drag coefficient of spheres. C_D depends on Reynolds number (Re) and in typical sprays (Re: 10 -10000), C_D is expressed by (Heskestad et al., 1981):

$$C_D = B \,\mathrm{Re}^{\frac{-1}{2}} \tag{23}$$

where, B = 12.6 (Heskestad et al., 1981) and $\mathrm{Re} = \frac{d_d u_r}{\nu_a}$. Now substituting eqn (23) into eqn (22) gives:

$$F_d = \frac{B \nu_a^{\frac{1}{2}} \pi \rho_a d_d^{\frac{3}{2}}}{8} (u_d - u_a)^{\frac{3}{2}} \tag{24}$$

From equations (21), (24), (19) and (20), the following differential equations for the water droplet velocity (u_d) and the air velocity into the spray (u_a) can be written:

$$\frac{du_d}{dz} = -\frac{g}{u_d} - \frac{3}{4} B \nu^{\frac{1}{2}} \left(\frac{\rho_a}{\rho_w} \right) d_d^{\frac{-3}{2}} \frac{\left(u_d - u_a\right)^{\frac{3}{2}}}{u_d} \tag{25}$$

$$\frac{du_a}{dz} = -\frac{1}{2} \frac{u_a}{A_s} \frac{dA_s}{dz} + \frac{3}{8} Q_w B \nu^{\frac{1}{2}} d_d^{\frac{-3}{2}} \frac{\left(u_d - u_a\right)^{\frac{3}{2}}}{u_d u_a} \tag{26}$$

4.3 Discussion on the Equations

Integration of the above equations should provide an estimate of the air entrainment into a spray. However, equations (25) and (26) are difficult to solve analytically because the initial drop and air velocities need to be specified at a certain location near the drop source (nozzle), not exactly at the drop source. Water emerging from a spray actually does not break up into droplets at the nozzle tip. Usually flow from a nozzle can be divided into three regions. In the first region water comes and remains as solid water jet until the jet reaches a certain diameter. The second region is where the droplets are formed. Finally in the third region the flow of water drops is actually occurred. The following sketch shows conical spray pattern from a nozzle (Fig. 41).

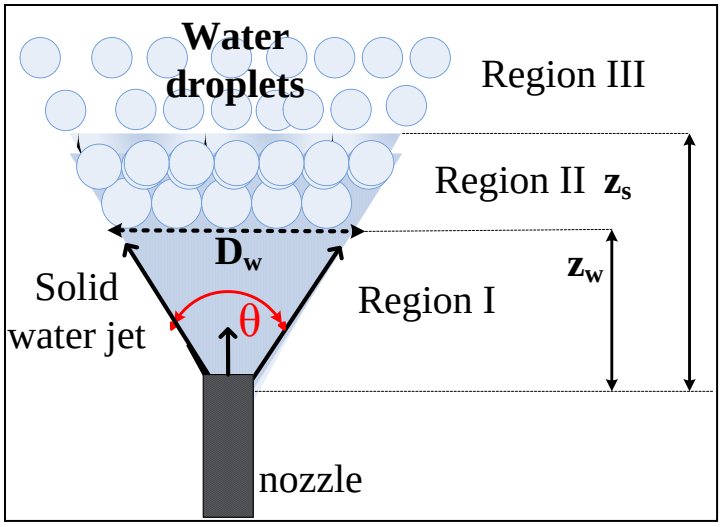

Fig. 41. Upward water spray from a conical nozzle.

In Fig. 41, D_w is the diameter of the solid water jet which breaks up into droplets at z_w vertical distance from the nozzle and z_s is the vertical location where droplets starts to flow. Generally to solve equations (25) and (26), initial air and water drop velocities should be specified at a location, z_s, just beyond the boundary of the spray nozzle. It turns out that if z_s/z_w remains within certain limits, the solutions of the flow is insensitive to (1) the precise value of z_s/z_w and (2) the value of initial air velocity imposed for a given initial drop velocity. It was also identified that at z_s/z_w =1 and initial air velocity (u_{a0}) equal to the initial drop velocity (u_{d0}) is acceptable for a large variety of spray nozzles (Heskestad et al., 1981). Thus the equations appeared be solvable numerically considering the above facts. However, it is still necessary to know the spray cross sectional area, $A_s\ (z)$, the effective drop diameter, d_d, and the initial drop velocity, u_{d0} in order to solve the equations.

The spray cross sectional area, A_s *(z)*, at any axial distance can actually be replaced with spray angle. If a nozzle creates a conical angle of θ, then, instead of A_s *(z)*, the following relationships can be used in equation (26):

$$A_s(z) = \pi \frac{z^2}{\left(\tan\frac{\theta}{2}\right)^2} \tag{27}$$

and $$\frac{dA_s}{dz} = 2\pi \frac{z}{\left(\tan\frac{\theta}{2}\right)^2} \tag{28}$$

For a practical spray nozzle, the initial drop velocity can be related to the average velocity from the nozzle. This relationship is expressed as

$$C_M = \frac{Q_w \rho_w u_{d0}}{Q_w \rho_w U_n} = \frac{u_{d0}}{U_n} \tag{29a}$$

where C_M is called momentum coefficient and U_n is the water velocity from the nozzle.

Or, $$u_{d0} = C_M Q_w \frac{4}{\pi D_n^2} \tag{29b}$$

where D_n is the nozzle diameter.

Usually nozzle diameter and flow rates at different pressure are provided in any nozzle specification. A nozzle actually produces a range of droplet sizes from the solid liquid stream. It is found that effective diameter lies somewhere between the sauter mean diameter to volume mean diameter (Heskestad et al., 1981). These diameters do not differs greatly in water sprays and since the air entrainment is not very sensitive to the difference between these two sizes, the sauter mean diameter is considered for this research as effective drop diameter. Literature search has revealed the existence of a

relationship to determine the effective drop size from any nozzle specification (Bennet & Eisenklam, 1969; Briffa & Dombrowski, 1966; Heskestad et al., 1981). The relationship is expressed as

$$d_d = r\left(\frac{D_n}{U_n}\right)^{\frac{2}{3}} \tag{30}$$

where, r is a constant of proportionality generally dependent on the relative geometry of the nozzle.

Now the equations (27)-(30) can be used to identify the necessary spray information of spray cross sectional area, $A_s\,(z)$, the initial drop velocity, u_{d0} and the effective drop diameter, d_d in order to solve the equations (25) and (26). After careful analysis of their developed model, for a downward spray, Heskestad et al. (1981) discovered that nondimensional forms of the equation produced accurate results. The same method is utilized here to solve the equations for the studied upward flow.

4.4 Nondimensionalized Equations

Considering the initial drop velocity, u_{d0} as the characteristic velocity, and the diameter of the solid water jet, D_w which carries the flow rate Q_w at a velocity of u_{d0} as the characteristic length, the following normalized relationship was obtained.

$u_d^* = \frac{u_d}{u_{d0}}$, normalized drop velocity

$u_a^* = \frac{u_a}{u_{d0}}$, normalized air velocity

$z^* = \frac{z}{D_w}$, normalized axial distance

The normalized relationships are also based on the idea of Heskestad et al. (1981). The governing equations (25) and (26) are normalized with the characteristic quantities and expressing the local sectional flow area A_s, in terms of spray angle θ. Finally the following nondimensional relationships are obtained:

$$\frac{du_d^*}{dz^*} = -\frac{\alpha}{u_d^*} - \beta \frac{\left(u_d^* - u_a^*\right)^{\frac{3}{2}}}{u_d^*} \tag{31}$$

$$\frac{du_d^*}{dz^*} = -\frac{u_a^*}{z^*} + \gamma\beta \frac{\left(u_d^* - u_a^*\right)^{\frac{3}{2}}}{u_d^* u_a^* \left(z^*\right)^2} \tag{32}$$

Here the parameters α, β, γ and ξ can be called as gravity parameter, viscous-interaction parameter (related to discharge velocity), geometric parameter (related to cone angle) and geometric parameter (related to nozzle size) respectively.

$$\alpha = \left(\frac{\xi}{\beta}\right)^4 \tag{33}$$

$$\beta = \frac{3}{4} B\nu^{\frac{1}{2}} \left(\frac{\rho_a}{\rho_w}\right) D_w d_d^{\frac{-3}{2}} u_{d0}^{\frac{-1}{2}} \tag{34a}$$

Or, $$\beta = \frac{3}{4} B\nu^{\frac{1}{2}} \left(\frac{\rho_a}{\rho_w}\right) \frac{U_n^{0.5}}{C_M r^{\frac{-3}{2}}} \tag{34b}$$

$$\gamma = \frac{1}{8} \left(\frac{\rho_w}{\rho_a}\right) \frac{1}{\tan^2 \frac{\theta}{2}} \tag{35}$$

$$\xi = \frac{3}{4} B \nu^{\frac{1}{2}} \left(\frac{\rho_a}{\rho_w} \right) g^{\frac{1}{4}} \frac{D_n^{0.25}}{C_M^{\frac{13}{8}} r^{\frac{3}{2}}} \tag{36}$$

4.5 Numerical Solution

The normalized equations (31) and (32) have been solved numerically to estimate the air entrainment rate into a large number of upward conical sprays selecting systematic variations in the parameters γ, β, and ξ. A Visual C^{++} program has been developed to solve the normalized differential equations using fourth order Ranga-Kutta method. The program was verified with the results from the downward spray model of Heskestad et al. (1981). The program showed good agreements with their published data.

Fig. 42 and Fig. 43 show the results of non dimensional entrainment velocity, u_a^* and entrainment flow, $Q_a^* = \frac{Q_a}{Q_w}$, at different non dimensional axial locations from the apex of the spray cone, $z^* = \frac{z}{D_w}$. In the study two cone angles (30 and 60), two nozzle pressures (P1 and P2 where P2=2*P1) and two flow directions have been chosen to study effect of spray cone and discharge velocity (i.e. pressure) for both upward and downward spray of constant diameter nozzle in entrainment velocity and entrainment rate.

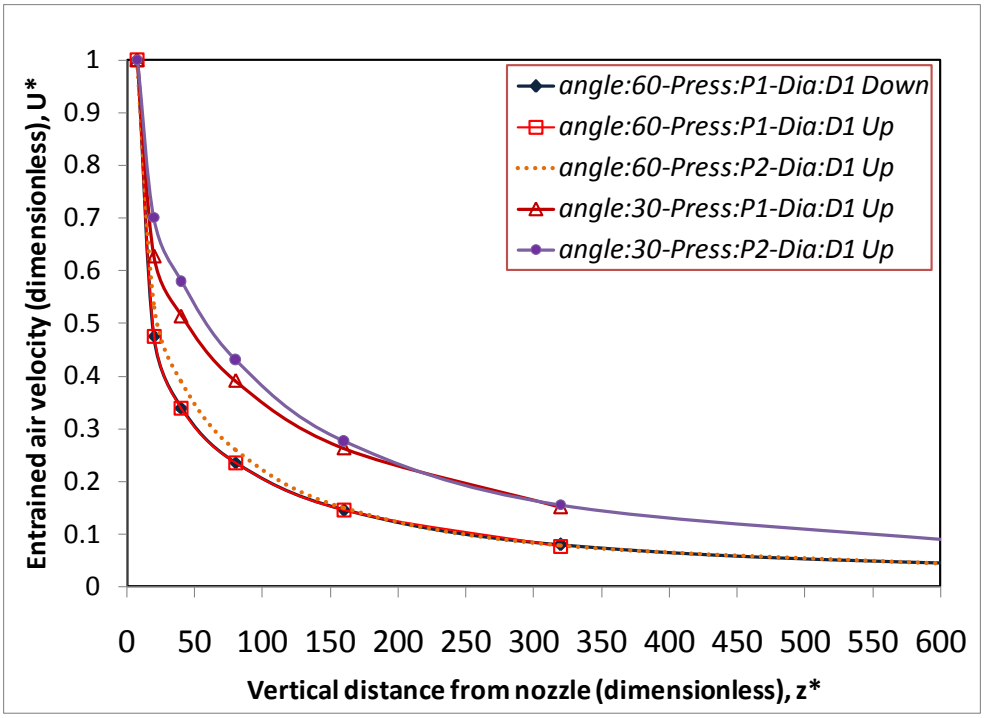

Fig. 42. Dimensionless air entrainment velocities into different conical sprays.

Fig. 42 shows that non dimensional velocities of entrained air for the nozzles of same cone angle and pressure but different directions (downward and upward) are exactly similar for the same distance from the nozzle. Only difference is that the curve for the upward spray (solid red line with red square marker) ends at z^*=325 where the curve for the downward spray (solid blue line with solid blue diamond marker) becomes flatter at higher z^*. This indicates that the upward flow for a spray is limited to certain axial distance at certain pressure and angle, where as a nozzle can be mounted at much higher location to flow downward. However for both sprays velocity decreases as the distance increases. If a upward spray is at same angle and diameter but operates at two times higher pressure (red dotted line), very less change in the velocity is observed.

Higher pressure only helps the water drops to reach higher elevation. Instead of doubling the pressure, if the cone angle is reduced to half (solid brown line with triangular marker) then the entrainment velocity increases quite a bit, though the distance covered is the same. Finally if both the pressure and angle is changed (double pressure and half angle) the velocity as well as the coverage increases (purple solid line with circular marker). Thus the results show that spray angle is more important than pressure to increase air velocity inside a spray. For an upward spray, pressure is the important factor only when we care about height coverage.

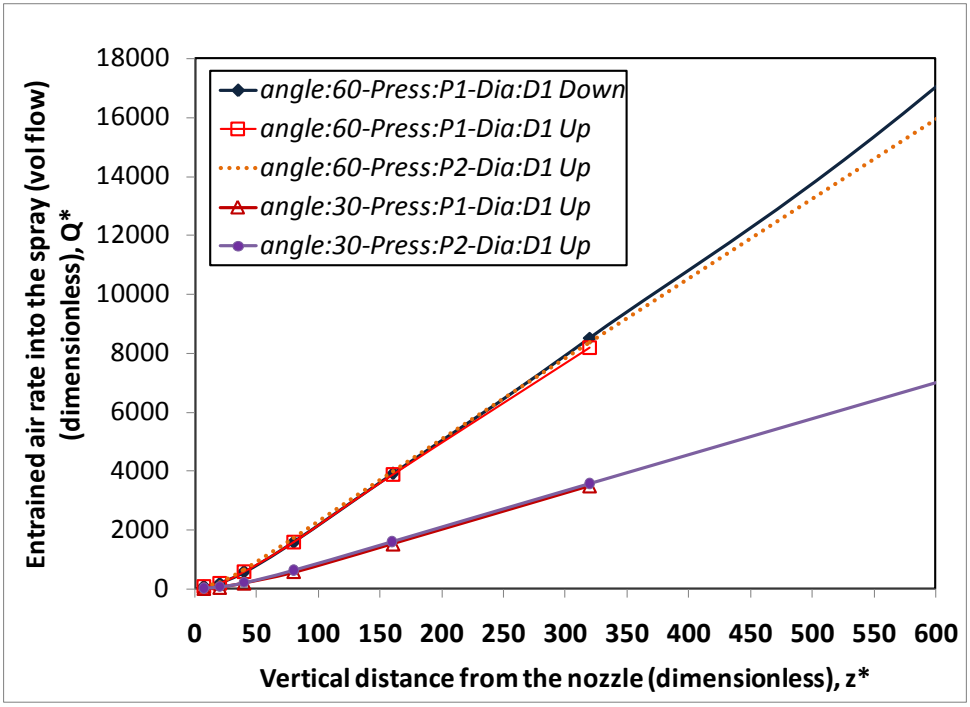

Fig. 43. Dimensionless entrainment rate into different conical sprays.

Fig. 43 shows that volumetric air flow rate increases as the distance from the nozzle increases. This is obvious as the conical spray area increases along the spray axis. Results of the sprays at similar conditions (angle 60° and pressure P1) and different flow directions (up and down) show that entrainment flow rates do not vary at all, only the distance covered are changed. Increasing the pressure of the upward 60° spray does not provide any higher air rate only it covers much higher elevation. However reducing the angle to 30° for the upward spray significantly decreases the air rate, as the spray area decreases. The overall study clearly indicates that the width (angle) of a spray significantly affects the air entrainment rate into the spray.

4.6 Summary

A simple theoretical model has been developed for air entrainment flow in a water spray discharging vertically upward in quiescent space. The equations were derived and solved based on the model developed by Heskestad et al. (1981). To solve the model equation a Visual C^{++} program has been developed with fourth order Ranga-Kutta method. The program has been verified with results of Heskestad et al. (1981). In the study two cone angles (30° and 60°), two nozzle pressures (P1 and P2 where P2=2*P1) and two flow directions (up and down) have been chosen to study effect of spray cone and discharge velocity (i.e. pressure) of constant diameter nozzles in entrainment velocity and entrainment rate. It appears that the theoretical solution of the model can be used to obtain good estimates for the entrainment flow in sprays of different configurations.

5 EXPERIMENTAL RESULTS*

5.1 Introduction

The objective of the experiments are to determine the effectiveness of different representative types of water curtains in controlling LNG vapor produced from the liquid spills. The change in concentration and temperature of an LNG vapor cloud, dispersing both naturally (by wind) and forcefully (by water curtain), was the main focus of these experiments. Therefore concentration (methane) and temperature data were measured at different downwind distances and elevations, to evaluate the acting mechanisms of a water curtain when interact with an LNG vapor cloud. The water spray nozzles used in the experiments were chosen to represent the three main categories of nozzles, full cone, fan, and fog. Generally, sizes of the droplet sizes produced by the conical, fan and fog nozzles are respectively considered as medium, coarse and very fine. Detail information on the nozzles and types of water curtains used in the experiments is provided previously in section 3.

---

* Parts of this section are reprinted with permissions from (1) "Experimental Study of Effective Water Spray Curtain Application in Dispersing Liquefied Natural Gas Vapor Clouds" by Rana, M. A., Cormier, B. R., Suardin, J. A., Zhang, Y. and Mannan, M. S., 2008. *Process Safety Progress*, 27 (4), 345-353, Copyright [2008] by John Wiley & Sons, Inc., and (2) "Use of Water Spray Curtain to Disperse LNG Vapor Clouds" by Rana, M. A., Guo, Y. and Mannan, M. S., 2009. *Journal of Loss Prevention in the Process Industries*, 22, 707-718, Copyright [2009] by Elsevier Ltd.

This section details the results of the experiments conducted in this study. So far four out-door experiments were conducted on different weather conditions and Table 10 shows the weather conditions during the experiments.

Table 10. Weather conditions during the experiments.

Conditions	2006 Expt.	2007 Expt.	2008 Expt.	2009 Expt.
Month	April	November	March	March
Wind speed (m/s)	2.5 ±0.8	2.2 ± 0.6	4.5 ±1.0	5.1 ± 1.2
Wind direction (from)	North to east	South-west to south-east	South to east	South-south-east
Ambient temperature (°C)	26 ± 0.1	22.5 ± 1.5	22.5 ±0.2	28.4 ±0.3
Relative humidity (%)	64.5 ± 0.6	25.5 ± 3.5	50.6 ±0.7	38 ±0.5
Solar Flux (W/m^2)	N/A	250 ± 12	N/A	590.7±87.5
Water temperature (°C)	N/A	19.5 ± 1.5	17.5 ± 2.5	26.5 ± 1.5

5.2 Experiment of 2006

5.2.1 General Description

In this experiment, LNG was continuously released from the tanker onto the water surface with a discharge pipe connected to the insulated pipe line. The end of the discharge pipe was bended to 45° angle to reduce turbulence. The average flow rate from the pipe was 7.5×10^{-2} m^3/min (20 GPM). An LNG pool of 2.5 m diameter (approximately) was observed to be formed on the water surface almost instantly and the pool geometry reached steady state rapidly in 1 to 2 minutes. Vapor produced from the pool evaporation dispersed downwind (towards south-west) as a vapor cloud and the cloud concentrations were measured in different points with point gas detectors. The

measurement unit is %LFL (or % LEL). Note that 100% LFL equals 5% v/v methane concentration in air.

5.2.2 Results and Discussion

Three flat fan nozzles were used in the experiments. About 13 minutes after the start of LNG release, the water curtains were activated to control the concentration of the dispersing vapor cloud. The LNG release was continued during the entire time the water curtains were active. Gas detectors were located in both upwind and downwind locations of the water curtain region, and the data were recorded without and with spray activation. Water flow rate and water curtain pressure were not measured in this experiment. Fig. 44 shows continuous gas concentration (% LFL) reading versus time at two points, just before and after the water curtain location.

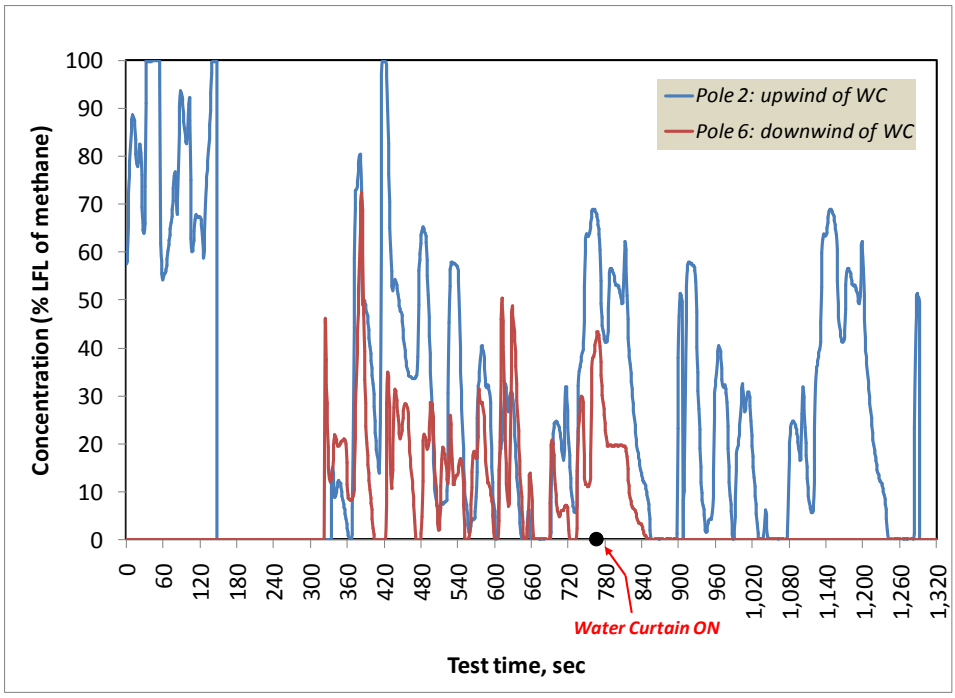

Fig. 44. Ground level (0.3m elevation) methane concentration at two downwind distances. Locations of Pole 2, Pole 6 and the water curtain are 4.0m, 10.0m and 8.5m respectively, from the pit edge.

Fig. 44 shows the ground level (0.3 m from ground) gas concentration data recorded at 4 m and 10 m downwind from the pit edge. Blue line (Pole 2) in the figure represents data at 4 m and the red line (Pole 6) represents data at 10 m. The water curtain was placed 8.5 m downwind (Fig. 22). It is already mentioned before that the water curtain was activated approximately 766 s after starting the continuous LNG release. So for each measurement point concentration data before 766 s is without the water curtain action and after that it is with the action. After the water curtain activation, it actually did not affect the vapor cloud concentration at 4.0 m location (before the water curtain region). However it did affect the vapor concentration at 10 m location (after the water

curtain region). The average peak concentration at 4 m location (blue line) is 61.7 (± 25.1) % LFL. The average peak concentration at 10 m is divided into two parts (red line). Without the water curtain action the average was 32.6 (± 10.3) % LFL and with the action it was very close to 0 % LFL. This data indicate that actually the water curtain did reduce the LNG vapor concentration. However the concentration at the smaller distance, closer to the spill, was already very low (below LFL, i.e. 5% v/v). So the location of the water curtain needed to be much closer to the spill to actually identify the effectiveness of the water curtain. The low concentration reading at this distance was mainly due to early dilution of the gas cloud from air entrainment from the high wind speed and high evaporation rate. That is why the cloud already stated to move up before reaching 4 m and 10 m distance. So when the light cloud interacted with the water curtain, the dispersion was facilitated by the higher momentum from the spray. That is why the concentration at 10 m distance after the curtain activation was almost zero.

During the experiment though the average wind speed was around 2.5 m/s, the high wind speed was almost 5.3 m/s. The higher evaporation rate was due to the spill surface. In this experiment, LNG was released on 45 m^2 of water surface at a very low rate. So the water acted as an infinite heat source for the LNG pool and produced vapor at a higher evaporation rate. Cormier (2008) discussed in detail about the evaporation rate calculation procedure for the experiment and estimated that the mass evaporation rate from the water surface was between 0.2 kg/m^2s and 0.8 kg/m^2, in different location of the pool, depending on the region of turbulence. The highest value of the evaporation rate (0.8 kg/m^2 s) was estimated almost underneath of the pipe where the LNG was

discharged. Again the lowest evaporation rate (0.2 kg/m^2 s) was estimated near the outer edge of the LNG pool where the LNG steadily spread onto the water surface. Thus the high evaporation rate and wind speed reduced the LFL distance significantly. Cormier (2008) also discussed that the total LFL distance observed without using any water curtain was 18.2 meters, where as with the water curtain it reduced to 15 meters. Thus the water curtains used in April 2006 showed that can control and disperse LNG vapor cloud. The experiment also proved their effectiveness in reducing downwind LFL concentration (methane). However the experiment did not identify the actual mechanism behind the effectiveness. So more experiments were developed to fill up the gap and the experiments conducted in the following years were more detailed.

5.3 Experiment of 2007

5.3.1 General Description

A total of four tests were completed in a 1½ hour period. Two types of water spray curtains were used in individual test sets. The first set of tests was conducted with the full cone spray curtain and the second set was with flat fan curtain. The water curtains were directed vertically upward and positioned perpendicularly to the prevailing wind direction, at a fixed downwind distance from the spill location. Test started with continuous spill of liquid LNG onto the concrete ground. As soon as the liquid touched the concrete ground it vaporized. A visible white condensate cloud was then produced as the very cold vapor condenses the water content in the air. The white vapor cloud was observed to disperse naturally towards the prevailing wind direction. The white cloud

formation mainly depends on the humidity of the ambient air, so it may or may not totally represent the actual size of a methane cloud. After achieving a reasonable sized visible vapor cloud flow, the water spray curtain was turned on to disperse the cloud forcefully, continuing the LNG release on the ground. Several minutes after the water activation, the LNG flow was turned off from the tanker. The curtain was kept on until the visible white cloud almost disappeared. Fig. 45 shows two photographs captured from the test.

Fig. 45. LNG dispersion tests. Top: without water curtain, bottom: with full cone water curtain. Reprinted from Rana et al. (2009).

During the tests, the wind speed averaged 2 m/s (4.5 miles per hour) and blew mainly from the south-west to south-east region. The average ambient temperature during the tests was 22.5 (± 1.5) °C and humidity was 25.5 (± 3.5) %. Table 11 includes the average flow rates and total flow time of LNG and water and average pressure of water at the curtain inlet for each test.

Table 11. Average flow rate and pressure data for 2007 experiment. Modified from Rana et al. (2009).

Measured Parameters	**Conical Water Curtain (7 nozzles)**		**Fan Water Curtain (1 nozzle)**	
	Test 1a	**Test 1b**	**Test 2a**	**Test 2b**
LNG flow rate, m^3/s	$(2.5\pm 0.5) \times 10^{-3}$	$(3.8\pm 0.7) \times 10^{-3}$	$(3.5 \pm 0.25) \times 10^{-3}$	$(3.4 \pm 0.75) \times 10^{-3}$
LNG total, m^3	1.35 ± 0.3	1.87 ± 0.3	1.25 ± 0.09	0.71 ± 0.16
Water pressure, kPa [psi]	275.8 ± 34.5 [40 ± 5]	304.5 ± 34.5 [45 ± 5]	551.4 ± 34.5 [80 ± 5]	620.4 ± 34.5 [90 ± 5]
Total water flow rate, m^3/s	$(15.5 \pm 4.7) \times 10^{-3}$	$(15.5 \pm 1.0) \times 10^{-3}$	$(15.1 \pm 4.6) \times 10^{-3}$	$(15.5 \pm 2.3) \times 10^{-3}$
Water flow rate per nozzle, m^3/s	$(2.2\pm 0.7) \times 10^{-3}$	$(2.2 \pm 0.14) \times 10^{-3}$	$(15.1 \pm 4.6) \times 10^{-3}$	$(15.1 \pm 4.6) \times 10^{-3}$
Water total, m^3	9.1± 2.8	5.4 ± 0.35	5.3 ± 1.6	3.16 ± 0.47

Procedures for the entire experiment were similar as mentioned earlier in section 3. However Table 11 clearly indicates that the times of water turning on and LNG release discontinuing are different for the tests. As these field tests deal with flammable LNG vapor, whose phenomena of flow and dispersion are still completely unknown, the decisions of turning on the water curtain and turning off the LNG flow mostly depended on the situation during each test. For example, the water curtain was activated much later

for test 1a than the test 2a (480 s for 1a and 231 s for 2a). The first reason for this was that the LNG pipeline was not pre-cooled before conducting the full cone test (1a), which reduced liquid flow at the discharge point and all of LNG was coming as vapor initially until the pipeline was completely cooled down. However during the test 2a, as the pipe line was already used twice, it was somewhat cooled, and it took much shorter time to get liquid out at the pipe discharge. So the water curtain activation time is higher in the first test.

Another main reason of the long wait in the first test was the wind's behavior. As already mentioned the test set up was based on predicted wind direction. At the start of test 1a, wind direction suddenly changed from the setup direction. So initially LNG vapor cloud was not exactly moving towards the water curtain, which was placed 7m downwind from the spill location. However the wind direction changed back towards the setup again within short time. This major factor of change in wind direction mainly delayed the water curtain activation time even though the wait for the pipe cooling was over. The readings of the gas detectors located at different downwind direction presented later in this section also identifies the situation that initial concentration sensing times are different for two the tests.

LNG was continuously released on concrete ground surface and the spill area was fixed by enclosing the area with wooden bars (1.5m × 1.5m × 0.13m) to obtain a fixed pool size. LNG flow was discontinued when a pool of a reasonable depth (approximately 0.1-0.13 m) was achieved, to avoid overflow from the enclosure. In test 1a LNG was released for a long period of time inside the enclosed spill area due to the

late activation of water curtain. So a reasonable liquid pool was created within 70 seconds of the water activation. However during test 2a, to achieve a reasonable LNG depth in the spill, it took almost 125 s after the curtain activation. That is why the LNG release discontinuing times are also different from each other. However the slight difference in the procedure should not have significant effect in the test results. Only the sizes of the vapor cloud during the LNG- water curtain interaction were slightly different due to the time difference. As the evaporation rate of LNG reduces overtime from spilling on concrete, the vapor cloud for test 1a was expected to be slightly smaller than test 2a at the time when the water curtains were activated.

Full cone curtain pressure was measured at the curtain pipe inlet and flat fan curtain pressure was measured at the spray head. As the full cone curtain was fabricated with seven smaller nozzles where as only one nozzle was used for the flat fan curtain, less pressure was achieved in the full cone curtain. Studying the test data, Fig. 36 and Fig. 37, it can be identified that each full cone nozzle operated around 34 – 42 kPa and at these pressures, the range of SMD of the droplets is 1.4 – 1.3 mm. On the other hand the flat fan curtain operated around 516 -586 kPa range and thus the range of SMD of the droplets at these pressures is 1.6-1.5 mm.

Water curtain coverage depended on the water pressure. So the heights of the curtains were different for different test. Fig. 46 and Table 12 show the average water curtain heights in the experiment. The total height of the water curtains were measured from pictures and videos. The height was measured by comparing with 2.3 m high tripod poles.

Fig. 46. Water curtain coverage in 2007 experiments.

Table 12. Heights covered by the water curtains in 2007 experiment.

Test	Water Curtain	Coverage (Avg Height), m
1a	Full Cone	2.8
1b		2.9
2a	Flat Fan	4.64
2b		6.55

Approximated widths of the water curtains are also determined from the experiment. This width, which is the downwind length of the curtain, is approximated form the shape of the water curtain actually produced during the tests. The upward full cone curtain though created a conical spray shape; it leaned towards the wind direction by wind speed. As the shape was conical, the width changes along the height. At 2.1-2.4m height from the nozzle the width was observed to be approximately 3.23m. For the convenience of analysis, the shape of this curtain is assumed rectangular for simplicity and a constant value of 1.6m (half of 3.23m) is considered as the width from the spray point. On the other hand the fan spray created a flat flow and also leaned towards

downwind due to wind speed. Its width fluctuated between 0.45-0.55 m during the test. In this analysis the shape of this curtain is also assumed rectangular and a constant value of 0.5m (average) is considered as the width, from the spray point.

5.3.2 Results and Discussion

5.3.2.1 Imaging

All tests were videotaped using digital, hydrocarbon and Infrared (IR) cameras. The hydrocarbon and IR cameras were used to differentiate between the dispersion of flammable hydrocarbon and the visible condensate cloud. Fig. 47- Fig. 49 show clips from the videos of the tests captured with the regular and hydrocarbon cameras, almost at the same time.

Fig. 47. Spill and natural dispersion. Left: regular image, right: hydrocarbon camera image.

Fig. 48. Forced dispersion with full cone spray curtain. Left: regular image, right: hydrocarbon camera image.

Fig. 49. Forced dispersion with flat fan curtain. Left: regular image, right: hydrocarbon camera image. Reprinted from Rana et al. (2008).

The regular image in Fig. 47 shows a smaller visible condensate cloud but hydrocarbon camera image shows actual size of the flammable cloud. In Fig. 48 and Fig. 49, the regular camera image shows that white condensate cloud becomes invisible after it crosses the spray area. The black areas of the hydrocarbon camera image show the presence of colder hydrocarbon in the gas-air-water vapor cloud. The light darker area after the spray indicates that still there are some colder hydrocarbons (which are not visible) and the concentration/temperature is lower.

5.3.2.2 Concentration and Temperature

LNG was continuously released on concrete ground surface into an enclosed area (1.5m × 1.5m × 0.13m) to obtain a fixed pool size. Concentration and temperature of the dispersing LNG vapor (methane) cloud was measured continuously during each test. Prior to the experiment, the gas detectors were calibrated with methane gas (50-50% CH_4-Air Mixture) to measure methane concentration in % volume/volume unit. The schematic of the setup (Fig. 28) indicates that the data collection points in each test were distributed at five different downwind distances from the spill (x_1-x_3 & x_5-x_6) and at two (y_{-2}, y_2) or four (y_{-3}, y_{-2}, y_2 & y_3) crosswind positions and three elevations (z_1-z_3). The water curtains were positioned at x_4 (= 7.0m) downwind distance from the LNG release spot in both the tests. Fig. 50 is an example of readings at 0.5m elevation and three downwind locations. In the figure, red, brown and blue colors represent measurement at 1 m, 3.3 m and 11.3 m downwind distances respectively.

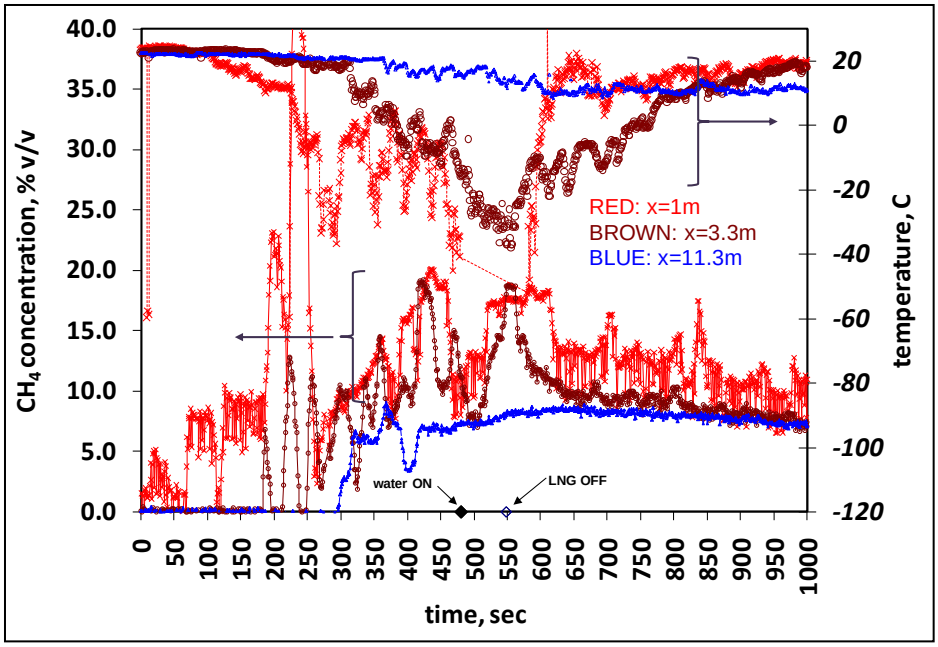

Fig. 50. Concentration and temperature measurement during test 1a at 0.5 m elevation of three downwind locations. Modified from Rana et al. (2008).

From the above figure it is clear that during the time of continued LNG release, near ground level concentration, closer to the release point is higher and becomes lower as the cloud proceeds downwind. And for the temperature, cloud temperature is colder near the release and approaches atmospheric temperature as the cloud moves further. So the data shows dispersion of LNG vapor cloud. Measurements can be divided in to two parts: (i) natural dispersion of LNG vapor measurements: when there is no interaction between water and LNG vapor; and (ii) forced dispersion of the LNG vapor measurements: after the interaction between water curtain and the LNG vapor. Fig. 51 shows the schematic of the test procedure and the natural and the forced dispersion processes considered in a test.

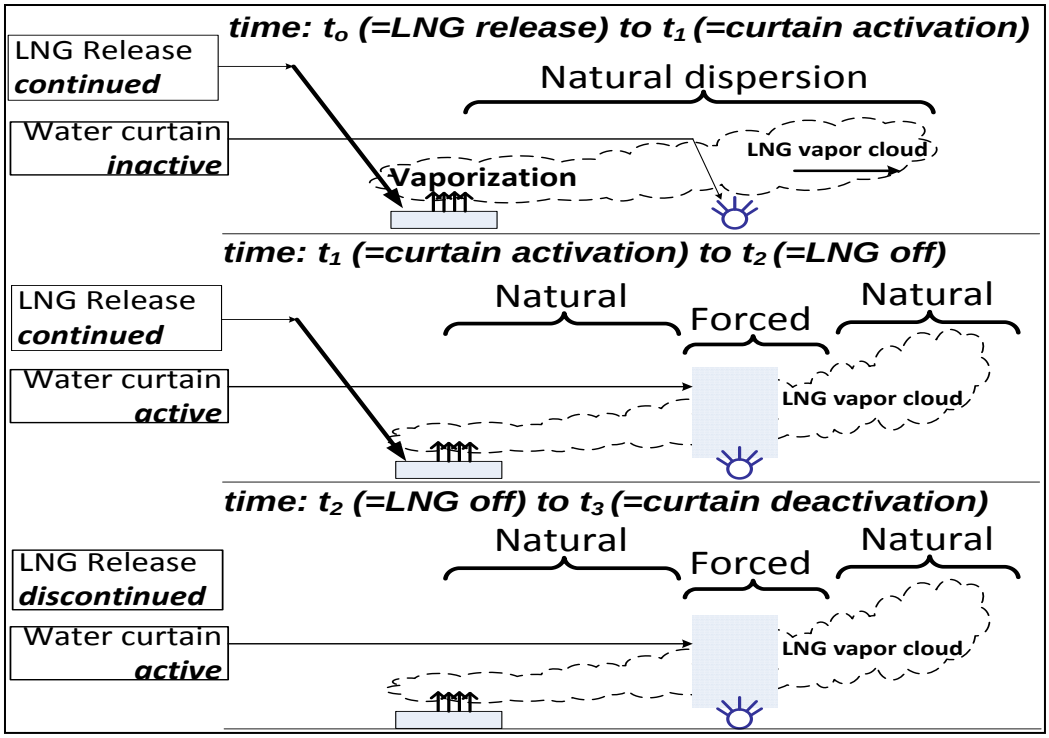

Fig. 51. Test procedure and dispersion process. Reprinted from Rana et al. (2009).

To determine the effect of water curtain in controlling LNG vapor cloud, data collected at three elevations of x_2 (=3.3m) and x_5 (=11.3m) downwind distances are considered in the research for analysis purpose. Here one test for the full cone (test 1a) and one test for flat fan (test 2a) curtain are considered to discuss in detail.

Before the analysis all the flow sensor, thermocouple and gas detector data were carefully reviewed and synchronized with the captured video as there was time lag among the LNG flow, temperature and concentration data. Some fluctuations were observed in the recorded concentration and temperature data, especially close to the spill area, due to the wind gustiness and crosswind turbulence. Turbulence created very close to the spill spot due to momentum of LNG flow from the pipe, flashing and evaporation

speed might cause additional fluctuation in the reading. Concentration and temperature data at three elevations (z_1-z_3) of the two horizontal locations (x_2 and x_5) are first averaged and then analyzed. The readings of the similar four crosswind (y direction) sensors located at one elevation (z direction) of one horizontal position (x direction) are averaged to get one concentration or temperature data at that (x, z) location. Fig. 52 to Fig. 55 summarize the average concentration and temperature readings for two tests with two types of water curtain. The charts show average data at three heights (z_1= 0.5 m, z_2= 1.2 m and z_3= 2.1 m) of two (x_2= 3.3 m and x_5= 11.3 m) downwind distances.

In the analysis, the selected downwind positions are just before and after the water curtain region. This means that data at 3.3m (x_2) distance are always due to natural dispersion of LNG, considering the fact that the vapor never interacted with the water curtain at this position. As the 3.3m downwind location is in between the spill area and the spray, LNG vapor was observed to have very insignificant effects by the spray here. Due to the wind, the water spray was also observed to lean towards the wind direction and thus not affecting the vapor coming to it. For these reasons, it is assumed that there is no effect of the water spray on the LNG vapor before the spray area. However, as 11.3 m (x_5) downwind position is after the water curtain region, the test data here are divided into two parts based on the test procedure: (i) natural dispersion data before the water curtain activation and (ii) forced dispersion data after the water curtain activation.

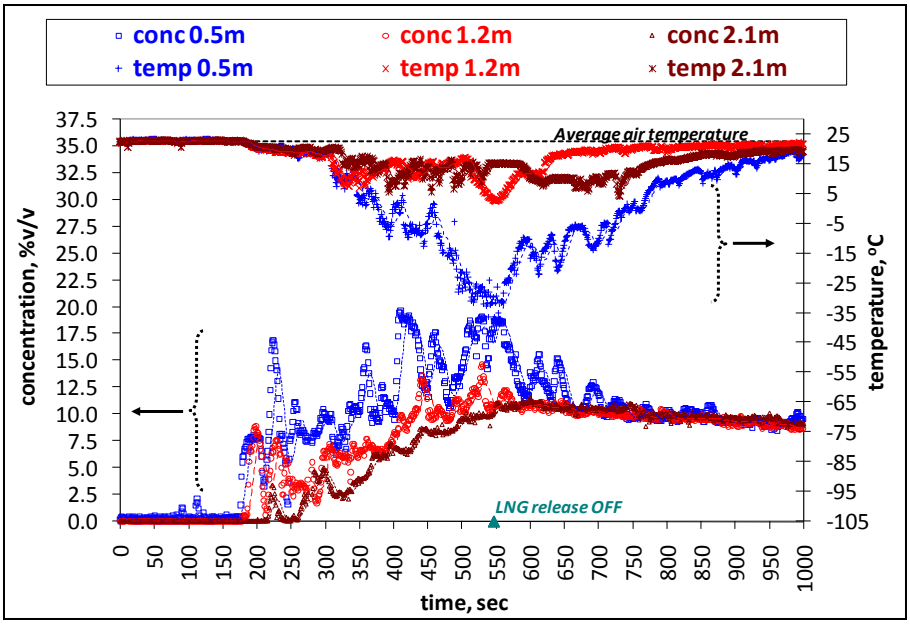

Fig. 52. Average data at (x_2=) 3.3m downwind: full cone spray curtain, test 1a. Reprinted from Rana et al. (2009).

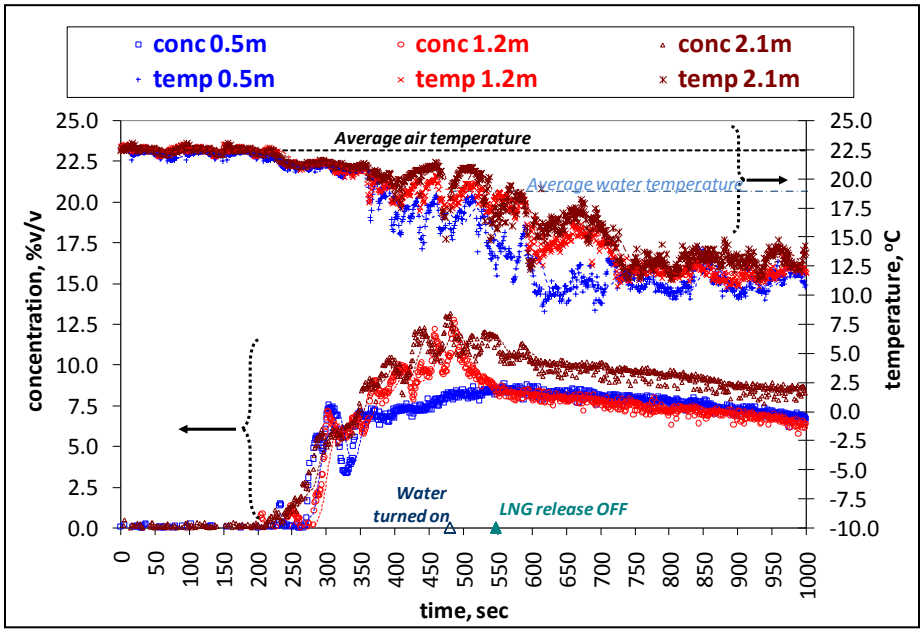

Fig. 53. Average data at (x_5=) 11.3m downwind: full cone spray curtain, test 1a. Reprinted from Rana et al. (2009).

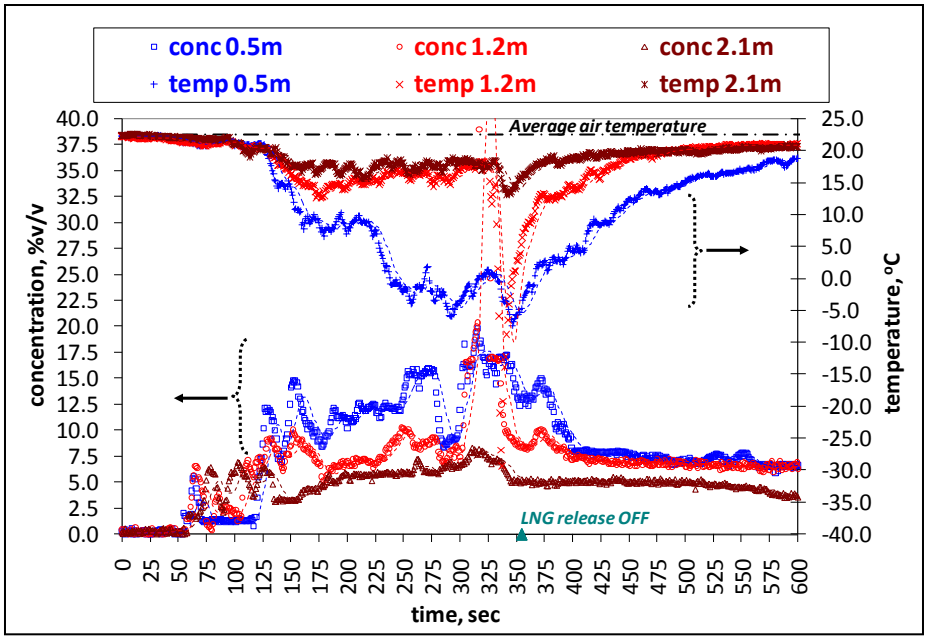

Fig. 54. Average data at (x_2=) 3.3m downwind of release: fan spray curtain, test 2a. Reprinted from Rana et al. (2009).

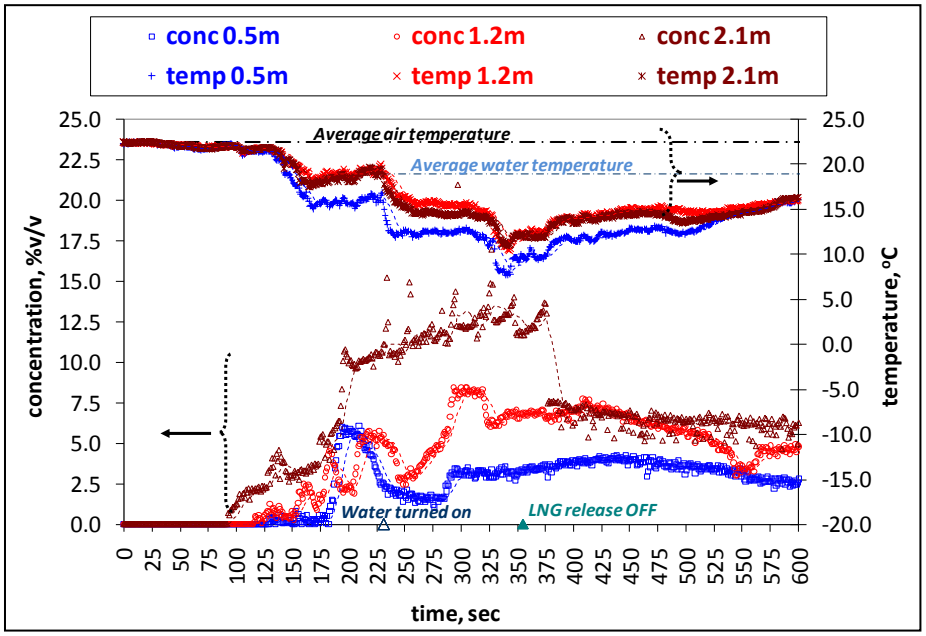

Fig. 55. Average data at (x_5=) 11.3m downwind: fan spray curtain, test 2a. Reprinted from Rana et al. (2009).

Natural dispersion: Concentration at 3.3 m downwind of the spill started to increase as LNG release was continuous (Fig. 52 and Fig. 54). Average CH_4 concentrations at 3.3m continued to increase as the LNG release was continued for some time after turning the water sprays on. This is obvious as water action does not affect the LNG vapor at this location. 3.3m downwind concentrations at 0.5m above the ground are higher than concentrations at 1.2 m and 2.1 m elevation for both the tests. However, Fig. 53 and Fig. 55 show that concentration reading, due to natural dispersion, near the ground (0.5 m) at 11.3 m downwind, is smaller than the higher elevations (both 1.2 m and 2.1 m) readings. Thus data clearly demonstrates that LNG vapor naturally gets diluted, lighter and disperses upward as it travels further downwind.

Temperature data recorded during the natural dispersion actually demonstrate air temperature. Fig. 52 and Fig. 54 show that average temperature 0.5 m above the ground is lower than temperatures at 1.2 m and 2.1 m heights for both the tests. The temperature data during the natural dispersion are consistence with the average concentration data, but only closer to the spill location (3.3 m). It means that the cloud is colder and heavier near the ground. Fig. 53 and Fig. 55 show that temperature data during natural dispersion at 11.3 m downwind distance become inconsistent with the concentration data of the same location. Though ground level concentration (0.5 m) is low at this location (11.3 m), temperature is still lower than the two upper elevations (1.2 m and 2.1 m). It means that though LNG vapor naturally disperses upward and ground concentration reduces as it travels downwind, vapors close to the ground are still cold and heavy.

Forced dispersion: Data at 11.3 m, after the water curtain activation (at 480 s for test 1a and at 240 s for test2a) are considered effected by the forced dispersion (Fig. 53 and Fig. 55). Different behavior of concentrations due to forced dispersion at 11.3 m downwind distance in two tests proves that the action mechanisms are different for the two curtains. In the full cone test, concentrations at 1.2 m and 2.1 m heights started decreasing immediately after the spray was turned on. The concentration plot at 0.5 m height indicates a slight reduction in the rate of increase in concentration when the LNG release was still continued. Again for the flat fan test, rate of concentration increase was reduced due to the forced dispersion when the LNG was still releasing from the pipe. Gas concentrations at 11.3 m downwind of the release for both the curtains continued to decrease after discontinuing the LNG flow.

Fig. 53 shows concentration at 1.2 m height becomes the lowest and at 2.1 m becomes the highest by the full cone curtain action. The change in CH_4 concentrations after the full cone spray region (11.3 m) at 2.1 m high is not very significant as the vapor cloud could cross over the top of the water curtain without complete interaction. The results indicate that the full cone water curtain could not provide enough momentum to the cloud. Observation during the tests showed that this curtain produced enough turbulence around it due to spiral flow pattern. Therefore the reduction in gas concentration is mainly by better mixing with air. This discussion is also supported by analysis provided later in this section.

Fig. 55 shows that the concentration at 0.5 m height is the lowest and 2.1 m height is the highest for the flat fan test. The change in concentration at 2.1 m height for

the flat fan curtain is very significant. Comparison of CH_4 concentration profiles at 0.5 m above ground for 11.3 m and 3.3 m downwind (Fig. 54 and Fig. 55) show significant difference. For 1.2m above ground, average concentrations at 3.3 m downwind are higher than 11.3 m downwind, both before and during water curtain application. However for 2.1 m above ground, average concentrations at 11.3 m downwind are higher than 3.3 m downwind, both before and during the entire period of water curtain action. This difference indicates that the flat fan water curtain was dispersing the LNG vapor upward through mainly by imparting momentum to the cloud than mixing and diluting it with air. This discussion is also supported by analysis provided later in this section.

The temperature data recorded during the forced dispersion at 11.3 m downwind distance were not the air temperature any more. When the water was turned on all of the sensors at this position got wet and read only the water temperature. The average water temperature during the tests was 19.5° C. Average temperature profile at 0.5 m height is always the lowest for both the test, which indicates the cloud is still heavier at ground level than higher level. In Fig. 53, temperature at all the heights starts to decrease initially when the curtain was turned on. The curves become constant below 15° C after the release was stopped. In Fig. 55 temperature profile is consistent with the previous test only during water curtain action and continued LNG flow. After the release was discontinued, temperature starts to increase. The difference between the temperature data from these two tests indicates that the full cone water curtain warms up the cloud more than the flat fan spray curtain by transferring more heat.

5.3.2.3 Vaporization of LNG

One of the critical parameters controlling the dispersion of LNG vapor is the rate of vapor produced. To understand the effect of a water curtain of a certain size, the information on the size of the vapor cloud is essential. During the tests LNG was delivered from the tanker with a stainless steel pipeline connected to a flexible hose and released to the LNG release spot. The tanker contained commercially available LNG with a composition of 99.8% methane. Thus, the hydrocarbon vapor generated was mainly composed of methane. The temperature and pressure were 100 kPa and 110 K in the tanker. LNG was released from the truck at an average rate of 2.5×10^{-3} m^3/s (39.3 GPM) for 9.8 minutes and 3.5×10^{-3} m^3/s (55.9 GPM) for 6 minutes in the full cone (1a) and fan curtain (2a) tests, respectively. It was observed that when LNG comes out of the pipe, some vapors were generated immediately due to flashing. It is also possible to form some aerosol, which is a suspension of liquid droplets so small that they will not settle out of the vapor/air mixture. The vapor and aerosol immediately contributed to the vapor cloud that formed. Most of the liquid reached the concrete surface and formed a liquid pool that evaporated. The total vapor evolved from the pool was the primary source for the vapor cloud. Fig. 56 illustrates the vapor formation process from the liquid spill.

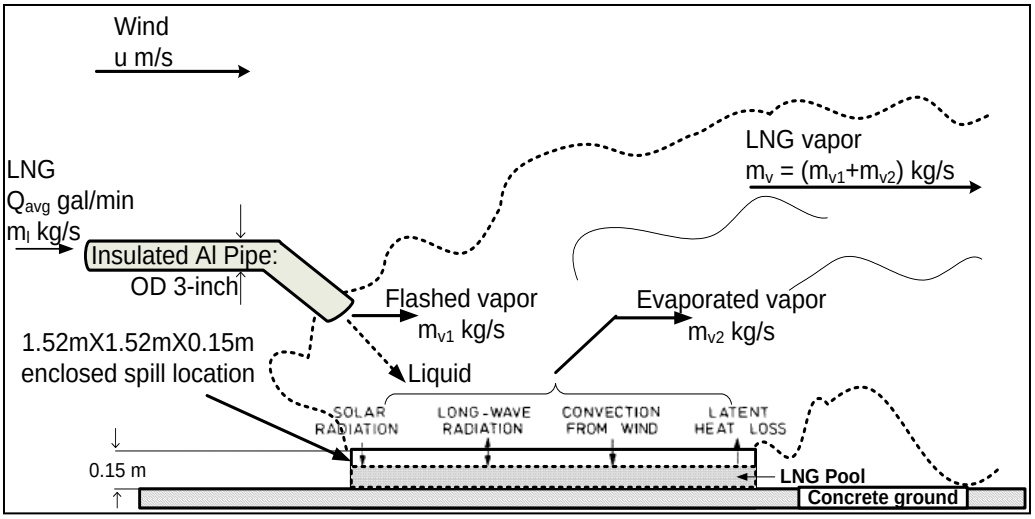

Fig. 56. Formation of LNG vapor cloud from continuous liquid release. Reprinted from Rana et al. (2009).

Direct measurements to determine the vapor generation during the LNG release were not taken. Only the liquid (LNG) flow rate in the pipeline was measured 1.5-2.5 m away from the LNG truck. So in this analysis, analytical relationships for the LNG vapor production are used. One relationship derived by Briscoe and Shaw (1980), and Hissong (2007) are used to calculate total vapor generation or vaporization rate. The final form of the relationship is:

$$m_{vapor} = m_{flash} + m_{evap} \quad \text{(kg/s)} \tag{37}$$

Here $$m_{flash} = f \times m_{liquid} \quad \text{(kg/s)} \tag{38}$$

$$m_{liquid} = \rho_{LNG} \times Q_{liquid} \quad \text{(kg/s)} \tag{39}$$

$$m_{evap} = m_{sub} + m_{air} + m_{rad} \quad \text{(kg/s)} \tag{40}$$

$$m_{sub} = \frac{k_s (T_s - T_L)}{L(\pi \alpha t)^{1/2}} A_{pool} \quad \text{(kg/s)} \tag{41}$$

$$m_{air} = h_a A_{pool} \frac{T_a - T_L}{L} \quad \text{(kg/s)} \tag{42}$$

$$m_{rad} = \frac{q_{rad} A_{pool}}{L} \quad \text{(kg/s)} \tag{43}$$

Vapor coming out from the discharge pipeline was observed during the tests. Due to the specification of the LNG discharge line, some of the LNG flashes before reaching the discharge point of the hose because of heat transfer and some pressure drop. Study with the piping system of the Fire School has shown that 5 to 20 % hydrocarbon vapors can be produced along the pipeline, used in the tests, due to heat transfer from the pipeline (Cormier, 2007). Since this vapor fraction was not measured in the test, and it was observed that the volume of the flashed white vapor cloud emerging from the pipe is large, an average of 20% flashing at the pipe outlet due to heat transfer is assumed constant throughout the vaporization calculation, ignoring the pressure drop effects.

Though an enclosed area of 1.52m × 1.52m was made to contain LNG release with several precautions to stop leakage, LNG leaked outside of the area. Approximate size of the pool was measured after each test from the ice footprint remained on the ground. The average measured pool area was approximately 5m^2. Temperature of the ground surface was approximately 25°C during the tests. Main difficulty in the application of this relationship (Eqn 37) is the choice of appropriate values for the thermodynamic properties. Vapor rate calculations are conducted considering pure

methane's physical properties; liquid temperature (-160°C), liquid density (450 kg/m^3) and heat of vaporization (510 kJ/kg). Calculations also assume constant LNG flow rate (mass flow rate) from the pipe. For the ground thermodynamic property, k_s= 1.7 W/mK and $\alpha = 4.16 \times 10^{-7}$ m^2/s are assumed as the properties of concrete. The assumptions are based on the values provided by Briscoe and Shaw (1980). To determine the heat transfer to the LNG pool from the air, h_a is calculated from the formula provided by Hissong (2007). The formula for h_a for heat transfer to horizontal surface is:

$$h_a = 0.037 \left(\frac{L_i u_a \rho_a}{\mu_a}\right)^{0.8} \left(\frac{C_a \mu_a}{k_a}\right)^{\frac{1}{3}} \frac{k_a}{L_i} (T_a - T_L) A_{pool} \quad (44)$$

All of the values required to solve the above equation are the properties of ambient air at film conditions except L_i, which is the length of the liquid pool. Here "film conditions" means the average of the ambient air temperature and the pool (liquid LNG) temperature (Hissong, 2007). Fig. 57 and Fig. 58 show vapor rates calculated for the tests.

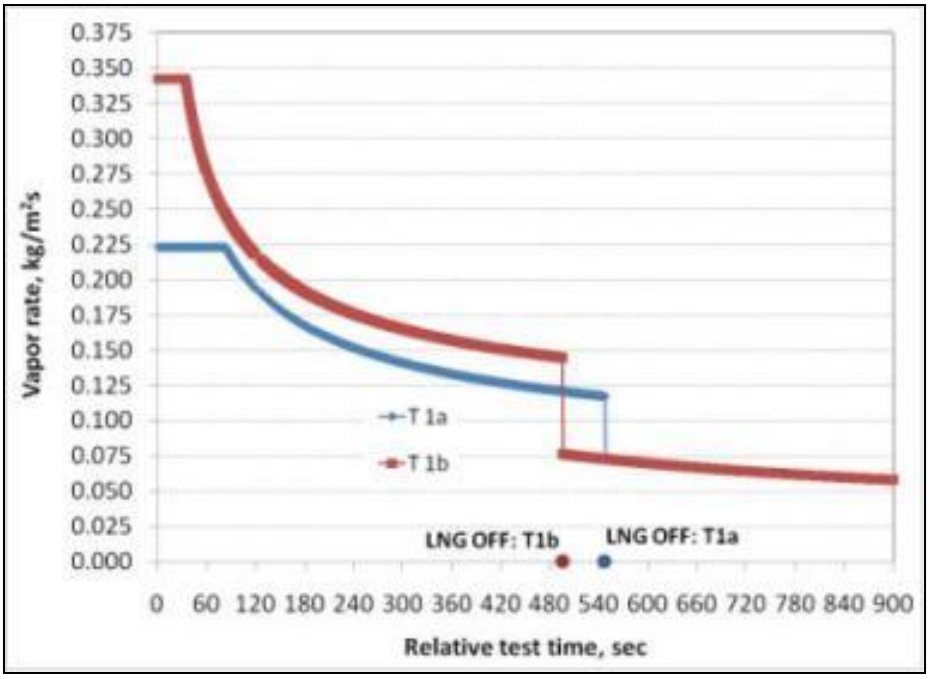

Fig. 57. Vapor flow rate for full cone curtain tests (test 1a and 1b).

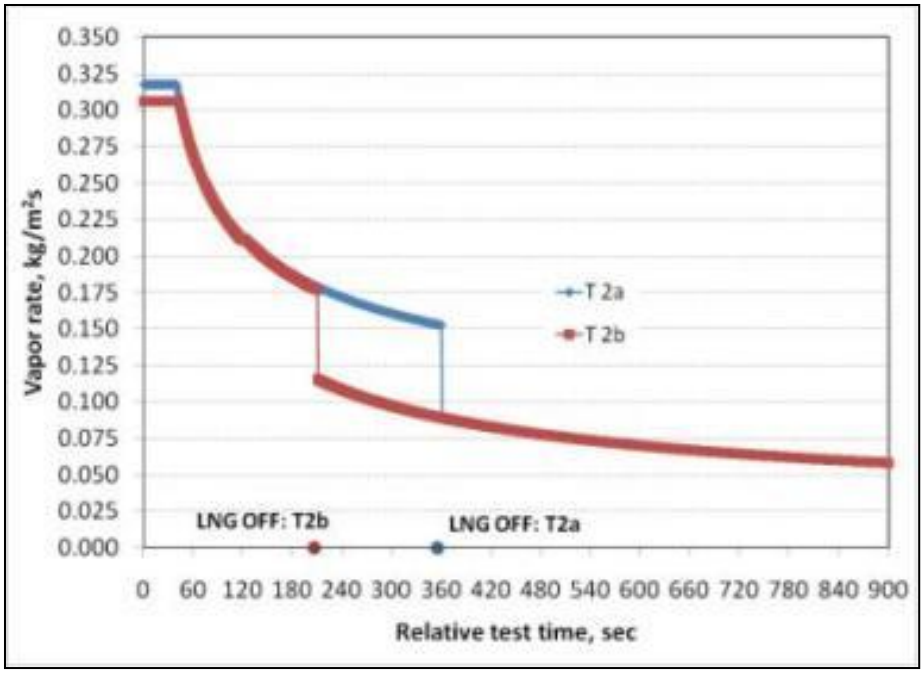

Fig. 58. Vapor flow rate for flat fan curtain tests (test 2a and test 2b).

The figures indicate that the LNG vaporization rate decreased overtime as the spill surface cooled down. During the continued LNG flow, due to the flashing from the pipe, vaporization rate is higher than when LNG flow was turned off. The calculations assume that the vaporization rate is uniform throughout the spill surface area of $5m^2$.

5.3.2.4 Dilution by Water Curtain

The main purpose of water curtain is to reduce the LNG vapor concentration downwind of the curtain through forced dispersion. So the curtain effectiveness is analyzed in terms of dilution and strength ratio in this paper. Dilution ratio is defined here as the ratio of the average concentrations at 3.3 m and 11.3 m downwind distances and at each height. In the calculations, the downwind progress of cloud is considered by assuming that the cloud moves downwind with the constant speed of the wind. The following relationship illustrates dilution ratio (DR) at a certain height:

$$DR = \left. \frac{C_{x_5 t_2}}{C_{x_2 t_1}} \right|_z \tag{45}$$

The time required for a parcel of the cloud to travel a certain distance is given by:

$$\Delta t = t_2 - t_1 = \frac{x_5 - x_2}{u_W} \quad \textbf{(s)} \tag{46}$$

During the tests the total volumetric flow rate of water was measured. The effect of water curtain in diluting the vapor cloud is analyzed in terms of strength ratio. Strength ratio (SR) is defined as the ratio of water mass flux and LNG vapor mass flux at

the curtain location. The calculation of SR also considers the downwind progression of cloud assumption stated before. The following equation illustrates the strength ratio (SR) at the curtain location at a certain height:

$$SR = \left.\frac{\dot{m}_{water}}{\dot{m}_{vapor}}\right|_{z} \quad (\frac{kg/m^2 s}{kg/m^2 s}) \tag{47}$$

As DR is the ratio of concentration at two downwind positions, an effective water curtain is expected to reduce the ratio to very lower value. Again as the water flux is always almost constant; SR is then inversely proportional to the vapor flux. So a lower SR value indicates larger vapor flux and vice versa. The area considered for the water mass flux is the water flow surface area and the area considered for the vapor flux is the measure pool area. Fig. 59 and Fig. 60 show the dilution and strength ratio results for the two tests.

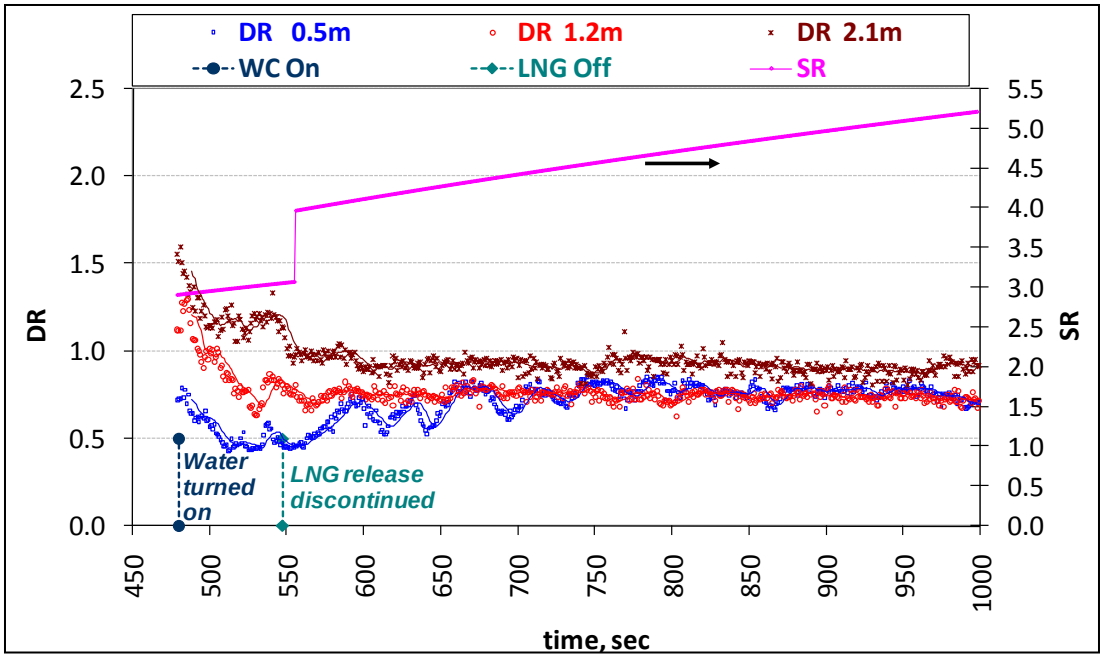

Fig. 59. Dilution and strength ratio: test 1a. Reprinted from Rana et al. (2009).

In Fig. 59, the dilution ratio decreases after the water application for each height until the LNG release was continued. The curves then become almost flat for the higher elevations but slightly increase at 0.5m after the LNG release was discontinued. DR for 2.1 and 1.2 meters, which are greater than 1.0, indicate that initially concentrations at 11.3m downwind distance were much higher than 3.3m distance for these heights. Eventually during the forced dispersion, when the water curtain is active, the ratios become lower than 1.0. The average concentration change by the full cone spray decrease but the curves become flat over time after the LNG spill was stopped. This curtain shows more effectiveness during the lower SR. Because of spiral flow nature, it creates turbulence near the spray region, which allows better and efficient interaction of air with larger vapor flux could than the interaction of the same air with smaller cloud.

Again concentration change at ground level is not very significant because vapor might escape through the gaps. The concentration change for this curtain should be mainly due to effective mixing with air as it failed to push the vapor upward efficiently.

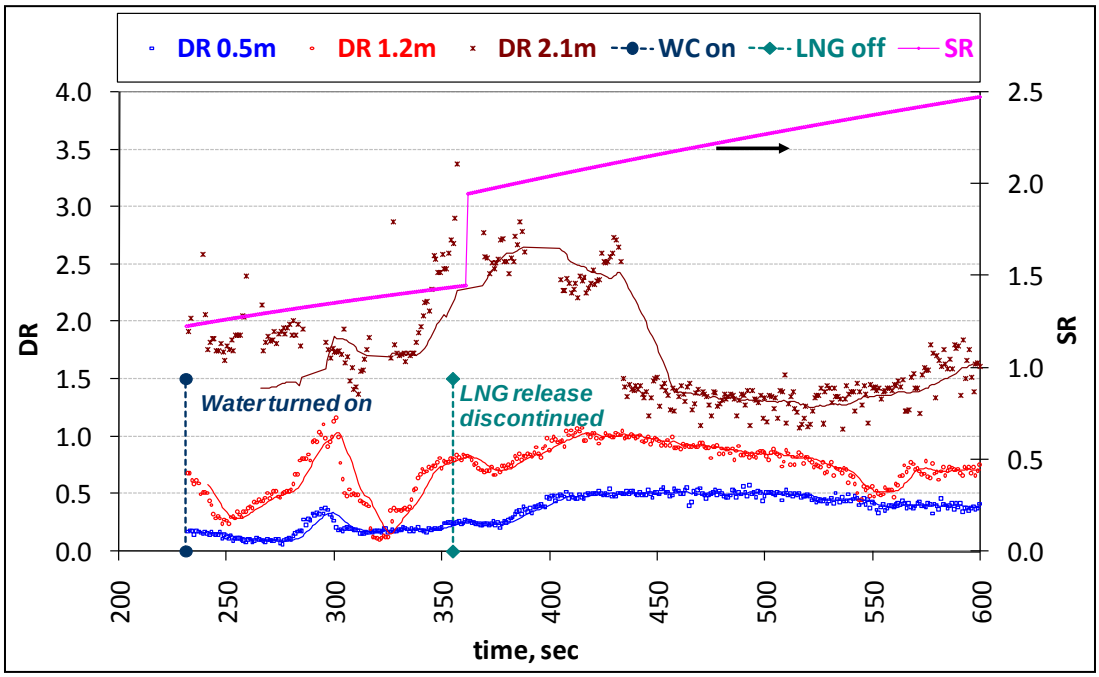

Fig. 60. Dilution and strength ratio: test 2a. Reprinted from Rana et al. (2009).

In Fig. 60, because of the water action, the dilution ratios decrease at 1.2 m and 2.1 m but remains constant at 0.5m after LNG release was discontinued. The curves remain almost steady for lower heights but increase at 2.1 m when the release was still continued. The dilution ratios at 2.1 m are always greater than 1.0. This indicates that concentrations at 11.3 m downwind distance were always much higher than the concentrations at 3.3 m distance at this height. The average concentration change by the

flat fan spray is because of momentum effect. This curtain shows more effectiveness during the higher strength ratio (SR). This is because of the fact that larger momentum creates a solid barrier to the passage of the cloud and pushes it upward. So the dilution by this curtain is mainly through mechanical effects, not by mixing. Above discussion are also supported by the study stated later in this section.

5.4 Experiment of 2008

5.4.1 General Description

The 2008 experiment was the repetition the previous experiment, with some modification in the spill area and spill discharge line. Similar water spray curtains were used in individual test sets and the first water curtain tests was conducted with the full cone spray curtain and the second set was with flat fan curtain. A total of three tests were completed during 2008 tests. The wind speed averaged 4.5 meters per second (10.3 miles per hour) and blew mainly from the south-west to south region. The average ambient temperature during the tests was 296 K and humidity was 50.6%. Table 13 includes the average flow rates and total flow time of LNG and water and average pressure of water at the curtain inlet for each test.

Table 13. Average flow and pressure data for 2008 experiment.

Measured Parameters	Test 1	Test 2: Full Cone	Test 3: Flat Fan
LNG flow rate, m^3/s	3.2×10^{-3}	2.9×10^{-3}	2.6×10^{-3}
LNG total, m^3	2.50	1.74	1.87
Water pressure, kPa [psi]	N/A [N/A]	241.3 ± 34.5 [35 ± 5]	317.1 ± 34.5 [46 ± 5]
Total water flow rate, m^3/s	N/A	26.3×10^{-3}	13.3×10^{-3}
Water flow rate per nozzle, m^3/s	N/A	3.3×10^{-3}	13.1×10^{-3}
Water total, m^3	N/A	26	10

5.4.2 Results and Discussion

During the experiment, gas detectors and thermocouples were placed so that they could cover more downwind distance than the 2007 experiment. The tests were conducted for longer time than the previous year. However data shows very small concentrations and almost ambient temperatures of the LNG vapor cloud were recorded at in different downwind distances and heights. Only the sensors placed much closed to the spill area (at 1m distance) detected concentration and temperature. Readings in further downwind locations were so low that it seemed that the detectors and thermocouples did not sense any vapor cloud to respond. Fig. 61 shows the detector and thermocouple reading 1 m downwind from the spill for test 1 and test 2.

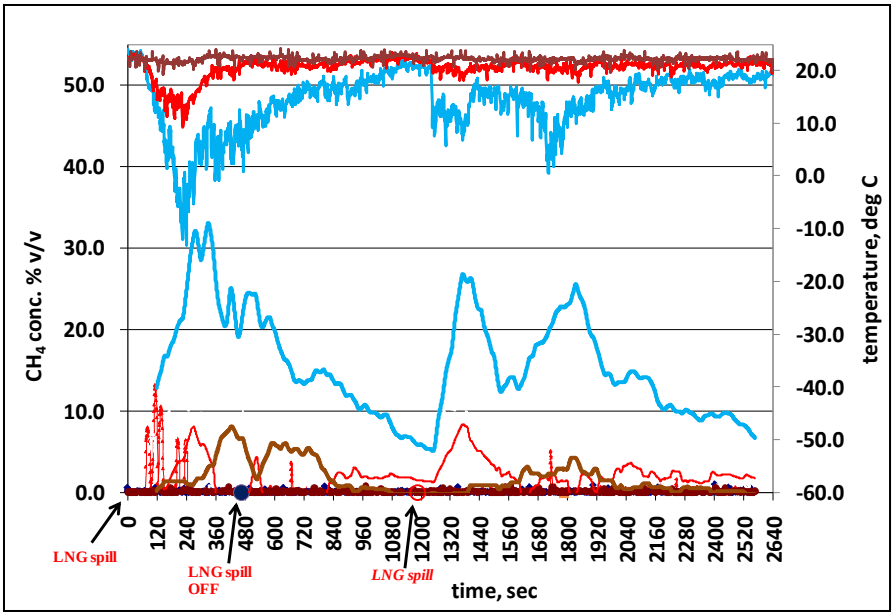

Fig. 61. Concentration and temperature reading at the spill source: 2008 experiment.

In the above figure, the blue line, red line and the brown line is for the sensors at 0.5 m, 1.2 m and 2.1 m elevations respectively The second spill in the figure represent start of the second test. Two causes were identified for the very low readings (almost 0 %v/v) at far downwind distances. First one is the very high wind speed and turbulence occurred during the tests. Because of these, LNG vapor might got diluted and dispersed very early and fast. The higher wind speed expedited the natural dispersion process and the cloud was diluted below flammable limit without the aid of the water curtain.

The second cause is the low rate of evaporation. The setup of the spill area for these tests slightly differs from 2007 tests. The spill container in these tests was a box with 2-inches thick concrete base. The LNG release pipe size was also modified to L-shaped pipe with larger diameter. These two changes affected a lot in vapor generation.

The pipe shape and size reduced vapor flashing (almost none) and turbulence and the spill box reduced heat from the base. Thus the vapor production was significantly reduced and it affected the downwind concentration.

In the tests temperatures of concrete surface were measured. The thermocouple positions inside the base are shown in Fig. 30. Fig. 62 shows the temperature inside the concrete base during the LNG spill for test 1 and test 2.

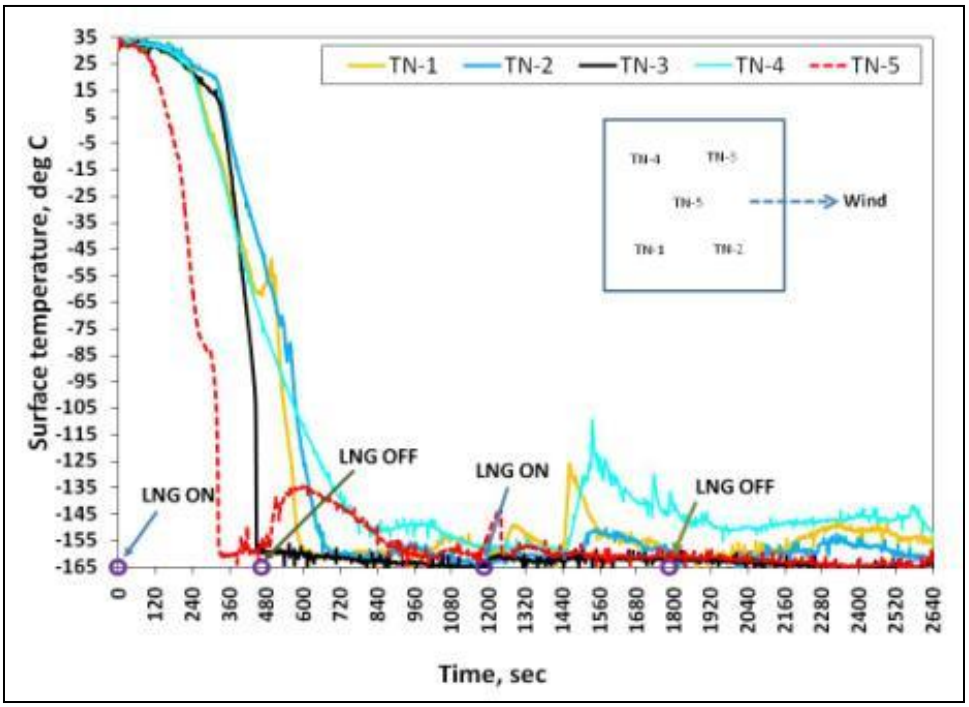

Fig. 62. Temperature of the concrete surface.

The above figure shows the effect of the temperature of LNG in cooling down the concrete base. The mid thermocouple (TN-5) cool down faster than the others as it was closer to the top surface. So it is obvious that the heat transfer from the base reduces

significantly and heat transfer from the surroundings dominates in LNG vaporization. The volumetric LNG flow rate from the truck to the spill location was also recorded in the tests. The vaporization process for these tests is described by the following Fig. 63.

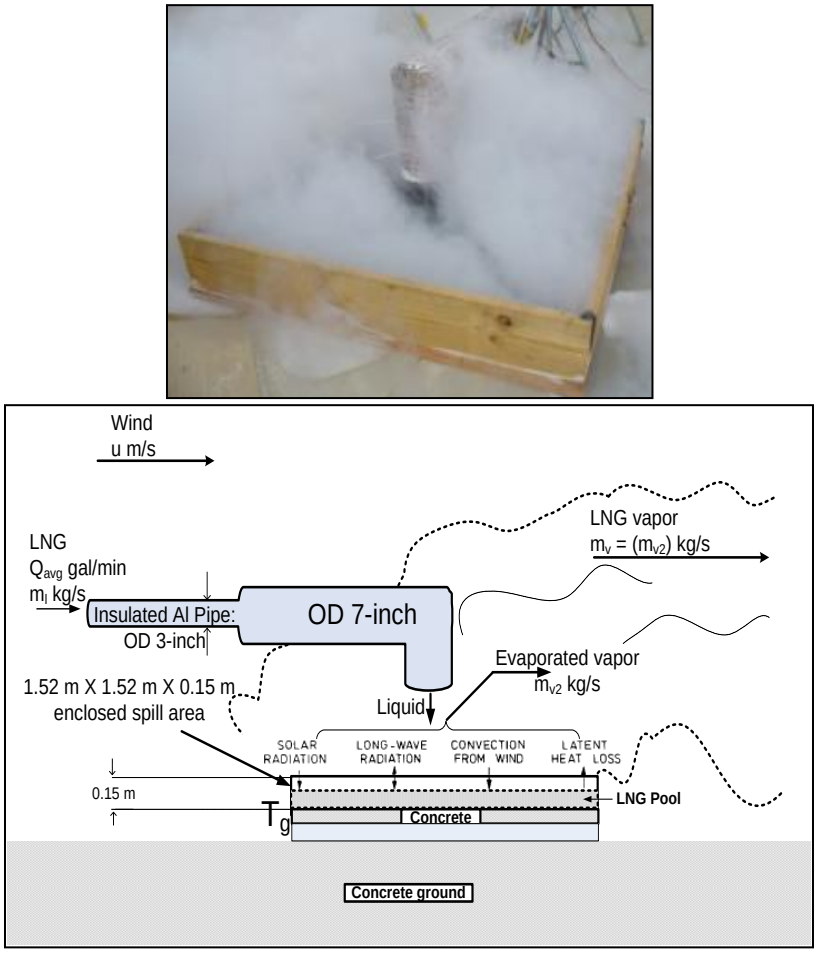

Fig. 63. Formation of LNG vapor cloud from continuous liquid release, 2008 tests.

Vapor generation from the spill for the tests was calculated with the similar analytical relationships described in section 5.3.2.3 are used. Average temperature of the

base is considered in this calculation. Fig. 64 illustrates the vapor rate from the liquid spill for test 1. Here calculation assumes that vaporization rate is uniform throughout the spill surface area.

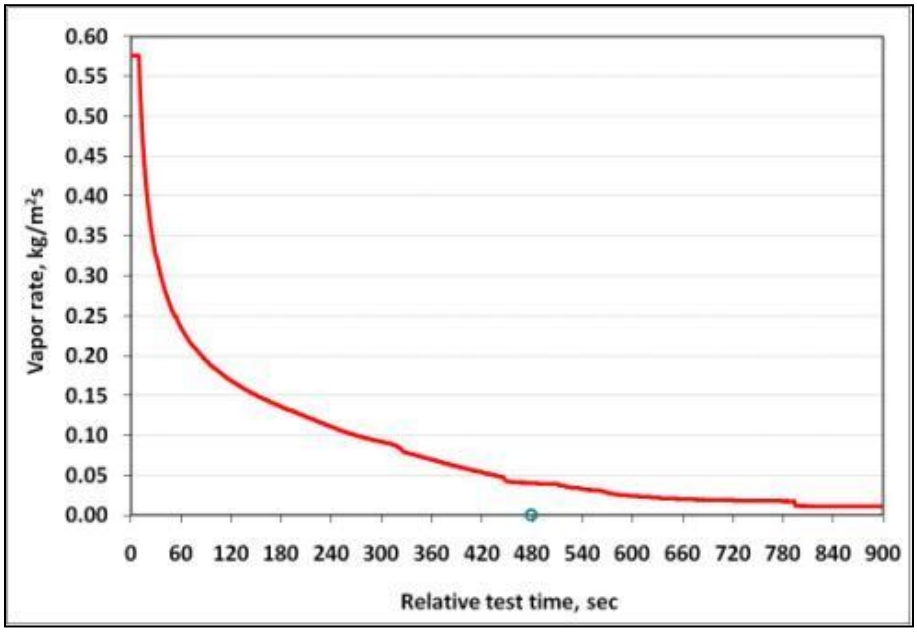

Fig. 64. Vapor rate for test 1 of 2008 experiment.

The above plot, which is for the first spill, demonstrates that the surface cooled very fast and vapor was generated only due to heat transfer from the air. The second and third spill started within a very short time after the first and second spill respectively. From Fig. 62 and Fig. 64, it can be stated that, vaporization rate during the second and third spill, in which water curtains were tested, were relatively lower and produced vapor cloud with smaller size which could not travel further downwind distance.

It is obvious from the test results that only heats from the air and atmosphere cannot produce significant amount of LNG vapor though the liquid release is continuous. In the tests the surface cooled down faster due to very small thickness of the base. Heat transfer from the surface/substrate is the main factor in vapor generation from LNG pool to create a reasonable vapor cloud to travel far downwind distances. Because of higher wind speed, turbulence and atmospheric temperature, the smaller vapor cloud produced from the pool was diluted very early and quite rapidly to become a lighter cloud and thus dispersed upward. Thus as the vapor could not travel much longer horizontal distances, the gas detectors placed in far downwind locations, after the spray area, did not record any significant concentration for further analysis.

5.5 Experiment of 2009

5.5.1 General Description

Spill tests were conducted with three types of water curtains. A total of four spill tests were completed in a 1½ to 2 hour period. The simulated scenario for the tests was continuous LNG release from pipe on a surface. In each test, release was conducted from the 7" OD heavily insulated Al-pipe on top of the surface of water which filled Pit 1 (3.05 m x 3.05 m x 1.22 m). To limit the spread of the LNG pool only to the area of 1.52 m x1.52 m, on the water surface, it was enclosed with four wooden bars of 0.15 m heights. 1.22m deep water settled below the LNG spill area. The test data can be divided into four tests with three water curtains. Two of these water curtains were directed vertically upward and the other one was downward and all positioned perpendicularly to

the prevailing wind direction, at fixed downwind distances from the spill location. The downward curtain was placed closer to the spill than the others. All of the curtains were tested individually at first and finally all together. The chronological order of the curtain tests was: (a) test 1: upward conical, (b) test 2: upward fan, (c) test 3: downward conical, (d) test 4: all three combined. LNG vapor was allowed to disperse naturally for some time between consecutive two tests. The following figure (Fig. 65) shows a snapshot from the first test.

Fig. 65. LNG dispersion test of 2009.

It was observed during the 2007 and 2008 experiments that due to unsteady wind direction and wind's crosswind turbulence, LNG vapor did not always travel straight to the setup. As the outdoor LNG test setup is always based on predicted wind direction and working in the flammable and cryogenic LNG cloud is restricted, the setup cannot be relocated according to the change of wind direction once a test is started. So this time

the vapor dispersion path was covered with barrier walls on the two sides to prevent the vapor from going sideways and escaping the setup. The new setup with barriers performed well as expected.

During the tests, wind blew mainly from the south to north region at 5 m/s average speed and wooden walls were placed in the east and west sides of the dispersion path to guide the vapor towards the curtains and sensors. The average ambient temperature was 28.3º C and humidity was around 40% (RH). Approximately 8.5 m^3 (2300 gal) LNG and 36 m^3 (9600 gal) water were used in the tests. Table 14 includes the average flow rates and total flow time of water and average pressure of water at the curtain inlet for each test.

Table 14. Average water flow rate and pressure data for 2009 experiment.

Measured Parameters	Test 1	Test 2	Test 3	Test 4
	Upward conical (8)	**Upward fan (1)**	**Downward Conical (6)**	**All: combined**
Water pressure, kPa [psi]	327.4 ± 17 [47.5 ± 2.5]	534.2 ± 17 [77.5 ± 2.5]	227.5 ± 13.8 [33 ± 2]	-- --
Total water flow rate, m^3/s	36.5×10^{-3}	11.4×10^{-3}	8.0×10^{-3}	4.55×10^{-2}
Water flow rate per nozzle, m^3/s	4.6×10^{-3}	11.4×10^{-3}	1.33×10^{-3}	--
Water total, m^3	14.6	3.9	1.84	16.38

Both LNG release time and water flow time (turning on and off) were different for the tests. As these field tests deal with flammable LNG vapor, whose phenomena of flow and dispersion are still completely unknown, the decisions of turning on and off the

water curtain and the LNG flow mostly depended on the situation during each test. The detail causes are similar to what has been discussed in section 5.3.

Pressures of both the conical curtains were measured at the curtain pipe inlets and flat fan curtain pressure was measured at the spray head. The conical curtains were fabricated with eight (for upward) and six (for downward) nozzles where as only one nozzle head was used for the flat fan curtain. So less pressure was achieved in the conical curtains. Studying the test data, Fig. 36 and Fig. 37, it can be identified that each upward cone nozzle (TF48) operated around 119-159 kPa and at these pressures, the range of SMD of the droplets is 0.98-0.89 mm. The pressure range was higher than 2007 tests and thus smaller drops could be produced this time. On the other hand the flat fan curtain operated around 259 kPa, which is much less than 2007 (and 2008) tests and the SMD of the droplets at these pressures is 1.94 mm (larger than 2007 and 2008). The working pressure for the downward nozzles (TF24) were 114-170 kPa at which it produces drops of diameter 0.62-54 mm.

Water curtain heights depended on the water pressure. So the heights of the curtains were different for different test. Table 15 lists the average water curtain heights achieved by the upward sprays during the tests. Fig. 66 shows the water curtain heights from snap shots. The total height of the water curtains were measured from pictures and videos. The height was measured by comparing with 2.3 m high tripod poles.

Table 15. Heights covered by the upward water curtains in 2009 experiment.

Test	Water Curtain	Coverage (Avg Height), m
1	Upward conical	4.6
2	Upward fan	4.9
4	All: Conical Fan	 3 4

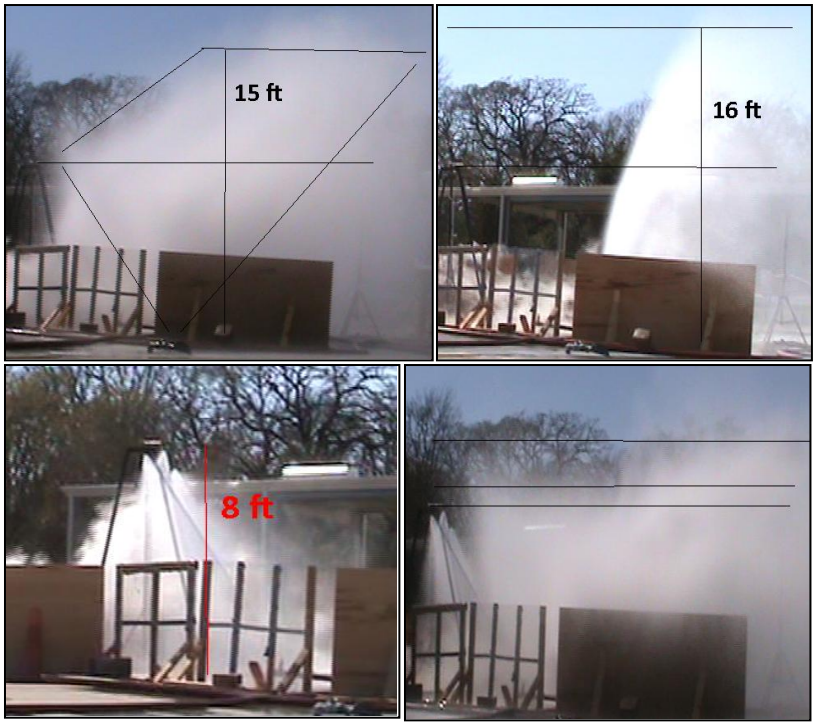

Fig. 66. Water curtain coverage in 2009 experiments. Top left: conical upward, top right: fan, bottom left: conical downward, and bottom right: combined.

5.5.2 Results and Discussion

5.5.2.1 Concentration

LNG was continuously released on water surface to obtain a fixed pool and produce almost a steady cloud. This time only concentration of the dispersing LNG

vapor (methane) cloud was measured continuously in different downwind distance. Though all of the gas detectors sense methane in % v/v level, the three detectors placed in the furthest distance measured methane in % LFL unit. Prior to the experiment, all the gas detectors were calibrated with methane gas to check their accuracy and sensing time. Fig. 32 and Table 7 of section 1 provide information of the test setup and sensors' position. The following figure (Fig. 67) shows average gas detector reading during the entire experiment at the pit edge (0 m) in three elevations. Blue, brown and purple colors represent concentration at 0.5 m, 1.2 m and 2.1 m respectively. The water curtains were located further downwind (see Table 8 for water curtain location). So the vapor cloud at this location was always free from the water curtains' affect when they were activated and gas concentration reading is for natural dispersion.

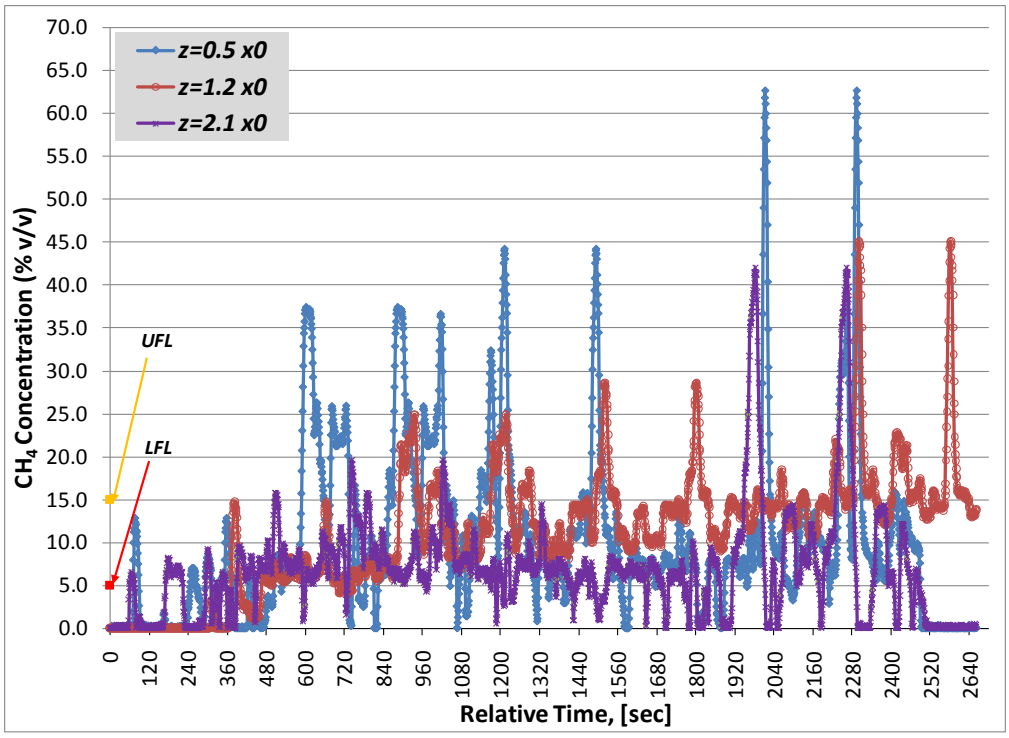

Fig. 67. Average concentration (natural dispersion) data at the pit edge (0 m downwind) all four tests of 2009.

Fluctuations are identified in the methane concentration readings because of location. This location was very close to the spill area and turbulence created by the momentum of the spill and vapor flow from the surface cause the fluctuations. Again as the wind's direction was frequently changing, vapor tried to drift sideways but the barriers prevented the cloud and guide it towards the water spray region. Thus the barriers also take part n creating the turbulence, which might also affect in dilution at this stage.

Concentration at 0 m downwind of the spill started to increase as LNG release was continuous. After the activation of the water curtains in different tests, it is

considered here that they did not affect the LNG vapor at this location because of the wind and vapor direction. Peaks of the concentrations indicate that at 0.5 m above the ground concentration are always higher than the other elevations during the whole time. Again reading at 1.2 m elevation, in this location, is smaller than 0.5 m but higher than 2.1 m. This is obvious as the LNG vapor was coming from the ground surface, concentration should be the maximum at the surface and the concentration should decrease along the cloud height near the spill source. Data also shows that the cloud concentration is always in the flammable region (5-15% v/v). Fig. 68 shows concentration reading approximately 10 m from the pit edge.

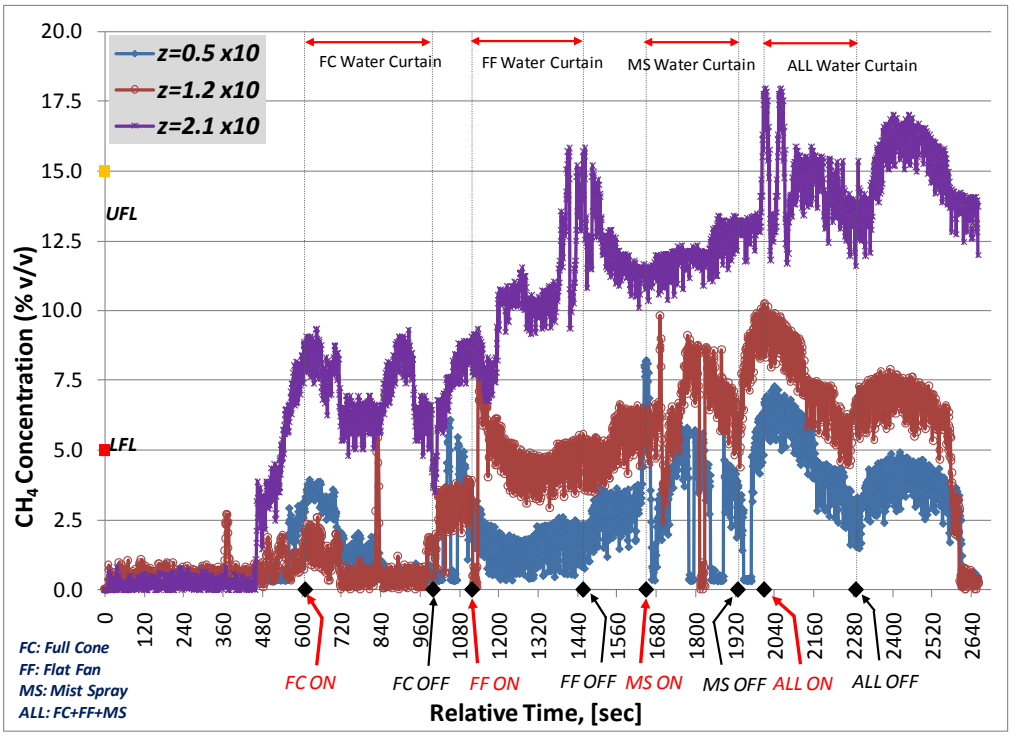

Fig. 68. Average concentration (both natural and forced dispersion) data 10 m from the pit edge for all four tests of 2009.

In the above figure, the blue, brown and purple colors represent data at 0.5 m, 1.2 m and 2.1 m respectively. The figure shows data for all the four runs. Due to time limitations, all of the tests were conducted simultaneously without allowing sufficient time between two runs to completely evaporate the pool from the previous spill. However this limitation should not affect the test result as the main objective of the tests was to identify the effects of each water curtain on continuous LNG release. Thus the figure shows both natural and forced dispersion data and it can be divided into four independent tests and each test duration is as follow:

- Test 1: upward conical curtain ($0 \text{ s} < t \leq 1000 \text{ s}$)
    - $0 \text{ s} < t \leq 600 \text{ s}$: natural dispersion – without curtain activation
    - $600 \text{ s} < t \leq 1000 \text{ s}$: forced dispersion – with water curtain
- Test 2: upward flat-fan curtain ($1005 \text{ s} < t \leq 1445 \text{ s}$)
    - $1005 \text{ s} < t \leq 1110 \text{ s}$: natural dispersion – without curtain activation
    - $1110 \text{ s} < t \leq 1445 \text{ s}$: forced dispersion – with water curtain
- Test 3: downward conical curtain ($1450 \text{ s} < t \leq 1920 \text{ s}$)
    - $1450 \text{ s} < t \leq 1650 \text{ s}$: natural dispersion – without curtain activation
    - $1650 \text{ s} < t \leq 1920 \text{ s}$: forced dispersion – with water curtain
- Test 4: combination of all curtains ($1925 \text{ s} < t \leq 2280 \text{ s}$)
    - $1925 \text{ s} < t \leq 2010 \text{ s}$: natural dispersion – without curtain activation
    - $2010 \text{ s} < t \leq 2280 \text{ s}$: forced dispersion – with water curtain

At 10 m downwind location, the ground level (0.5 m) concentration is the minimum and concentration at 2.1 m elevation is the maximum. Thus it is clear that

LNG vapor gets diluted, lighter and disperses upward as it travels further downwind even when the water curtains were inactive. The purpose of the water curtain is to enhance this dispersion process with some external force. The figure also shows that the ground level concentration at 10 m from the pit edge is almost below the lower flammability limit (5% v/v) but higher elevation cloud concentration is in the flammable zone.

From the spill time to the end of the data recording time, the cloud concentration at different height changed continuously. When no curtains were activated, concentrations continuously increased. Sharp increase in the concentration at the highest elevation demonstrates the natural dispersion process of LNG. Right after the water curtain activation, the concentration data can be considered to be affected by the forced dispersion. Different behavior of concentrations due to forced dispersion in four individual tests proves that the action mechanisms to control LNG vapor cloud were different for the three curtains as well as for the combined curtain. In test 1, concentration trends at all three heights started to decrease immediately after the spray was turned on and the trend continued. In test 2, although concentrations at all three elevations started to decrease immediately after the spray was turned on, concentration readings at 2.1 m started to rise, after some time. This increasing trend became higher than the natural dispersion case. However the concentrations at the lower elevations kept decreasing. In the third test, ground concentration (0.5 m) shows inconsistent decrease but the concentrations at higher elevations continued the increasing trend, but at smaller

rate. Finally the combined effect of all the curtains decreased the concentration in all elevations, but the decreasing rate at 2.1 m was lower than the other two elevations.

Thus all of the curtains show some effects in the LNG vapor cloud concentrations but the effects are different in terms of the mechanisms. The full cone water curtain could not provide enough momentum to the cloud. The reduction in gas concentration was mainly by mixing with air. However, the flat fan water curtain was dispersing the LNG vapor upward mainly by imparted momentum to the cloud, not by effective mixing and dilution with air. The results from the downward spray showed concentration increase in upper elevations. As the sprays were down facing, it was not possible for the water curtain to impart upper momentum to the cloud. Only potential cause is that the vapor became warm and dilute by the spray action. So the cloud dispersed upward and concentration at 2.1 m height increased. The analysis discussed more elaborately later in this current and the next sections.

To understand the effectiveness of the water curtains in reducing LFL distance, %LFL (0-5% v/v) concentration at similar elevations was measured 14 m from the spill edge in the tests. Data showed that LFL concentration was reduced significantly in all the three heights, in all four tests. Fig. 69 illustrates the LFL concentration data recorded at 14 m downwind distance from the spill.

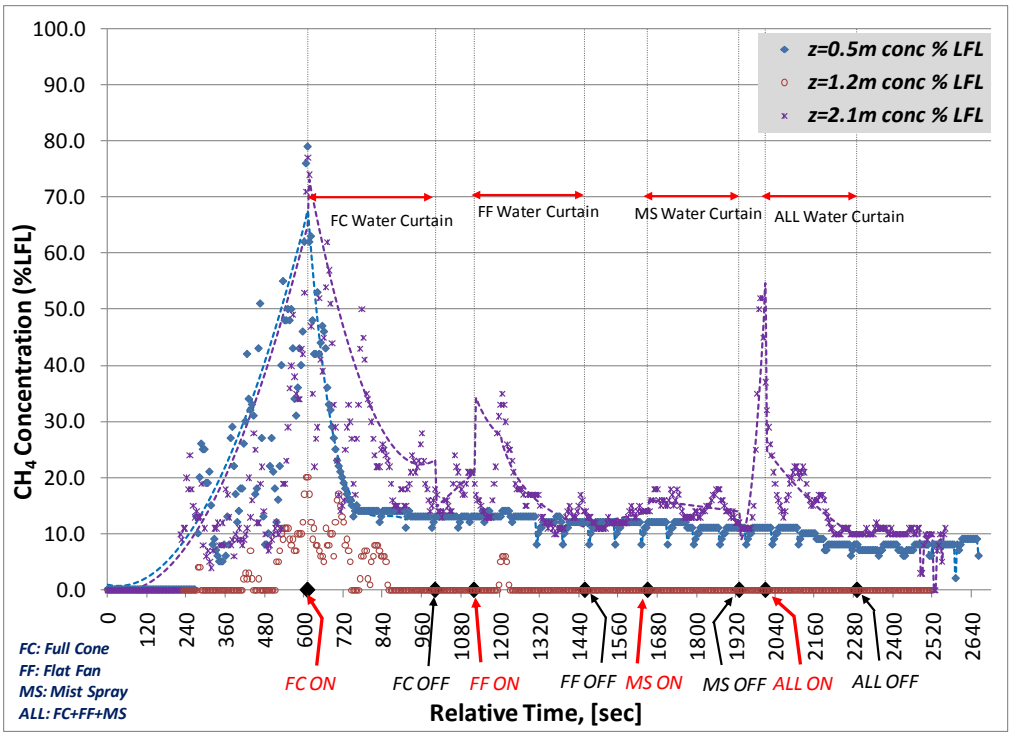

Fig. 69. LFL concentration (both natural and forced dispersion) data 14 m from the pit edge for all four tests of 2009.

5.5.2.2 Vaporization of LNG

In 2009 experiment, several thermocouples were placed in the LNG spill area below and above the water surface. Thermocouple locations are given in Fig. 33. Difference between two consecutive thermocouples' heights was 3.175 cm. The purpose of using these thermocouples was to measure the evaporation rate during the LNG release. The LNG spill area was enclosed to contain the liquid LNG during the tests with wooden bars. The area of the spill location was 1.52 m × 1.52 m and the depth of the enclosed area was 30.48 cm above the water surface. Nine thermocouples were placed in nine different elevations to cover 25.4 cm height from the water surface. Fig. 70 shows

the thermocouples' temperature reading at eight different heights from the water surface. One thermocouple installed at 22.225 cm elevation failed during the experiment.

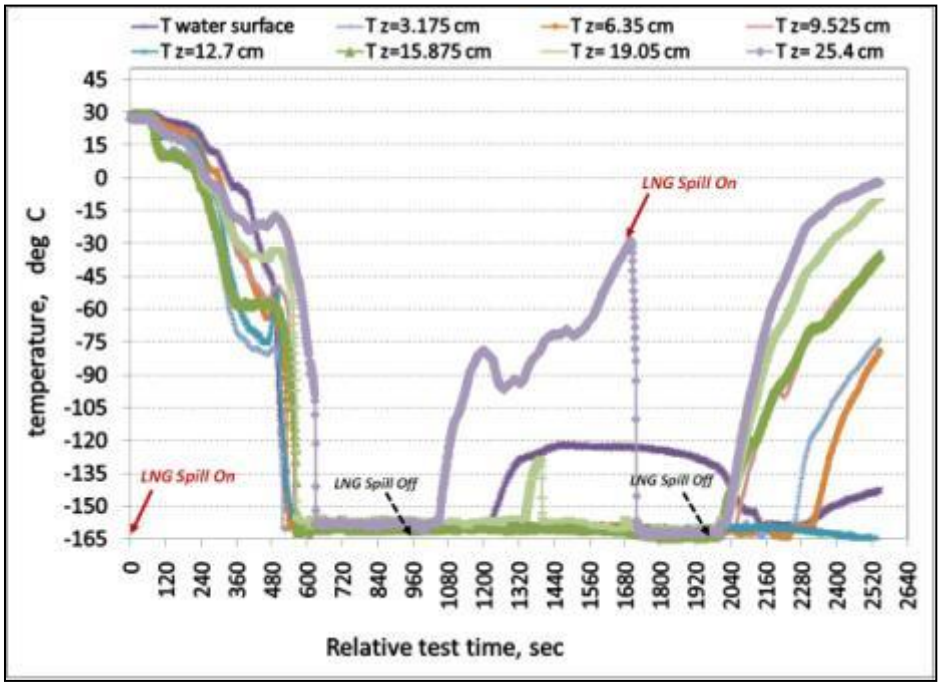

Fig. 70. Temperature measurement of the liquid pool at different heights for 2009 experiment.

When LNG was spilled onto the water surface, initially all of the liquid evaporated instantly due to large temperature difference between the LNG and the water. However continuous release of LNG eventually started to cool down the water and then LNG started to accumulate above water. As the pool was contained with a wooded enclosure, liquid level started to rise. Portion of the pool continued to evaporate due to the heat transfer from the water and the surrounding. A constant rate of 6×10^{-3} m^3/s

(approx) LNG release rate was maintained during the tests and it was turned on and off to avoid overflow from the spill enclosure. The above figure shows that the cryogenic LNG cooled down the water surface and the thermocouples, placed in different heights, rapidly. It indicates that the heat transfer from the water was enough to instantly vaporize the all of the continuously released liquid. Fig. 71 shows the vaporization rate calculated from the temperature data. Evaporation rate is calculated from the temperature reading by using the following relationship:

$$\textit{Evaporation Rate} = \textit{Release Rate} - \textit{Accumulation Rate} \tag{48}$$

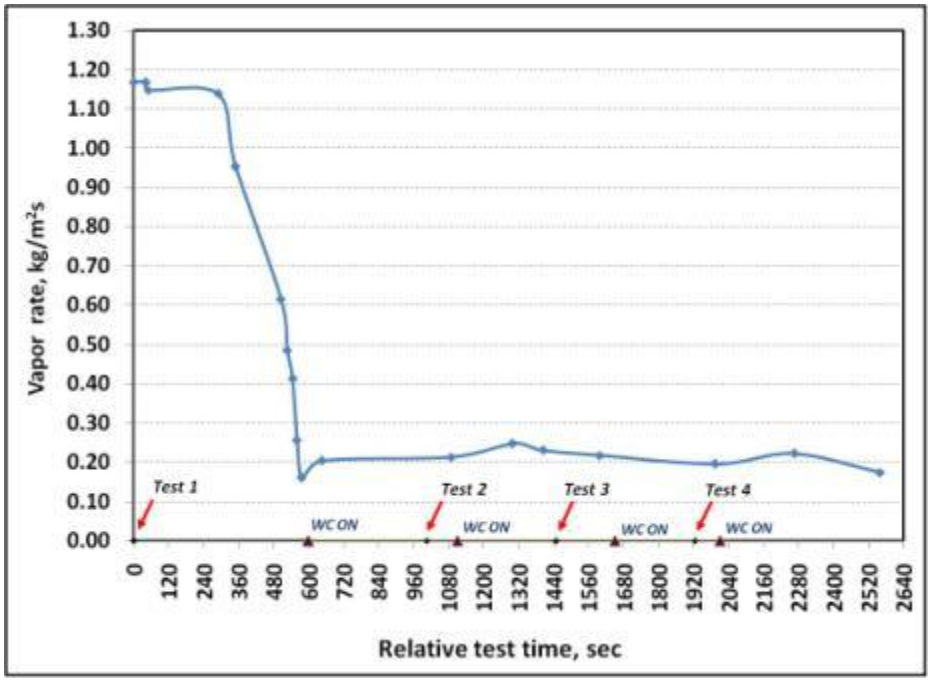

Fig. 71. Vapor rate from the LNG pool for 2009 experiment.

As the release rate is considered to be constant, accumulation rate is the main factor in calculating the evaporation rate. The accumulation rate was calculated form the temperature reading. Due to continuous LNG release (and evaporation), when LNG pool reached a certain height, the thermocouple positioned at that location instantly read the liquid temperature, -165° C (approximately). As LNG was continuously flowing, the thermocouple at that level and all the thermocouples below remain at -165° C (or very close). After some time, the temperature of another thermocouple installed at upper elevation changed to -165° C, as the liquid level continued to increase. The ratio of the difference between the heights (Δh) of the thermocouples and the time difference ($\Delta t=t_2-t_1$) for the liquid pool to reach from one thermocouple to another, gives the velocity ($\Delta h/\Delta t$) of liquid level rising. Accumulation rate is then calculated by multiplying this ratio with LNG density (450 kg/m^3). The accumulation rate calculated for a certain time difference is considered to happen at the average of those two times, i.e. at $(t_1+t_2)/2$. Results show that vaporization rate initially was close to the spill rate and then it decreased rapidly almost to a constant value. Throughout the period the water curtain remained active the vaporization rate remained constant at 0.2 ($\pm$0.05) kg/m^{2}s. The calculation assumes that the vaporization rate is uniform throughout the 1.52 m × 1.52 m spill surface area.

5.5.2.3 Dilution by Water Curtain

The water curtain effectiveness is analyzed here in terms of concentration ratio (dilution ratio). The ratio is defined here as the ratio of the average concentrations at 0 m

and 10 m downwind distances and at each height. The dilution ratio (DR) relationship provided earlier (eqn 45) in section 5.3.2.4 is similar to this concentration ratio used here. It is assumed that for each height concentration at 0 m is what coming into the water spray and concentration at 10 m is what going out of the spray. As this ratio is the ratio of concentrations at two downwind positions, an effective water curtain is expected to reduce the ratio to very lower value. In the calculations, the downwind progress of cloud is considered by assuming that the cloud moves downwind with the constant speed of the wind (5.1 m/s). Fig. 72 to Fig. 74 show the concentration ratio calculation results for the tests.

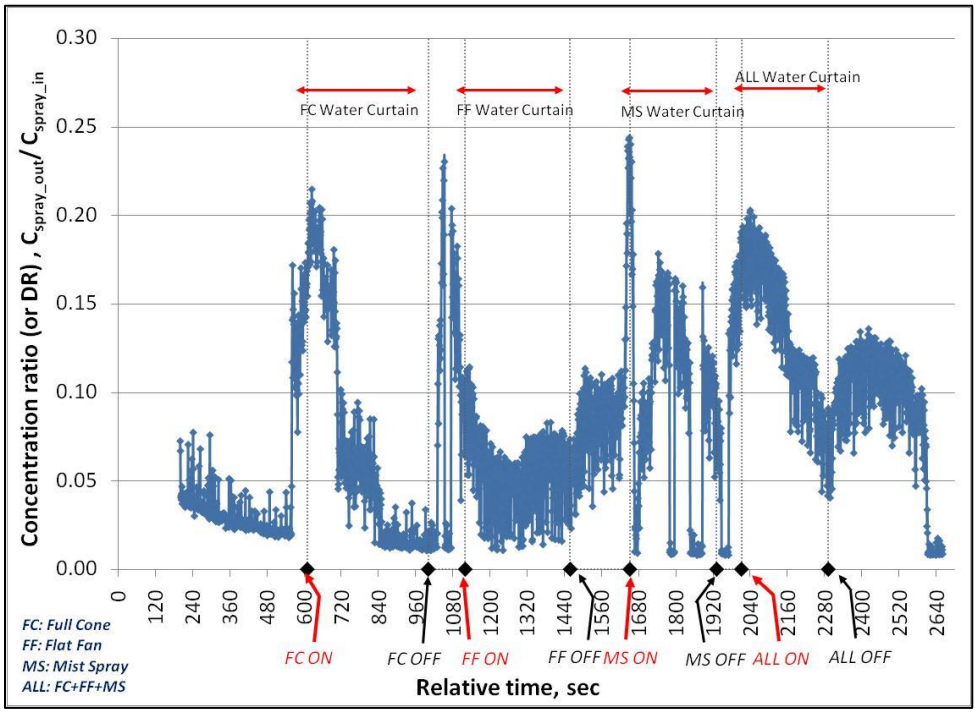

Fig. 72. Concentration ratio at 0.5m elevation in 2009 experiment.

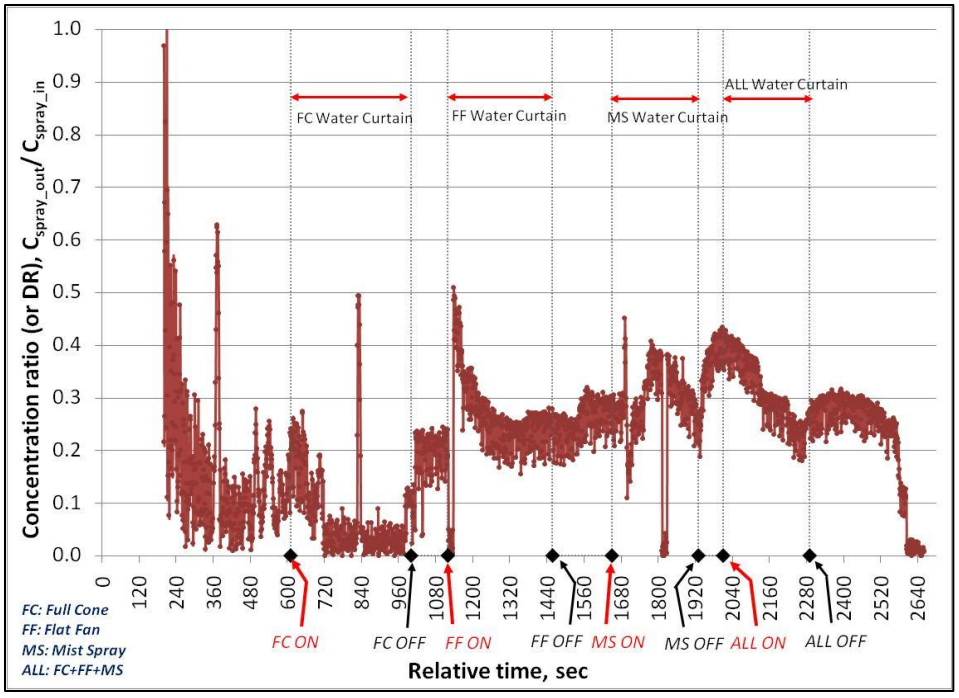

Fig. 73. Concentration ratio at 1.2 m elevation in 2009 experiment.

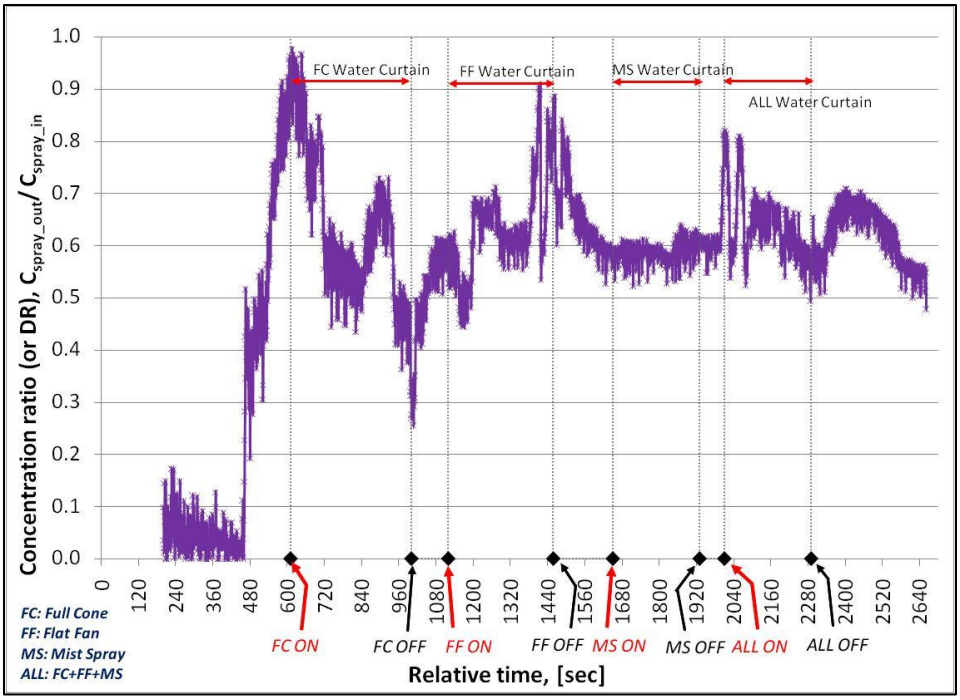

Fig. 74. Concentration ratio at 2.1 m elevation in 2009 experiment.

The figures identify that during the times when any of the sprays was active, the concentration ratios show increasing trends in all heights. This is obvious as the LNG spill on the water surface was continuous, concentration at 10 m distance should keep on increasing over time if there are no interruptions for any mitigation device. In the first test with the upward conical curtain, the ratios decreased right after the water application for each height. Decrease in the ratios for all the heights indicates that the curtain controlled the cloud mainly through dilution and mixing effects. As the concentration at 2.1 m did not increase, it means that it did not lift the cloud upward and thus could not provide enough momentum from the droplet velocity to the cloud. Results after the fan spray action show that the ratios decreased in 0.5 m and 1.2 m elevations but significantly increased at 2.1 m height. The larger (coarser) droplets of the spray mainly imparted high momentum to the cloud, which reduced the concentrations at the lower elevations but increased the 2.1 m elevation concentration right after the spray region. In the downward spray (mist type) calculations, the concentration ratio decreased at the ground level and remains almost constant throughout the water flow time at higher elevations of 1.2 m and 2.1 m. The fact is this spray could not impart upward momentum as it is faced downward. The concentrations at the upper portion of the vapor cloud only could increase if the cloud disperses upward by becoming lighter. So the spray was effective in warming or diluting the LNG cloud. The action of the combined water curtain system reduced the concentration ratio in all heights of the vapor cloud. So each of the curtains showed their efficiencies in different mechanisms and thus the cloud concentration downwind of the spray region was reduced. However, the reduction by the

combined action is not very significant compared to the single upward conical spray action. Based on the above results the conical spray was much more effective than the other two and combined in terms of dilution and mixing. The downward spray showed better results in terms of heat transfer. To support the above discussion and to determine the actual effectiveness of the sprays of different drop size, width and flow pattern, more analysis of the experimental data is conducted later in the section with support from some theoretical calculations.

5.6 Study of Water Spray Action Mechanisms

Generally some physical processes are involved when a water spray is used to control and disperse LNG vapor cloud. These processes may include (i) mechanical effects of creating a barrier to the passage of a gas cloud, (ii) entrainment of air into the water spray and dilution of the gas cloud with entrained air, (iii) thermal effects between the gas cloud, water droplets, and entrained air, and (iv) imparting upward momentum to an incoming cloud when the water flow is upward. Actual actions of a water spray may consist of all or any combination of these mechanisms. Since the overall interaction process among the vapor cloud, air and water droplets of a spray is a sophisticated phenomenon as well as complex, study of the spray mechanisms and their effects has been conducted individually in this research. As the effect of barrier was observed during the experiments; the study includes effects of heat transfer, air entrainment and momentum.

5.6.1 Heat Transfer by the Sprays

Heat transfer calculation is performed to identify the rate of heat transferred to the cloud by the water curtain during forced dispersion process. In the experiments, thermocouples were installed in the spray regions to measure the water temperature when the sprays were activated. Thus the water spray temperature was monitored. During the natural dispersion process, when the sprays were inactive, temperature readings were indicating the air/cloud temperature. As soon as the water was turned on the reading started to indicate the water drop temperatures because the thermocouples were in the spray area and water influenced the reading. Form the temperature reading the heat loss to the cloud (and air) per unit mass of water was determined by the following relationship:

$$q = c_{p_{water}} \left(\overline{T}_{water} - T_{reading} \right) \tag{49}$$

Thermocouples were installed in three elevations and in different crosswind locations in the spray area. It was observed that after the water curtain activation and due to LNG vapor –water interaction, the temperature reading reached water temperature instantly and then started to drop. The thermocouples placed in the LNG vapor cloud path showed more effective readings. These thermocouples were mainly located in the middle of the spray region. This phenomenon indicates that the water curtain was losing heat due to the better interaction with colder cloud (and also the air). Temperatures recorded in three elevations (0.5 m, 1.2 m and 2.1 m) were very close and so in the heat transfer calculation average of temperature recorded in different heights is used to represent average temperature of the spray region. Fig. 75 and Fig. 76 show the average

temperature change with respect to test time, calculated from average spray temperature in 2007 and 2009 experiments.

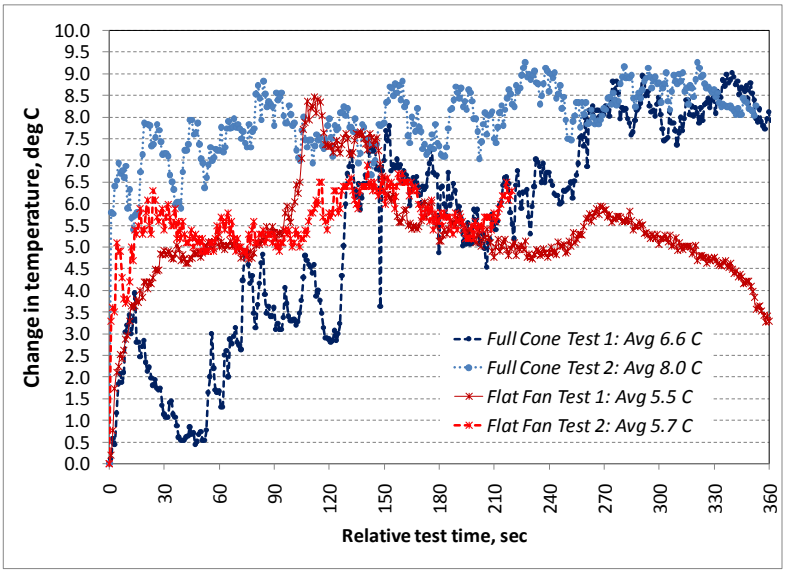

Fig. 75. Change in water spray temperature reading in 2007 experiment.

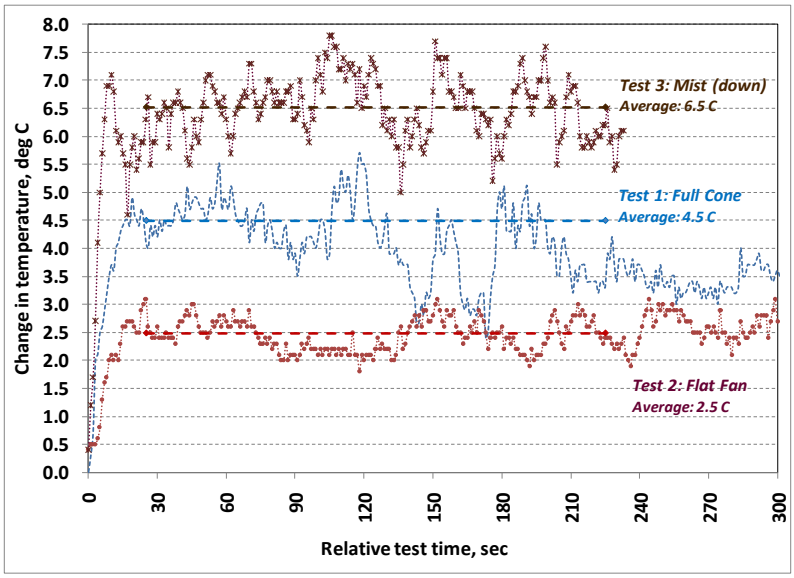

Fig. 76. Change in water spray temperature reading in 2009 experiment.

Initial water temperature for 2007 and 2009 experiments were 19.64 (±0.51) °C and 28 (±0.5) °C respectively. Table 16 lists the average temperature changes and calculations of heat loss by the water spray from the two experiments. Calculations were performed assuming $c_{p\ (water)} = 4.186$ J/gm°C.

Table 16. Average temperature change and heat loss calculation.

Experiment	Water Curtain [# of nozzle]	Water flow rate/nozzle $\times 10^3$ [m^3/s]	Droplet size (SMD) [mm]	Change in spray temperature, ΔT_w [°C]	Heat transfer by spray, q_{avg} [J/gm]
2007	Full Cone [7]	2.2 ±0.70	1.35 ±0.05	6.61 ± 2.2	27.67
		2.2 ±0.14		8.03 ± 0.65	33.61
	Flat Fan [1]	15.1 ±0.46	1.55 ±0.05	5.47 ± 0.98	22.90
		15.5 ±2.30		5.68 ± 0.50	23.78
2009	Full Cone [8]	4.6 ±0.70	0.935 ±0.045	4.50 ± 0.4	18.84
	Flat Fan [1]	11.4 ±0.50	1.94 ±0.05	2.50 ± 0.27	10.47
	Mist Cone [6]	1.33 ±0.07	0.58±0.04	6.50±0.55	27.21

The water curtain temperature change was not very significant and thus calculated heat released by the water curtain is also low. However it is clear from the results that full cone spray provides higher heat than the fan spray. Though the fan spray can give higher flow rate and larger crosswind coverage, temperature change by the cone spray is larger due to relatively smaller drop size and wider spray area (downwind). Although curtains were closer to the spill source as well as the water flow rates and water curtain coverage were relatively higher in 2009 tests compared to 2007 tests, the

temperature change and thus the calculated heat losses by the water were lower in 2009. It may be because the LNG vapor was already warmed up due to the difference in atmospheric conditions. The temperature, heat flux and wind speed were higher in 2009 than 2007. Therefore it can be concluded that water curtain is able to provide heat to the cloud due to heat transfer between droplets and LNG vapor cloud. Overall the results show that water curtain can provide heat to the mixed gas cloud and the full cone curtain is more effective in terms of heat transfer than the flat fan spray. However the mist type spray provided highest heat to the cloud in 2009 tests. So the heat transfer mainly depends on drop size and spray width.

It was also observed that methane concentration was somewhat little higher further downwind (13.7 m) than right after the spray region (11.3 m), for all the tests in 2007. This indicated that LNG vapor was not warm enough to become positively (/neutrally) buoyant. So instead of dispersing upward by the curtain action, LNG vapor fell down to the ground at further downwind distances. Ineffective heat transfer between water, LNG and air could not dilute the LNG vapor significantly. It could be implied from the results that the heat from both curtains was not adequate in 2007. This might be because of the water drop sizes and droplet terminal velocities. Both the droplet size and droplet velocity were not adequate enough to create large surface area and higher contact time to heat the vapor adequately. This situation did not repeat in 2009 because when the water curtain interacts with the LNG vapor, the cloud was already warmer naturally. Higher atmospheric temperature, solar flux and wind speed made the LNG vapor cloud warmer and lighter near the spill source, before it reaches the water curtain. So the heat

exchange between the water and vapor/air was not very significant and the water curtain increased the vapor cloud's dispersion process mainly by dilution and momentum effects.

5.6.2 Air Entrainment into Sprays

Water sprays are used for the dispersion of hazardous vapor clouds mainly using the feature of air entrainment into the spray. Air entrainment into the water spray occurs due to the momentum transfer between the water droplet and surrounding air. When entrained air comes into the cloud, the gas cloud concentration can be reduced depending on the degree of the mixing between them. A theoretical analysis of the air entrainment into the sprays is carried out in this research with the simple air entrainment model discussed earlier in section 4. 60° full cone and 180° fan type nozzles were used in 2007 experiment to make full cone and flat fan water curtains. Both of them were upward water curtains. In the 2009 experiments an additional downward water curtain made with 60° full cone spray were introduced.

This study mainly focuses on determining the entrained air velocity and volumetric air entrainment rate along the axis of the sprays used in the experiments. Though the experiments were conducted in an outdoor facility, this analysis considers quiescent surroundings and assumes that wind velocity has no effect on the air entrainment into the spray. The model, used for the analysis, can solve for both upward and downward conical sprays. However it was studied and mentioned with evidence by Heskestad et al. (1981) that this type of model can also accommodate nonconical spray

with appropriate approximation. The fan spray used in the research produces flat shaped flow pattern which is not constant along the height. It was observed that flow pattern makes approximately 15° angle at the nozzle tip. So to conduct calculation for the fan spray, a 15° conical flow pattern is considered to resemble a flatter spray pattern than usual wide conical spray. For the calculation it is necessary to have information on some parameters. The parameters, γ, β and ξ in the model depend on spray cone angle, discharge velocity and nozzle diameter. Information on cone angles and diameters are specified in the spray specifications and the discharge velocities used in the calculation were determined from experimental measurements of water flow rate and water pressure. The solution of the model is nondimensional form. The parameter C_M was used to convert the nondimensional result to dimensional form assuming $C_M = 0.95$. The assumption was made by considering the initial droplet velocity was almost equal (95%) to the nozzle discharge velocity. Sauter mean diameter (SMD) was considered for the drop size. For the water and air property it was assumed that $\rho_w = 1000$ kg/m^3, $\rho_a = 1.2$ kg/m^3 and $v_a = 15.11\times10^{-5}$ m^2/s. Fig. 77 and Fig. 78 show the theoretical calculation of entrained air velocity into the spray used in the experiments.

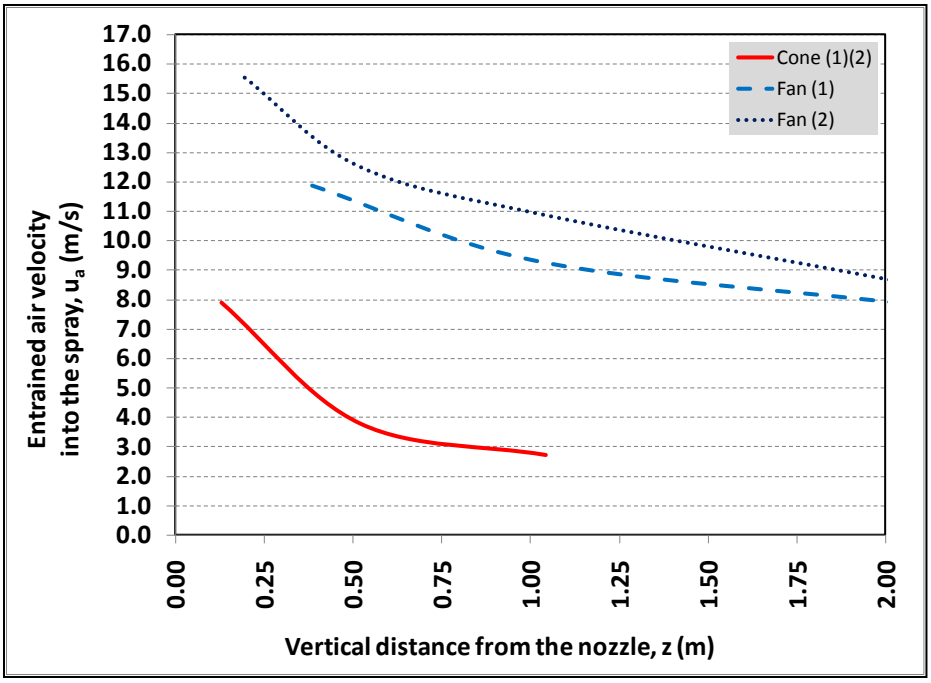

Fig. 77. Entrained air velocity into the sprays from 2007 experiment.

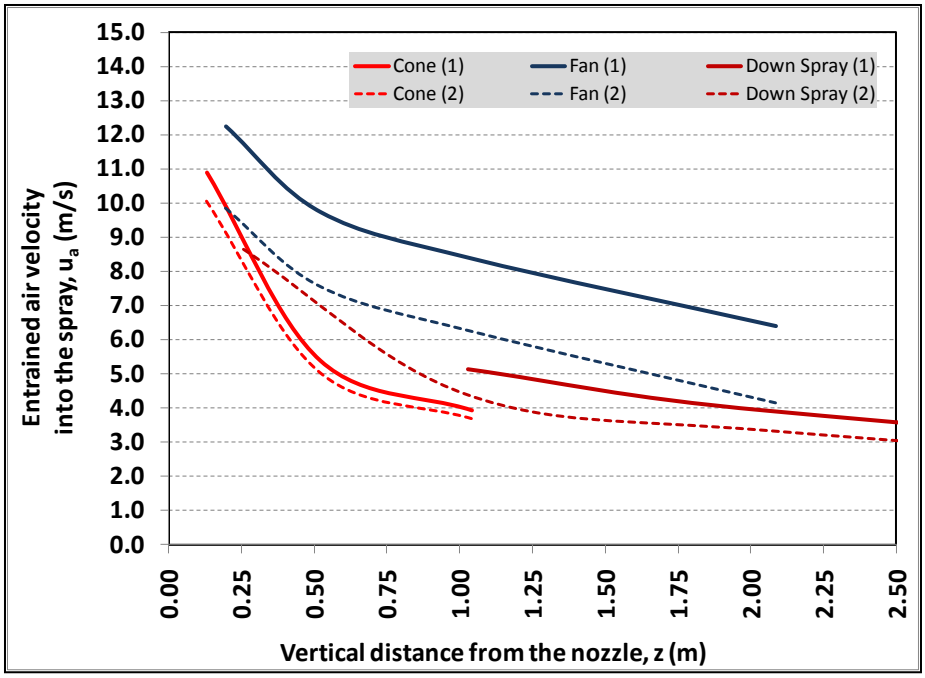

Fig. 78. Entrained air velocity into the sprays from 2009 experiment.

Fig. 77 shows theoretical calculation of upward air entrainment velocity along the axis of a single spray pointed vertically upward. The 2007 experiments included two tests with the full cone sprays and two tests with the fan sprays. As the conditions for the conical spray in two tests were almost similar, the figure shows one solid red line for this spray. The dotted and broken blue lines are for the fan spray tests. So from the figure it is clear that air velocity along the conical spray axis was much lower than for the fan spray. It also indicates that the conical spray could not provide higher coverage. This indicates that lower nozzle pressure and smaller drop size is not sufficient enough to entrain air of higher velocity and to create higher coverage when the flow is upward. Due to improved water curtain design, in the 2009 experiments (Fig. 78) higher pressure was achieved at the nozzle inlet and thus the upward conical spray entrained air at higher velocity along the axis and close to the nozzle tip it was almost close to the velocity of air entrained into fan spray. The downward conical spray entrained air at higher velocity than the upward conical spray as it was flowing in the downward direction. Downward spray also provided higher coverage depending on how high it was installed. The entrained air velocity into the upward fan spray was always larger than conical sprays, both upward and downward. This was because its nozzle pressure was much higher than the other two and its drops are also larger. For a similar flow direction large droplets entrain air at higher velocity than smaller droplets. Entrained air velocity creates air turbulence inside the spray region and thus influences the mixing of travelling vapor cloud with the entrained air. Overall the results show that air entrainment velocity is a strong function of spray angle, droplet size, droplet velocity, and spray direction.

According to the requirements, it is also necessary to flow air not only at a sufficient velocity, but also to deliver air in a sufficient quantity to ensure adequate dilution. The volumetric air entrainment rates were also calculated for each different spray nozzle used in the experiments. Fig. 79 and Fig. 80 show the theoretical calculation of volumetric air entrainment rate into the spray.

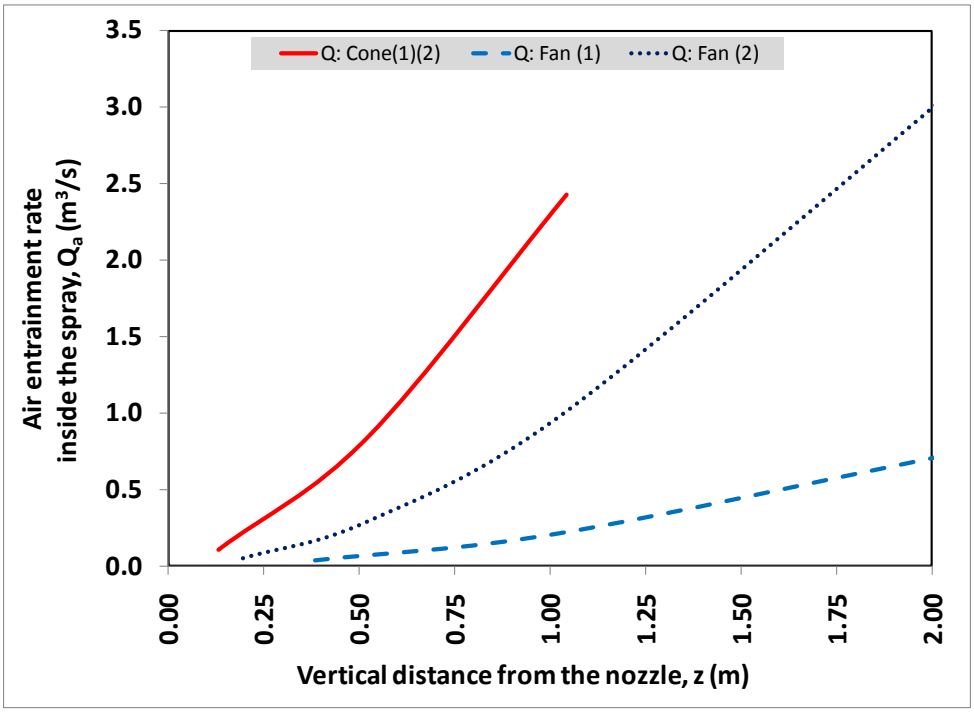

Fig. 79. Volumetric rate of entrained air into the sprays from 2007 experiment.

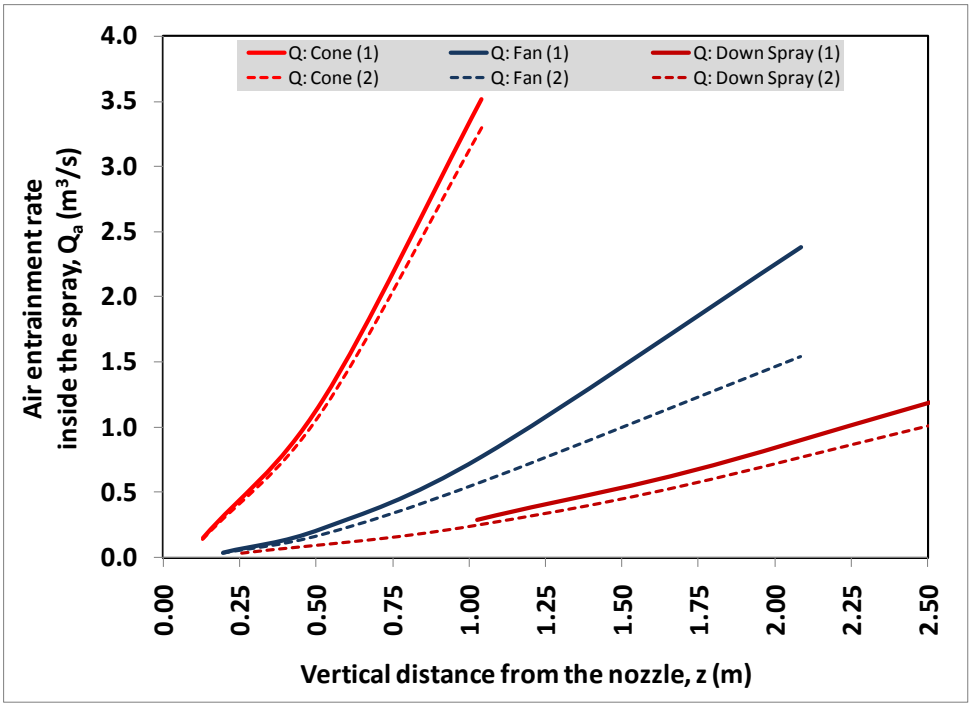

Fig. 80. Volumetric rate of entrained air into the sprays from 2009 experiment.

Volumetric air entrainment rate calculations show that the upward conical spray delivered more quantity of air inside the spray region among the three spray nozzles used in the tests. As the air entrainment rate depends both on air velocity along the spray and cross sectional area of the spray, the results show higher value for the upward conical spray. Therefore though the air velocity inside this spray is smaller than the upward fan spray, it should provide better dilution due to the larger quantity of air. The downward conical spray should deliver largest quantity of air inside the spray, as the droplets are the smallest among the three sprays. For the downward spray the volumetric air rate increases sharply along the vertical distance. The figure only shows the value up to certain heights. However the air velocity would also decrease along the distance until

it reaches the terminal velocity. Terminal velocity usually remains almost constant and causes poor mixing and dilution at that height due to less turbulence. So it can be concluded here that the upward conical spray with medium drop size and wider spray coverage shows best performance among the three sprays in terms of air entrainment and dilution.

5.6.3 Momentum by the Upward Sprays

The momentum imparted to the LNG vapor cloud by the water sprays depends on the nozzle pressure, droplet velocity and droplet size. Rate of momentum imparted to the cloud by the water droplets along the vertical spray distance were calculated theoretically with air entrainment model and are shown in Fig. 81 and Fig. 82. The calculations show that the momentum imparted by the fan spray along the spray axis is much higher than the momentum by the conical spray in both the experiments. So this indicates that the LNG vapor was uplifted to higher elevation by the fan spray where as the conical spray could not provide enough momentum to disperse the cloud upward.

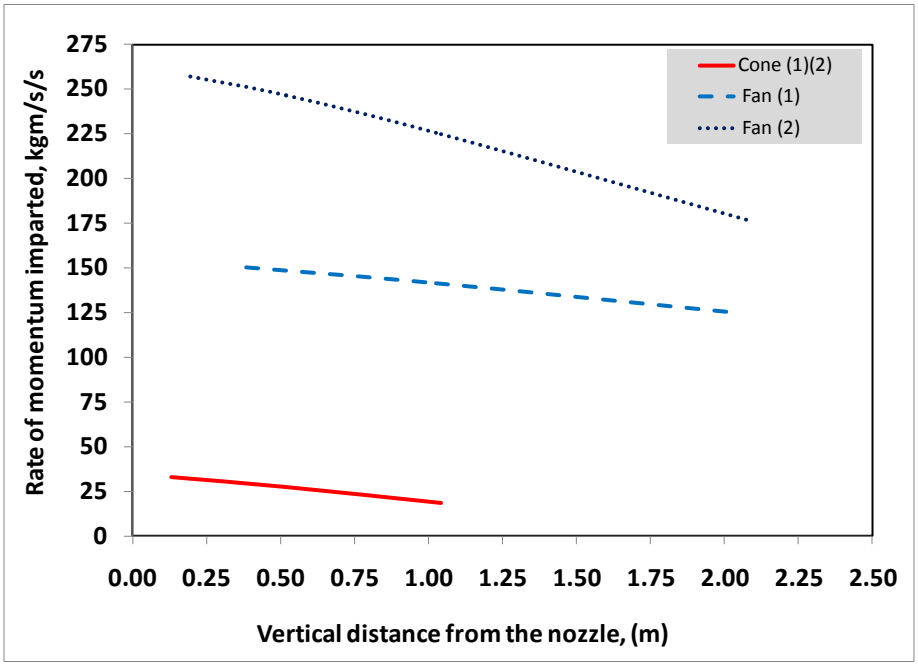

Fig. 81. Upward momentum from the water droplets from 2007 experiment.

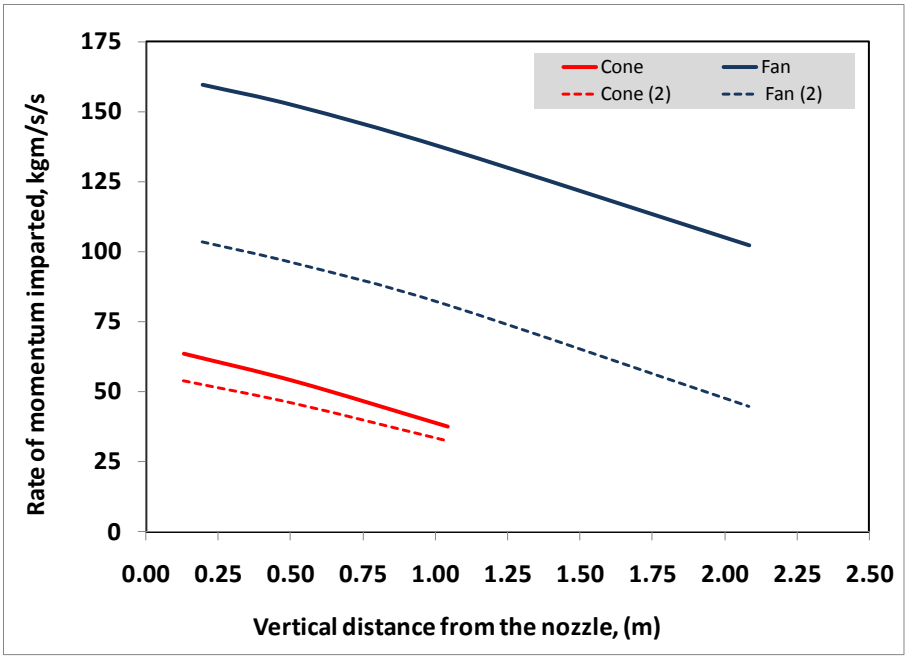

Fig. 82. Upward momentum from the water droplets from 2009 experiment.

5.7 Overall Effects in Forced Dispersion

More analyses are performed to determine the downwind trend of concentration at a certain height. Concentration profiles at three elevations (0.5m, 1.2m and 2.1m) is preferred for the analysis to study the overall dispersion effect of water curtain in reducing CH_4 concentration of the vapor cloud. Downwind concentrations at higher elevations (1.2 m and 2.1m) in this analysis also give an idea about the momentum effect of the water curtains to disperse LNG vapor upward. Previously, data showed concentrations at certain height and downwind locations at different times. This analysis selects point values of concentrations at different downwind distances by averaging concentration data within 1 to 1½ minutes before and after the water curtain activation, and after the LNG flow discontinuation. Fig. 83 and Fig. 84 show the effect of the two water curtains, in the downwind concentration trends near the ground level (at z=0.5 m). These figures are based on four tests conducted in 2007; two of which were with full cone curtains and the rest two were with the flat fan water curtains.

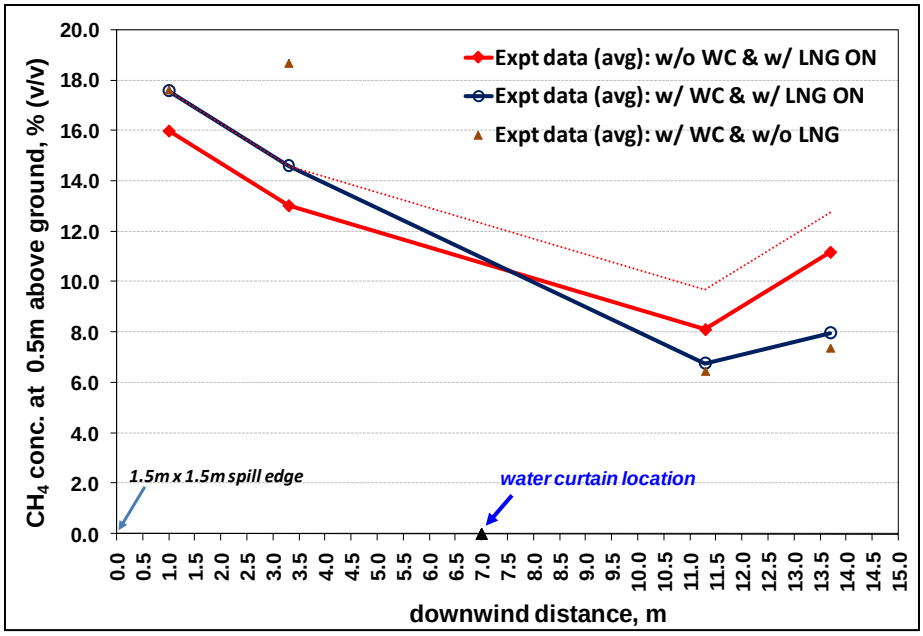

Fig. 83. Downwind concentration near ground level (at 0.5m elevation): full cone curtain test 2007.

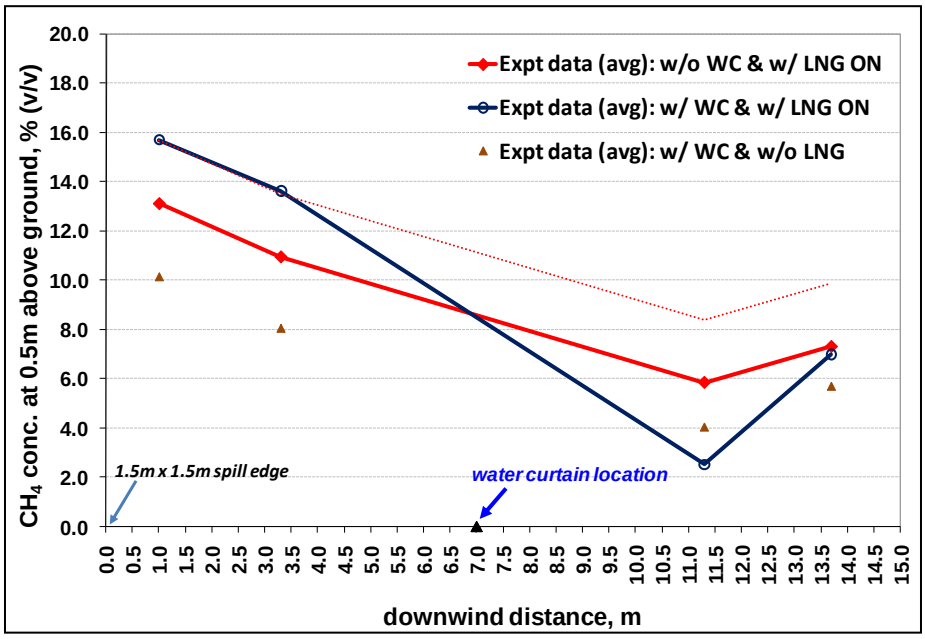

Fig. 84. Downwind concentration near ground level (at 0.5m elevation): flat fan curtain test 2007.

Near ground level concentration lines (at z=0.5 m) before the water curtain application (natural dispersion) show similar trends for downwind concentration profile for both the tests (red solid lines with solid red diamond markers). The trend changed after the water curtain application in both cases due to the forced dispersion process and the concentrations were different just after the water curtain region (blue solid lines with blue circular markers). Red dotted lines in the figures are the same lines as natural dispersion lines and represent the concentration line that would be expected if the water curtains were not active when they were activated. The brown triangular markers represent the data when there was no LNG release on the ground and water curtain action was continued.

According to the assumptions, forced dispersions should only be observed when the vapor passes through the water curtain width. As it is already mentioned earlier in that LNG vapor concentration eventually decreases as it travels downwind distances, the water curtains are expected to enhance this reduction of concentration by forced dispersion. In the following discussions, the location right after the water curtain (at 11.3 m) is the location of our interest to understand the water curtain effects. From the expected and actual data at the position just after the water curtain, additional decrease of LNG concentration by the water curtain is identified. For the full cone curtain the additional decrease in concentration is 30.5% where as for the flat fan curtain it is 70%. Use of the full cone water curtain (Fig. 83) for both discontinuous and continuous LNG flow situation shows similar results. However, the use of the flat fan curtain for the discontinuous flow situation failed (Fig. 84) to show any significant decrease in

concentration compared to the natural dispersion process. Again, from the careful observation of the above figures it can be stated that by placing the curtains closer to the spill location as well as increasing the spray width could give much higher reduction in ground level concentrations. This statement considers that the water curtain effect is more when the vapor concentration is higher or when the vapor is more concentrated.

Though LNG vapor concentration should eventually decrease as the cloud travels further downwind, concentrations (due to natural dispersion) at 13.7 m are higher than the previous location (11.3 m). Similar trends were identified in both the tests. It may be because the cloud was not quite light to disperse upward and/or vapor from the surface level ($0 \text{ m} < z < 0.5 \text{ m}$) moved to that elevation to increase the concentration. The data after the water curtain activation followed the similar trend and so at this point vapor came down as it was not lighter enough (the buoyancy was not changed from negative to positive effectively) or the vapor came up from the surface level. The causes of the effect of the curtains in decreasing CH_4 concentration can be studied more from the following concentration analysis at higher elevations. Fig. 85 and Fig. 86 show downwind concentration at 1.2 m elevations.

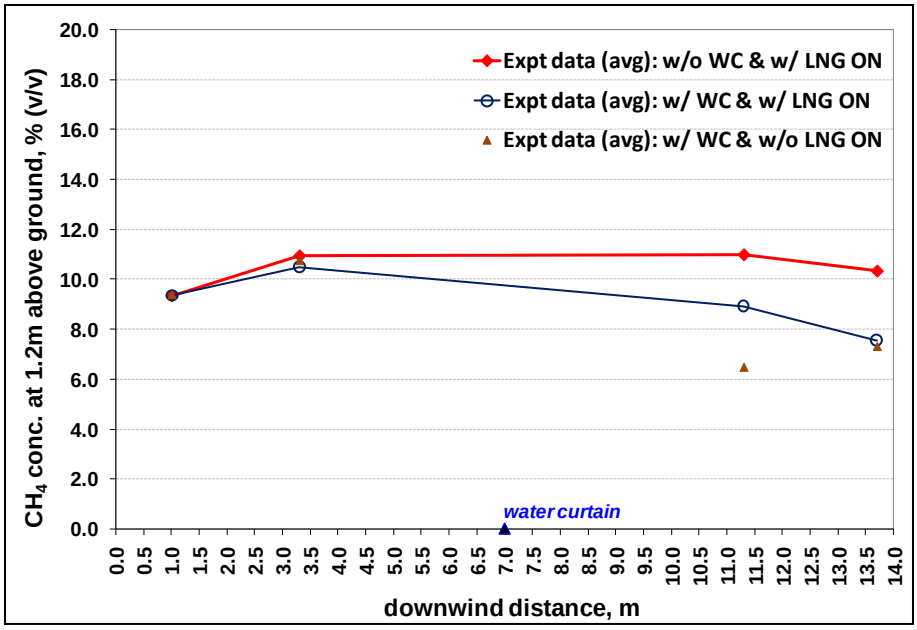

Fig. 85. Downwind concentration at 1.2m elevation: full cone curtain test 2007.

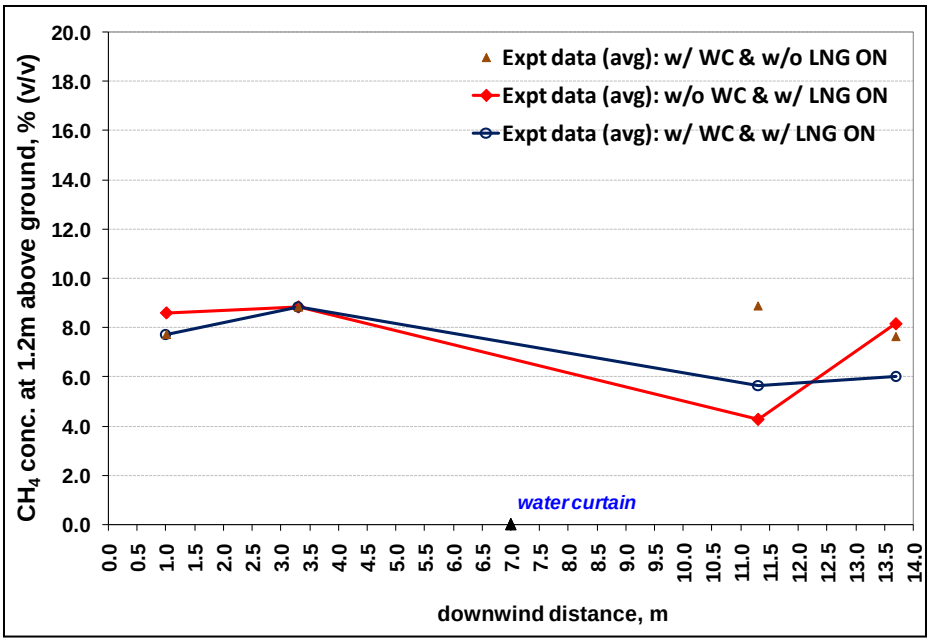

Fig. 86. Downwind concentration at 1.2m elevation: flat fan curtain test 2007.

The downwind concentration trends at 1.2 m are different for the two tests. In Fig. 85 and Fig. 86, the red lines represent concentration trend when the curtain was not applied and the blue lines represent the case of curtain application during LNG flow. The brown triangles represent the data of water curtain application when LNG flow was discontinuous. The full cone test data shows that the water curtain reduced the CH_4 concentration at 11.3 m distance for both LNG continuous and discontinuous situations. However Fig. 86 shows that the CH_4 concentration at 11.3m location actually is higher after water curtain activation. These observation imply that the full cone curtain actually diluted the vapor where as the fan curtain pushed the vapor upward more than diluting it. Higher elevation (2.1m) data presented in Fig. 87 and Fig. 88 are further studied to understand the dispersion process.

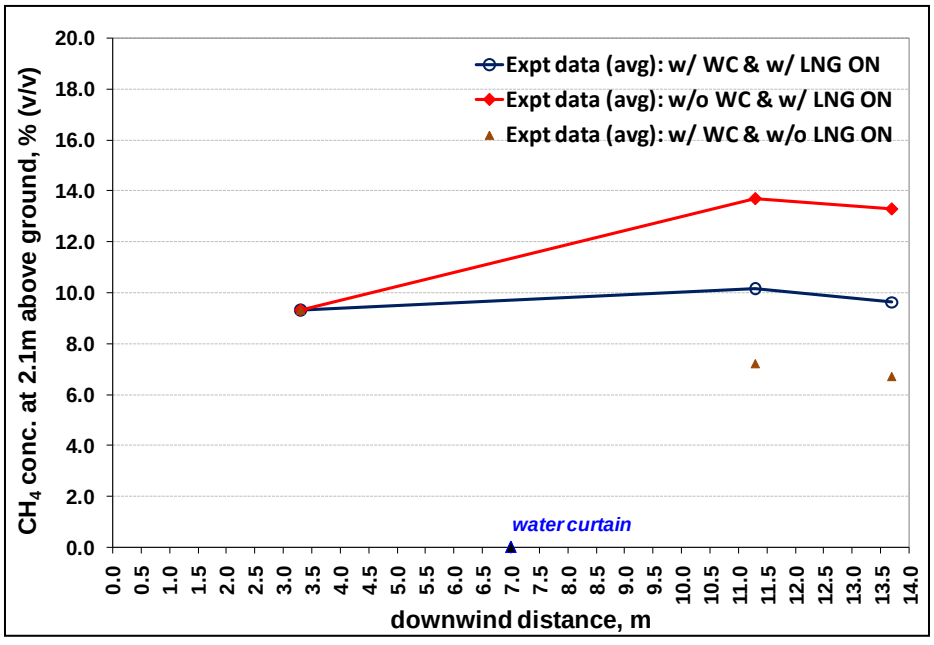

Fig. 87. Downwind concentration at 2.1m elevation: full cone curtain test 2007.

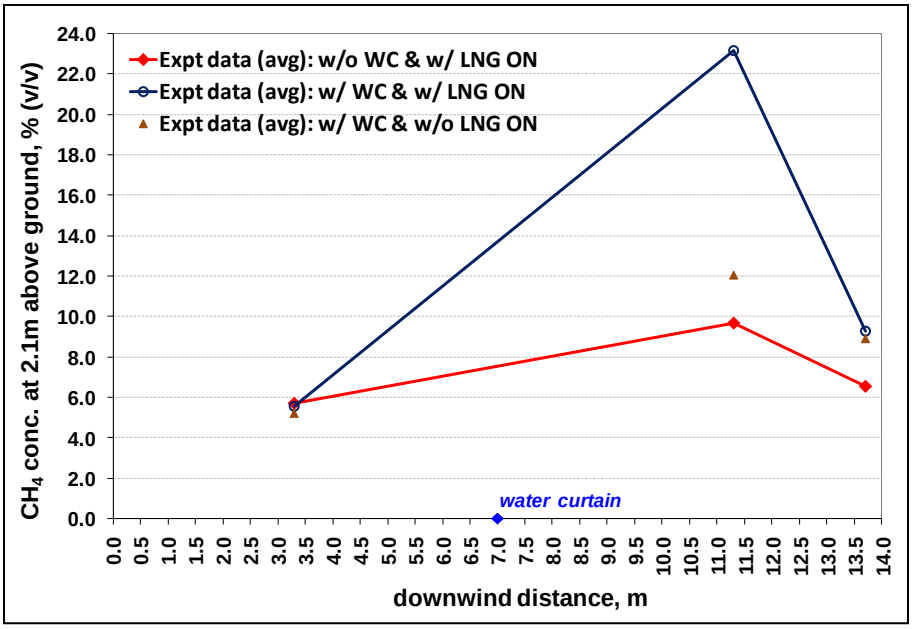

Fig. 88. Downwind concentration at 2.1m elevation: flat fan curtain test 2007.

Both the figures (Fig 87 and Fig 88) show that concentration of CH_4 increases at higher elevation as it travels forward naturally and that is obvious. By the flat fan curtain action the concentration increased to much more higher value when both the water and LNG flow was continued than natural dispersion situation (Fig. 88). CH_4 concentration increase during the discontinued LNG flow is lower even though it is higher than natural dispersion situation. However by the full cone curtain action (Fig. 87) the concentration is actually reduced for both LNG on and off situations.

To understand the overall effect of water curtains on the vapor cloud the following concentration contours (Fig. 89 and Fig. 90) were developed from the average experimental data. These contours show average vapor cloud concentrations, used in the above analysis, at different elevations and downwind distances.

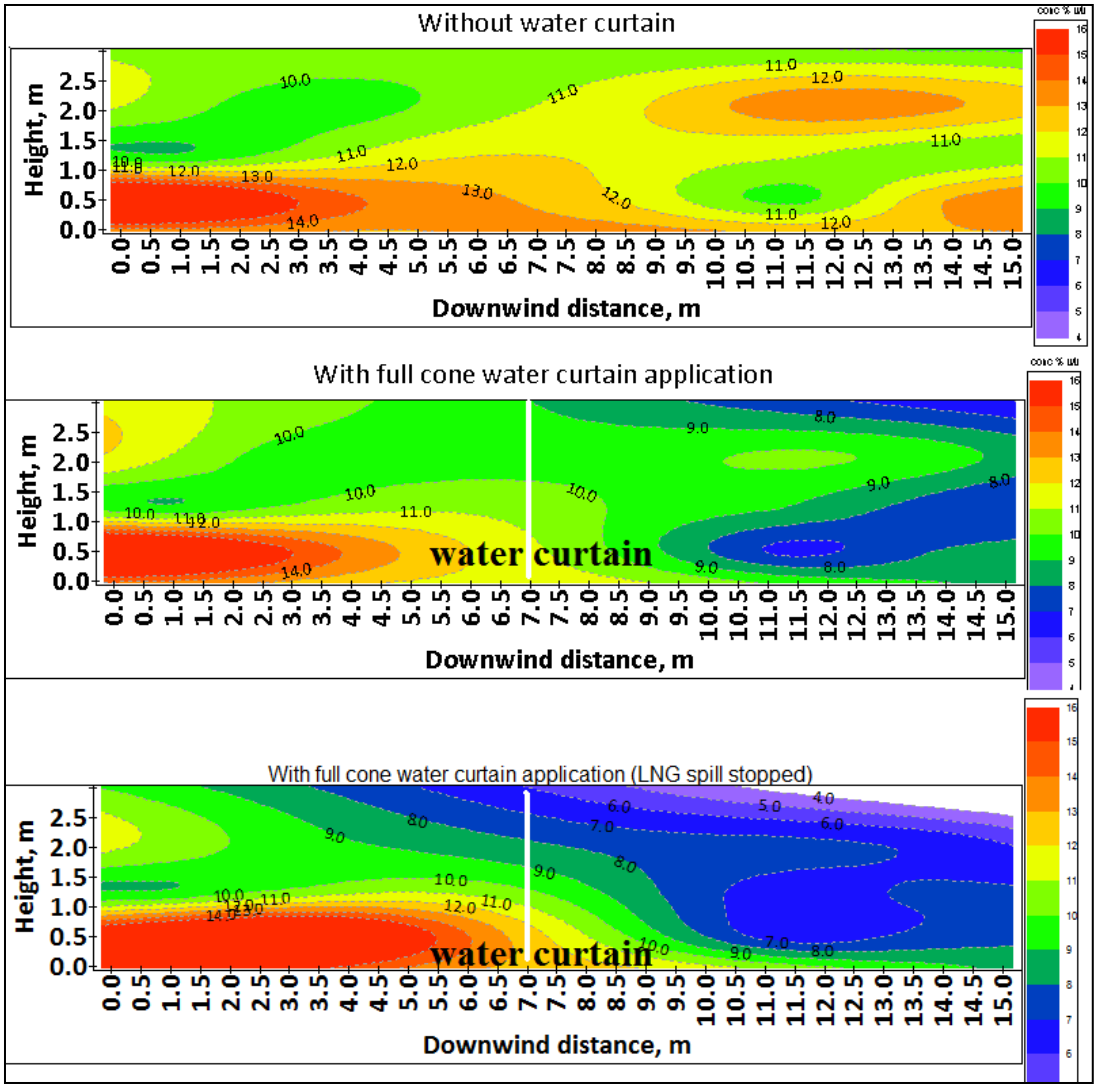

(Concentration range in the contour: 4 - 16 % v/v methane in air)

Fig. 89. Concentration contour without and with full cone water curtain action in 2007 experiment.

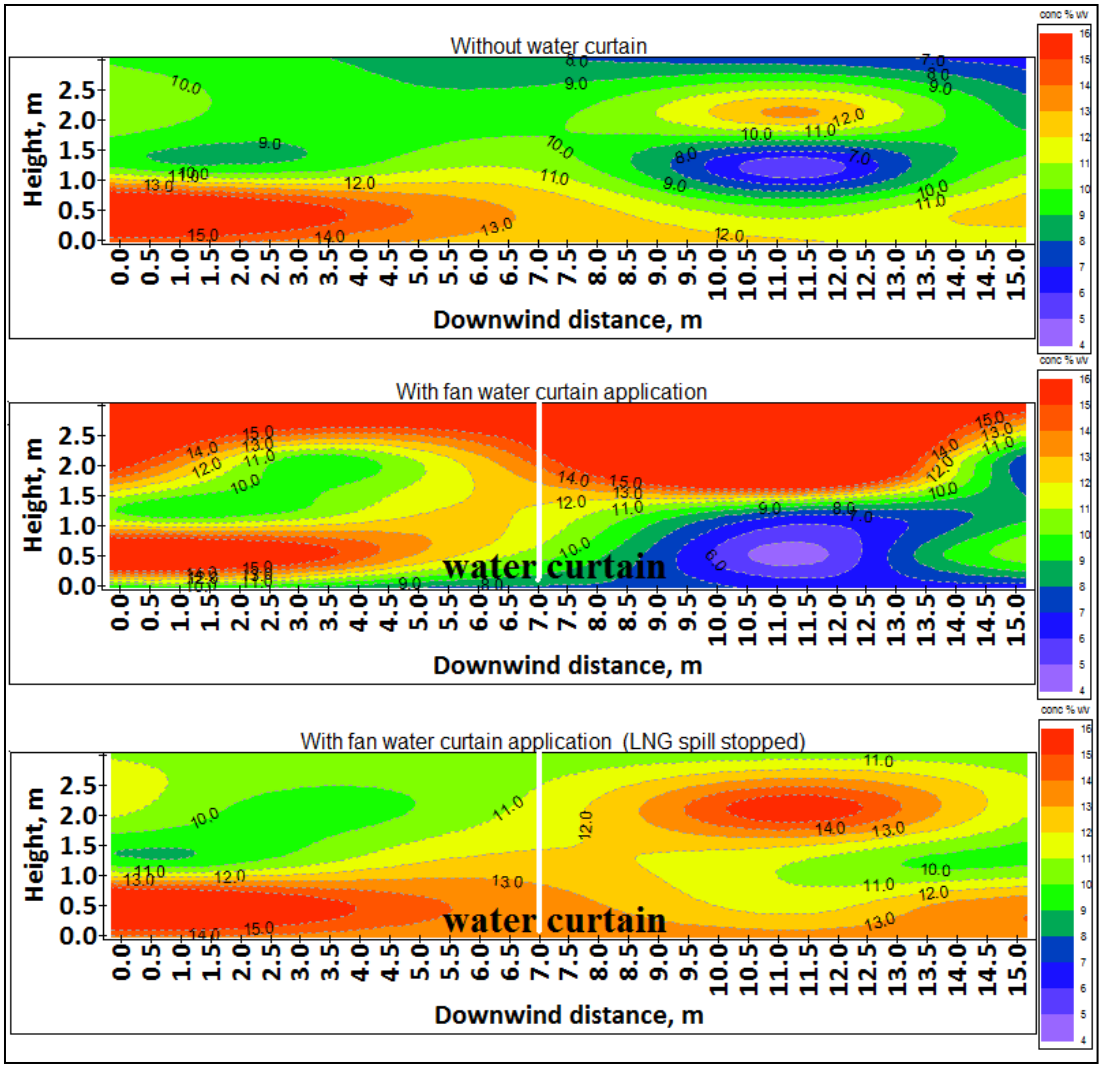

(Concentration range in the contour: 4 - 16 % v/v methane in air)

Fig. 90. Concentration contour without and with flat fan water curtain action in 2007 experiment.

The contours were developed with 3D Field Pro® software using minimum curvature method. It is already mentioned that these contours are developed from the experimental data of average concentration. Above figures show the LNG vapor dispersion process by the two types of water curtains from 2007 experiments. These

phenomena indicate that full cone actually reduced CH_4 methane concentration by mixing it with air and the flat fan imparted so much momentum to the cloud that the ground level concentration becomes very low and higher level concentration increased to a very high value. So it can be concluded that both of the curtains reduced the ground level concentration when LNG release was continued. During the time when LNG spill was discontinued the full cone curtain showed better efficiency than the fan curtain. Again the figures also indicate that none of the curtains were able to reduce the concentration below LFL within the measured distance in 2007 experiment.

In 2009 dispersed LNG vapor concentration data were collected without and with water curtains both before and after the water curtain regions. To understand the effects of the water curtains similar concentration trend analysis is conducted with the test data. Fig. 91 to Fig. 94 show the trend of downwind concentration (% v/v CH_4) of LNG vapor cloud at three different heights without and with water curtain action. Each of the individual figures is for individual tests conducted in 2009.

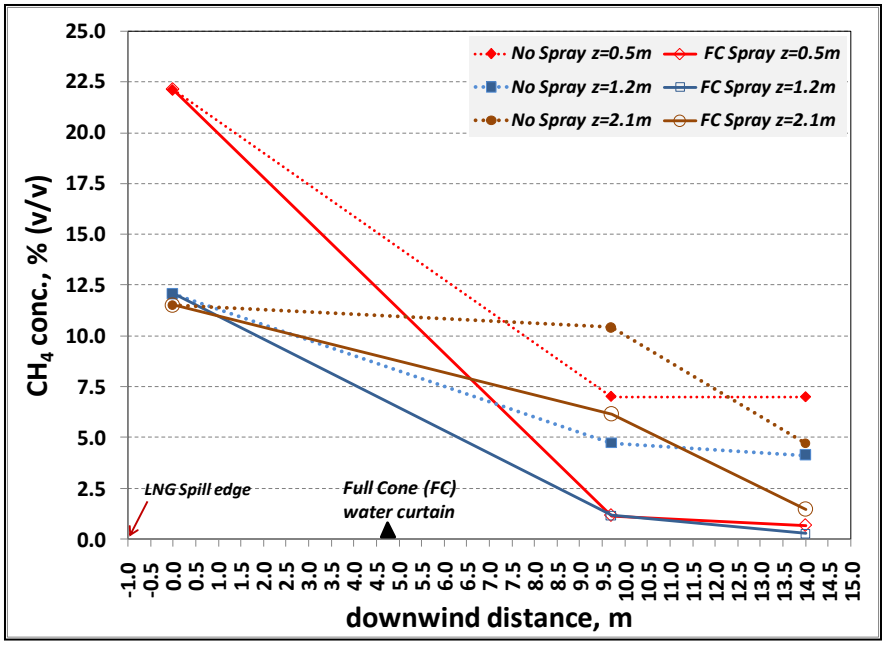

Fig. 91. Downwind concentration at three different heights without and with full cone water curtain in 2009 experiment.

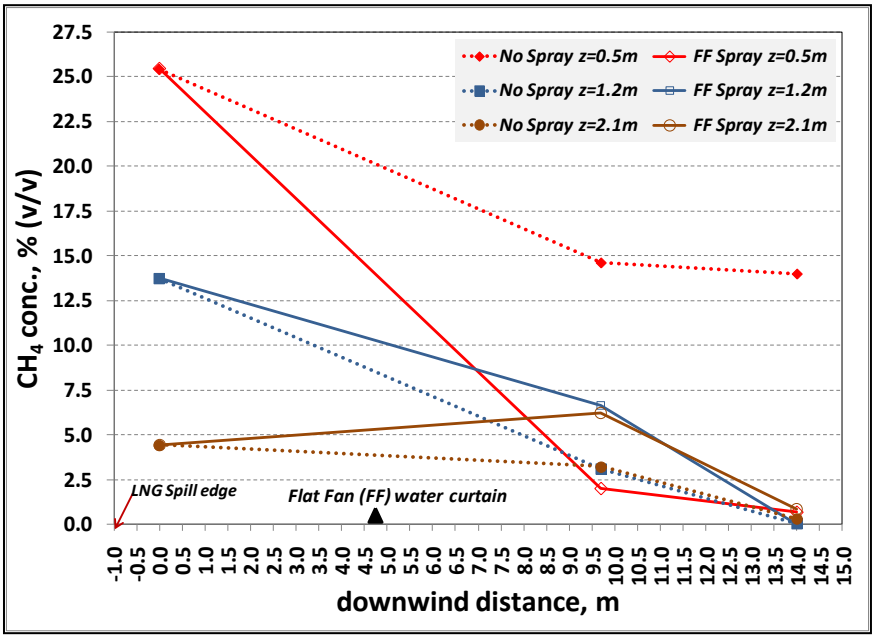

Fig. 92. Downwind concentration at three different heights without and with flat fan water curtain in 2009 experiment.

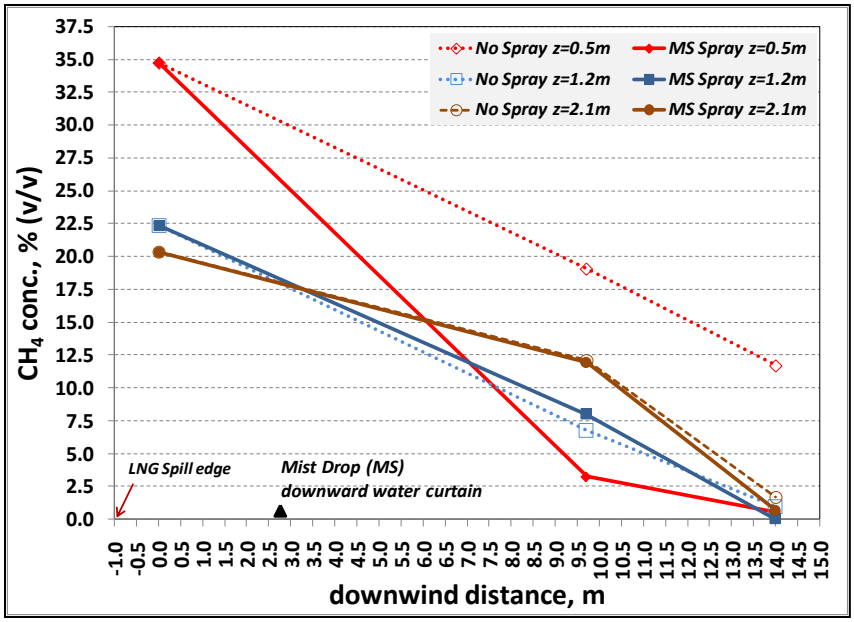

Fig. 93. Downwind concentration at three different heights without and with mist drop downward water curtain in 2009 experiment.

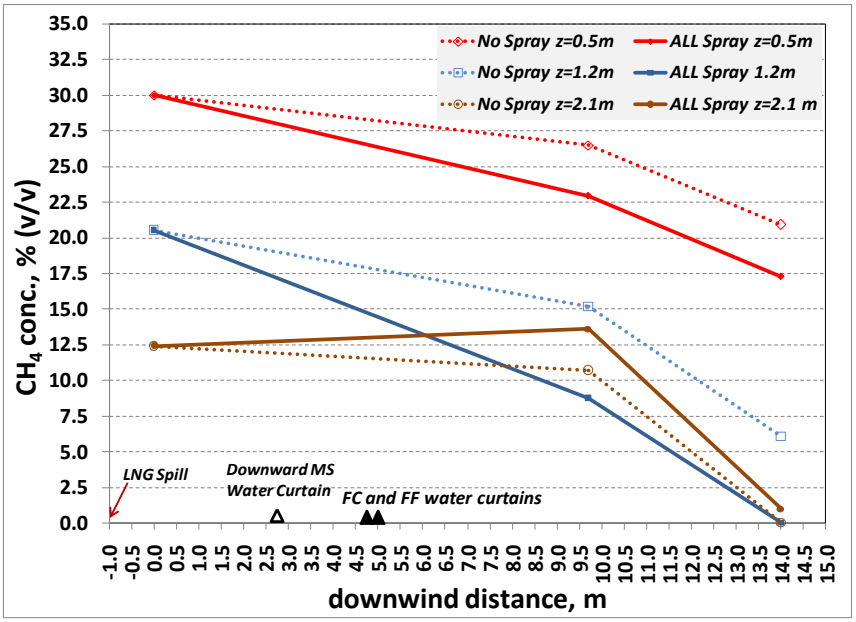

Fig. 94. Downwind concentration at three different heights without any spray and with combined water curtain system in 2009 experiments.

Dotted lines in the figures represent concentration trend without water spray and solid lines are for concentration trend with water spray action. Red, blue and brown is for concentration at 0.5 m, 1.2 m and 2.1 m respectively. Ground level concentration (at z=0.5 m) trend for each figure are similar, i.e., the water curtains were able to reduce the concentration at this height. The percent reduction in ground level concentration by the full cone, the fan, the mist (downward) and the mixed (combined) were 83, 86, 83 and 13% respectively. However the upper level concentration trends are different for different tests. Again it is noted that this time the concentration of CH_4 decreased for each height as it traveled forward further downwind distances which means the cloud was dispersing and moving upward (positive buoyancy) more efficiently than 2007 experiment.

Results show that water curtain reduced LNG vapor concentration as well as LFL distance in all the tests. From Fig. 91 it is clear that the gas concentration was reduced after the spray region in all three heights by the full cone water curtain. However Fig. 92 clearly shows that though the flat fan spray significantly reduced the ground level (0.5m) concentration, concentrations at higher levels (1.2m and 2.1m heights) were actually increased after the spray region (9.7 m). The result repeated the mechanisms identified in the 2007 experiments where the flat fan actually pushed the LNG vapor cloud upward to reduce the ground level concentration.

The downward conical curtain, mist curtain, reduced the ground concentration and increased the concentration at 2.1 m (Fig. 93). As this curtain could not provide upward momentum, this increase is due to the vapor's upward dispersion. So it is

obvious that this curtain warmed up the cloud to make it positively buoyant. In Fig. 94 the effect of all the curtains acting together is pictured. The mixed or combined curtains test show that the concentrations at 0.5 and 1.2 m were reduced; concentration at 2.1 m was increased. This can be caused by uplifting mechanism of the fan type curtain. Concentration contours are developed to understand the dispersion mechanisms of the water curtains with the similar procedure discussed earlier. Fig. 95 to Fig. 98 show the contours developed from 2009 experimental data.

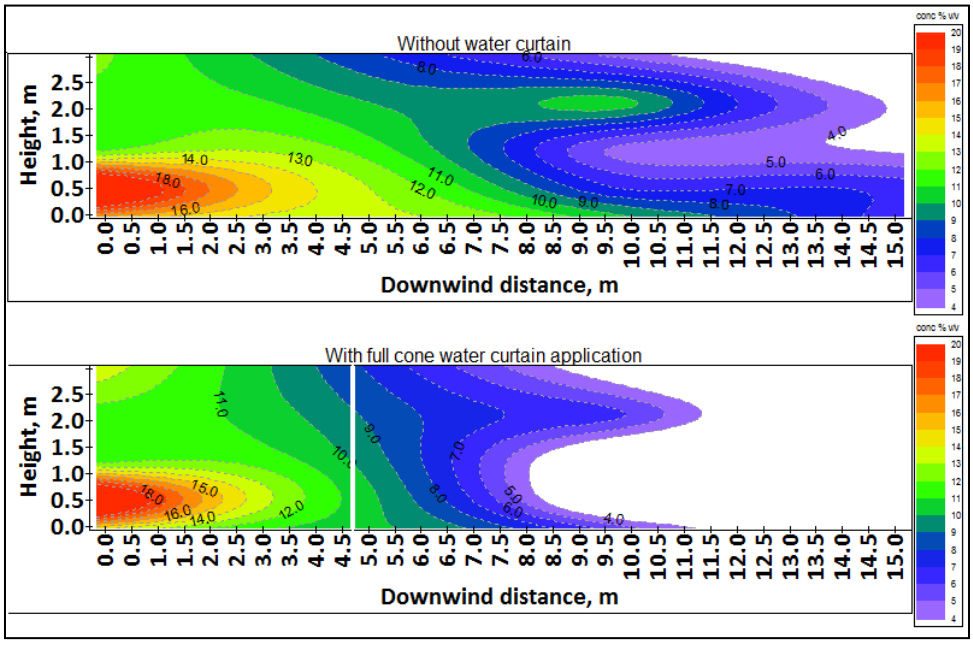

(Concentration range in the contour: 4 - 20 % v/v methane in air)

Fig. 95. Concentration contour without and with full cone water curtain action in 2009 experiment.

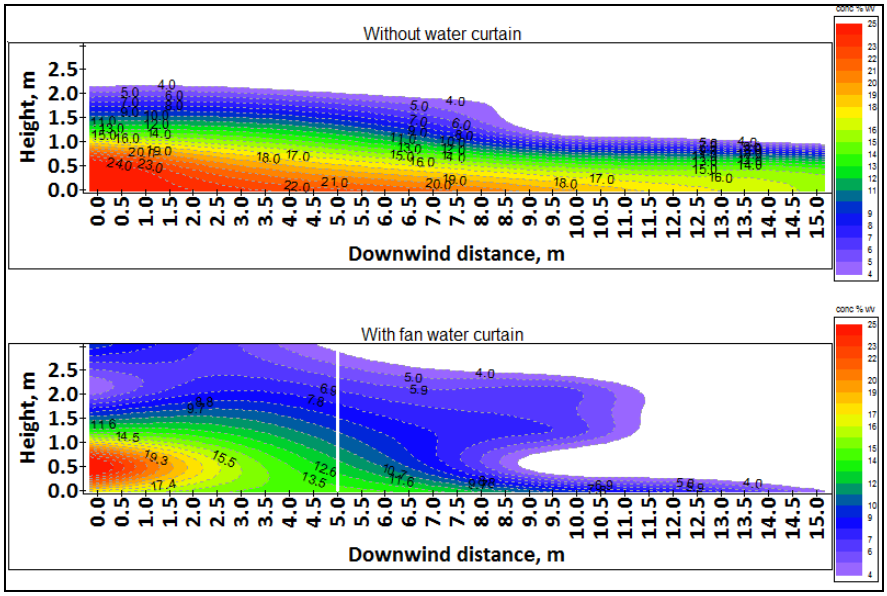

(Concentration range in the contour: 4 - 25 % v/v methane in air)

Fig. 96. Concentration contour without and with fan type water curtain action in 2009 experiment.

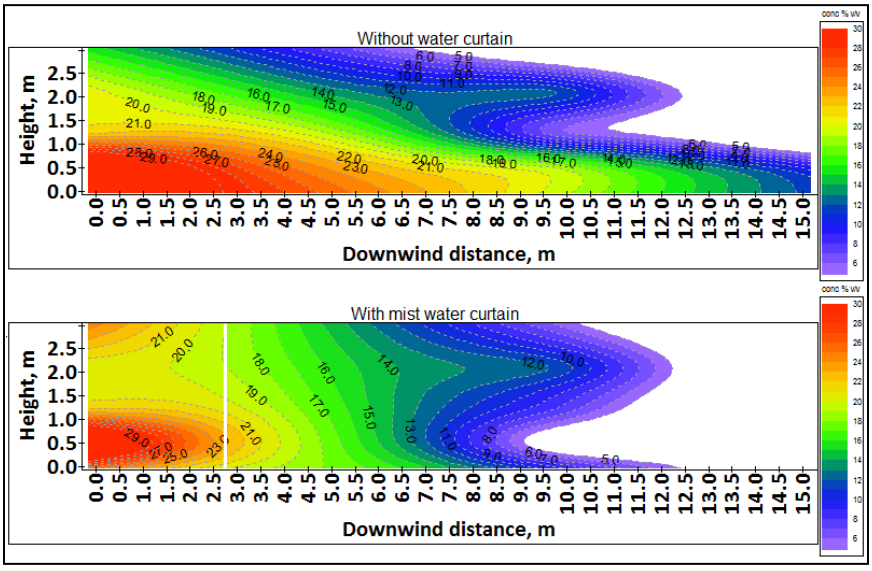

(Concentration range in the contour: 5 - 30 % v/v methane in air)

Fig. 97. Concentration contour without and with mist type water curtain action in 2009 experiment.

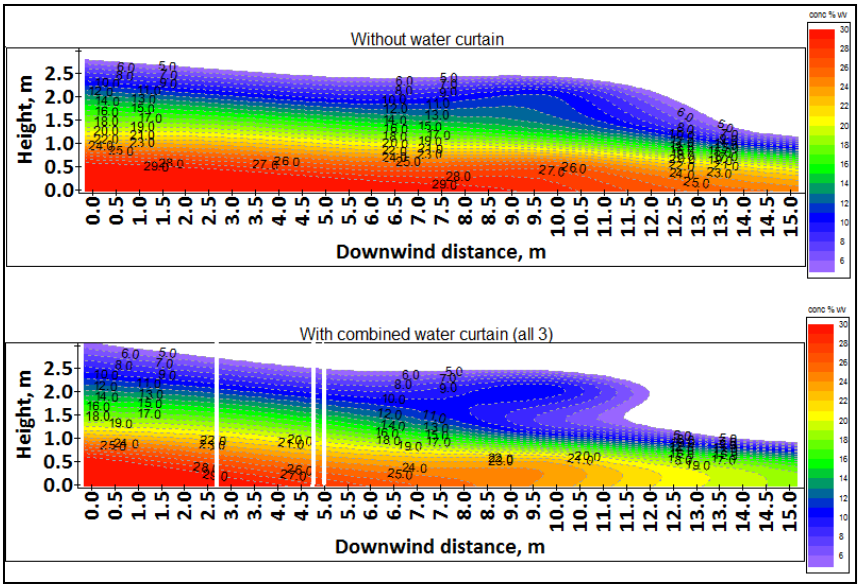

(Concentration range in the contour: 5 - 30 % v/v methane in air)

Fig. 98. Concentration contour without and with combined water curtain action in 2009 experiment.

The contours show that all of the water curtains reduced the downwind concentration of the LNG vapor cloud. However the performances of the water curtains are different in controlling the vapor cloud based on their drop size, width and flow pattern. The water curtain with higher width and medium droplet size, represented by the full cone curtain, implies very less momentum to the cloud to lift it upward and is more effective to reduce the LNG vapor concentration with the aid of dilution. On the other hand, water curtain with smaller width and larger droplet size, represented by the flat fan spray, provides effective momentum to reduce concentration. The water spray curtain with smaller droplets and downward flow reduced the concentration and shows good performance in warming up the cloud. Each water curtain effectively reduced the LFL

distance. The combined system though used more water and compared with all the action mechanisms it was not as effective as the individual ones. Overall the upward full cone water curtain, which has medium droplet size and wider coverage (60° conical) showed better performance.

5.8 Summary

Studies were performed to comprehend the effectiveness of different types of water curtain as LNG vapor control methods. Four experiments, in consecutive four years from 2006, were conducted to examine representative type upward conical, upward fan and downward mist (conical) spray curtains in dispersing LNG vapor cloud from a continuous release from pipe to the ground or water. The water curtains represent three main classes of water curtains used in the industries. The ranges of water droplets generated by the nozzles are different at same gage pressure.

Experimental data are analyzed to study the physical phenomena of air entrainment and dilution, heat transfer and mechanical effects of these water curtains. Study was performed to determine the effectiveness of these water curtains in reducing LNG vapor cloud concentration downwind. Results identify that the actions of all three water sprays can reduce the LNG concentration to some degree by dilution with air as well as by pushing the vapor upward. Water curtains also provide some amount of heat to the mixed gas cloud and air. If ineffective heat transfer between water, LNG and air fails to warm and dilute the LNG vapor significantly, the LNG vapor will rise up only for some instance due to curtain action (momentum) and then it will definitely fall back

at further distance. Difference in results from different experiments indicates that the effectiveness of the water curtain also depends on the weather condition and vaporization rate.

The overall performance of a water curtain depends on the magnitude of physical effects introduced by the curtain to the LNG cloud. But the magnitude of each mechanism introduced by different sprays is different based on the spray angle and direction, and water droplet size and velocity. Full cone reduced CH_4 concentration by mixing it with air and the flat fan imparted so much momentum to the cloud that the ground level concentration becomes very low and higher level concentration increased to a very high value. The downward mist sprays reduced concentration by warming up the cloud near ground level. So it can be concluded that all three curtains reduced the ground level concentration. However the upward full cone curtain (a) mixes vapor efficiently, (b) changes the cloud temperature; (c) provides inefficient momentum to the cloud to lift it upward; the flat fan curtain (a) imparts very high momentum; (b) provides very inefficient mixing with air as well as heating; and the downward mist spray (a) provides higher heat to the cloud compared to the other two sprays, (b) delivers some air into the spray to dilute the cloud; (c) does impart some upward momentum to uplift the cloud. Overall the upward conical sprays show best overall performance amongst the three sprays in terms of action mechanisms. Therefore in conclusion the air entrainment and dilution with some heat transfer is the dominant mechanism to control LNG vapor cloud.

6 CONCLUSIONS AND RECOMMENDATIONS FOR FUTURE WORK

6.1 Conclusions

The ability of water curtain to show different physical effects initiated an interest in the utilization of water curtain as a potential LNG vapor cloud mitigation measure. It is generally accepted that water curtains can be deployed to control vapor cloud movement from LNG spillages, which can reduce the flammable LNG vapor concentration effectively, by forced dispersion. At present the Mary Kay O'Connor Process Safety Center (MKOPSC) is conducting experimental and theoretical research on number of issues involved in LNG safety. The purpose of the research is to combine the theoretical understanding of the phenomenon with the field tests to make the results directly applicable to the current LNG industry needs. The research on the application of water curtain to control LNG vapor cloud, a part of the LNG safety research, has been presented in this dissertation.

A thorough literature review has revealed that water spray curtains are able to control an LNG vapor cloud and can reduce the methane concentration to some degree. Four physical mechanisms are involved when a water spray is activated on a vapor cloud. Among the four mechanisms, (1) air entrainment and dilution, (2) heat transfer, and (3) overall momentum actions are considered to be useful when applied to handle an LNG vapor cloud. However insufficient experimental work, conducted in late 70's and early 80's, could not establish the actual and most dominant phenomena involved during the LNG-water spray interaction. Because of low molecular weight (of methane) and

extremely low temperature, LNG vapor cloud dispersion behaves differently from other dense gases. Effectiveness of a water curtain, in terms of the degree of LNG vapor concentration reduction and temperature increase, of different types of water sprays of different flow configurations, drop sizes, covered heights and covered widths yet remained undetermined.

Four field experiments have been conducted in the last four consecutive years (since 2006) to (1) understand the underlying physical phenomena, and (2) determine the effect of several parameters controlling the physical processes during LNG vapor-water spray interaction. These experiments were developed from the knowledge of previous research, simulation works and experience to test representative types of water curtains with LNG spills under simulated conditions. Overall three types of water sprays are used in the research to represent three main classes of water curtains used in the industries. The sprays used are upward conical, upward fan and downward conical. The ranges of water droplets generated by the nozzles are different at the same gage pressure. Droplet sizes of the upward conical spray are small to medium where droplets produced by the upward fan spray are coarse. The downward cone spray produces mist like smaller droplets. The coverage by the two upward sprays is also different. The conical spray provides more downwind coverage (conical pattern) than the fan spray.

Experimental observation and detailed experimental data analysis, supported by some theoretical study prove that water curtains are able to control a drifting LNG vapor cloud and change the concentration along the cloud height. But the effectiveness of different water curtains is different, as the magnitude of the mechanisms involved are

different. The intent of this research is not to identify the type of water spray effective for LNG vapor, the intent is to determine the dominant mechanisms to control and disperse the cloud.

The upward full cone spray with wider spray angle and medium droplet size and droplet velocity creates high turbulence closer to the spray region. As it induces more air inside the spray, the mixing between the gas cloud and air is enhanced, though the air velocity into the spray is low to medium. The applied momentum to the cloud is not significant because of drop size and water pressure. On the other hand the upward fan spray cannot produce wide spray coverage as it is flat shaped. But it can create a solid barrier in the path of the cloud covering larger crosswind length and height, because of its coarse droplet size and water pressure. So the amount of air induced inside the spray is low though the air velocity is high. And the momentum it can apply from the bottom of a cloud is very high. In case of downward conical spray with smaller drop size, the heat transfer effects are better than the other two and the amount of air induced inside the spray is less than the upward conical spray with larger drop. It can warm up the LNG cloud more effectively than the other two because of drop size. However it is not realistic to warm up the cloud to a higher extent in outside spill conditions with the commercially available sprays. Overall it is concluded from the test that the upward full conical spray controlled and disperse more effectively. Therefore higher air entrainment and significant mixing with some heat transfer will more effectively handle an LNG vapor cloud, depending on the weather conditions and wind speed.

It should be noted that other factors also influence the water curtain actions. The performance of any water curtain also depends on the weather condition and vaporization from the substrate. It was determined from the experiments that the same water spray acts more effectively in a favorable weather (high wind and solar flux) than an unfavorable weather (low wind and solar flux) conditions. On the other hand the size of the cloud which interacts with the spray depends on the vaporization rate. A water curtain of a certain size only could handle a vapor cloud of a certain size. These experiments only deal with smaller spill size. The rate of evaporation mainly depends on the heat from the spill surface. Evaporation rate is higher when the release is on unconfined land or water than on confined land or water. A water curtain will show better performance if it interacts with a cloud which has high turbulence inside the cloud perimeter, i.e., when it is installed closer to the spill location. Shorter distance between the curtains and spill location also provides better coverage and high LNG-water spray interaction and thus the methane concentration can be significantly reduce to lower values.

6.2 Future Work

This section explains the limitations on the measurement, validation, and statistical problems that are encountered. While some of the gaps are identified, some of the findings in this research provide stepping stones for future research in order to close the gaps. There are several limitations in these experiments, as follows:

- Due to the gas detectors setup with long tubes a time lag of around 3 to 4 minutes was observed. The time to measure the gas concentration should be increased. Another problem was to keep a constant flow inside the tube. To overcome this limitation more detectors need to be placed physically in the test area.
- It was observed that cloud concentration reached lower value far downwind due to natural dilution. More gas detectors with lower level concentration measurement (100% LFL) should be used at further distances from the spill location.
- The gas detectors used in the experiments were not able to measure gas inside the spray. So alternate detectors are required to collect gas cloud information inside the spray.
- The water curtains could not be placed very close to the spill pit because of the downward slopes close to the pits. This design allows flowing water inside the LNG pool if the curtains are within 2 m of the pit. So alternate test setup should be considered to test the effect of water curtain location.
- Water pressure around the test site is limited which limits the use of number of nozzles during the tests. Also the size of the pipeline around the LNG training facility is not adequate to use multiple nozzles at higher pressure. This limitation affected the tests in creating a water curtain with a higher coverage.
- Some of the key parameters, like (i) the droplet size produced from a nozzle, and (ii) the droplet distribution in the spray area are very important to understand in detail the role of a spray nozzle. The actual drop size was not measured in the tests because of unavailability of appropriate measuring device which could be used safely outdoor

conditions in the presence of a flammable vapor cloud. Similarly the information on the distribution of water density in the space and change in droplet size along the height for the used curtains cannot be determined in this research due to the unavailability of exact information, lack of appropriate measurement devices and many limitations when dealing with LNG vapor out door. So future research should include these measurements.

- Each test had to stop within a short time because the large amount of water used would cause problems to some of the instruments located near the test area because of insufficient water drainage. All of the tests used LNG release with low flow rate to simulate a small spill. This also indicates that to control a large spill the required system has to provide sufficient water. In addition, draining the large amounts of water can present problems. In future this limitation should be considered.
- Humidity might have significant effects on both natural and forced dispersion of LNG vapor cloud. Though this research considered measuring the humidity in the dispersing cloud, due to some limitations (i.e. placement of the equipment away from water spray) measurements were not possible. So future research can determine the effect from experimental evidence.

One of the gaps in water curtain application research is that it is hard to predict the LNG vapor-water spray interaction as it is a complex phenomenon. An appropriate model for the case of an LNG release should describe the interaction of water droplets, LNG vapor, and air almost exactly in a certain atmospheric condition and should also be validated with field tests. This research produced many data that could be analyzed in

many different ways as well. Calculation or modeling of heat transfer and upward momentum has not been done rigorously in this research. Thus, future works must include more thorough measurement of water temperature, gas concentration and LNG vapor size by improving the experiment. Then, dilution and heat transfer in the spray can be modeled so it can be used for industrial scale-up where the possible release is larger than release used in this experiment. These calculations are also useful in determining the minimum required water droplet, width, location and height to reach effective suppression.

Currently, the knowledge and interest in computational fluid dynamics (CFD) is increasing specially in the LNG safety area. Some researchers also started working on CFD models to understand spray hydrodynamics. So water curtain models can also be developed through CFD modeling for LNG issues. The characteristics of the LNG vapor before and after water spray identified here can be used with proper scale-up. CFD models of sprays generally fall into two categories: Eulerian models and Lagrangian (or particle tracking) models. The first one usually models the spray as a continuum across the whole flow domain, while the latter model tracks the paths of droplets through domain. These models are useful, rapid and relatively inexpensive in providing almost accurate results. Most of these CFDs mainly focus on mitigating Cl_2, CO_2, NH_3 or HF release through dilution and absorption. However, for the case of LNG vapor release dispersion the absorption of gas into water should not be a contributing factor at all. Therefore, to disperse an LNG vapor cloud effectively, and to develop design guidelines for water curtain installation, these or other available CFD models can be studied

thoroughly and their assumptions can be modified accordingly. The applicability range of the CFD modeling also needs to be extended so that it can be used for any scale and comprehensive and authentic design guidelines of water curtain can be developed.

The research shows three types of representative water sprays of three different flow patterns of different droplet sizes control the LNG vapor cloud in terms of different physical processes. However to identify the effect of droplet sizes in forced dispersion of LNG, more tests need to be conducted with the same type of spray at different pressure or flow rate, i.e., with different droplet sizes. Future work of this research should address this effect as well as the effects of spray angle, spray momentum and location of the water curtain in controlling LNG cloud. However, to establish a definitive engineering guideline on water curtain design for LNG cloud dispersion controlled experiments for longer times and with different wind conditions are needed.

In the summary, this research is expected to help LNG industry by advancing the current understanding regarding suppression of LNG vapor dispersion and pool fire.

REFERENCES

Alessandri, E., Buchlin, J.M., Cavallini, A., Patel, M.K., & Galea, E. (1996). On the modelling of the thermal interactions between a spray curtain and an impinging cold gas cloud. In Centre for Numerical Modelling and Process Analysis, School of Computing and Mathematical Sciences, London, UK.

Angus. (2005). *Product specification sheet.* Oxfordshire, UK: Angus Fire Armour Limited.

Arthur D. Little. (1974). Evaluation of LNG vapor control methods. Report No 76285, submitted to the American Gas Association, Boston, MA: Arthur D. Little, Inc.

Atallah, S., Guzman, E., & Shah, J.N. (1988). Water spray barriers for LNG vapor mitigation. Report No 4015.1, Des Plaines, IL: Risk and Industrial Safety Consultants, Inc.

Bennat, F. G. S., & Eisenklam, P. (1969). Gaseous entrainment into axisymetric liquid sprays. *Journal of the Institute of Fuel*, *42*, 309.

BETE Fog Nozzle. (2007). *Product specification catalog: manual 110METRIC*. Greenfield, MA: BETE Fog Nozzle, Inc.

Binark, H., & Ranz, W.E. (1958). Induced air flows in fuel sprays. In Annual Meeting of American Society of Mechanical Engineers, Paper no 58-A-284, New York.

Bosanquet, C.H. (1957). The rise of a hot waste gas plume. *Journal of the Institute of Fuel*, *30*, 322-328.

Briffa, F., & Dombrowski, N. (1966). Entrainment of air into a liquid spray. *AIChE Journal*, *12* (4), 708-717.

Briscoe, F., & Shaw, P. (1980). Spread and evaporation of liquid. *Progress in Energy and Combustion Science, 6* (2), 127–140.

Brown, L.E., Martinsen, W.E., and Cornwell, J.B. (1983). Spill protection for liquefied gas facilities. In Spring Meeting of the American Petroleum Institute Committee on Safety and Fire Protection. Ft. Lauderdale, Florida.

Buchlin, J.M. (1994). Mitigation of problem clouds. *Journal of Loss Prevention in the Process Industries*, *7*, 167-174.

Buchlin, J.M., & Alessandri,E. (1997). Numerical simulation of the thermo hydraulic behavior of liquid sprays. In 13th Annual Conference on Liquid Atomization and Spray Systems, Florence, Italy.

Center for Chemical Process Safety (CCPS). (1997). *Guidelines for post release mitigation technology in the chemical process industry*. 58-90, New York: AIChE.

Center for Liquefied Natural Gas (CLNG). (2008). LNG Today, http://www.lngfacts.org / LNG-Today/Need-More.asp., Accessed December 2008.

Conch Methane Services (CMS). (1962). Characteristics of liquefied natural gas and their evaluation in relation to safe handling and above-ground storage practices. Technical Report - vol 1. London, England: Conch Methane Services, Ltd.

Cormier, B.R. (2007). Effect of tank pressure and insulation on LNG liquid flow rate - experience at Brayton Fire School. In Mary Kay O'Connor Process Safety Center Centerline Newsletters, 11 (2), 12-21.

Cormier, B. R. (2008). *Computational fluid dynamics for LLNG vapor dispersion modeling: a key parameters study*. PhD dissertation, Department of Chemical Engineering, Texas A&M University, College Station.

Cormier, B. R., Suardin, J. A., Rana, M.A., Zhang, Y., & Mannan, M. S. (2009). Development of design and safety specifications for LNG facilities based on experimental and theoretical research. *OPEC, Oil Prices and LNG, 12*, 295-424, Nova Science Publishers Inc. ISBN: 978-1-60692-897-4.

Dusserre, G., Dandrieux, A., & Thomas, O. (2003). The DVS model: a new concept for heavy gas dispersion by water curtain. *Environmental Modeling and Software*, *18*, 253-259.

Federal Energy Regulatory Commission (FERC). (2008). For Citizens, http://ferc.gov/for-citizens/citizen-guides/citz-guide-lng.pdf., Accessed August 2008.

Fthenakis, V. M. (1991). *Modeling of water spraying of toxic gas releases*. Ph.D. dissertation, Fluid Dynamics and Atmospheric Science Department, New York University, New York.

Fthenakis, V.M., & Zakkay, V. (1990). A theoretical study of absorption of toxic gases by spraying. *Journal of Loss Prevention in the Process Industries*, *3*, 197-206.

Gant, S. E. (2006). CFD modelling of water spray barriers. Report No. HSL/2006/7, Derbyshire, UK: Health and Safety Laboratory.

Gas Research Institute. (1982). Dispersal of LNG vapor clouds with water spray curtains. Annual Report – Phase 1, Report No GRI-80/0107, Chicago, IL: Gas Research Institute.

Gluckert, F.A. (1962). A theoretical correlation of spray-dryer performance. *AIChE Journal*, *8*, 460-466.

Hald, K., Dusserre, G., Dandrieux, A., & Buchlin, J.M. (2003). A methodology to investigate heavy gas dispersion by water-curtains. In Proceedings of European Safety and Reliability (ESREL) Conference, 741-746, Maastricht, Netherlands.

Hald, K., Dusserre, G., Dandrieux, A., & Buchlin, J.M. (2005). Heavy gas dispersion by water spray curtains: a research methodology. *Journal of Loss Prevention in the Process Industries*, *18*, 506-511.

Harris, N.C. (1981). The design of effective water sprays – what we need to know. In the Containment and Dispersion of Gases by Water Sprays, 7.1-7.5, North Western Branch Papers, Manchester, UK: Institution of Chemical Engineers.

Heskestad, G., Kung, H. C., & Todtenkopf, N. F. (1976). Air entrainment into water sprays and spray curtains. In Annual Meeting of American Society of Mechanical Engineers, Paper No 76-WA/FE-40, New York.

Heskestad, G., Kung, H. C., & Todtenkopf, N. (1981). Air entrainment into water sprays. Report No 22533, Reissue of RC77-TP-7 November 1977, Norwood, MA: Factory Mutual Research Corporation.

Heskestad, G., Meroney, R.N., & Kothari, K.M. (1983). Effectiveness of water spray curtains in dispersing LNG vapor clouds. In Proceedings of the American Gas Association Transmission Conference, Paper No 83-T-69, 169-183, Seattle, Washington.

Hissong, D.W. (2007). Keys to modeling LNG spills on water. *Journal of Hazardous Materials*, *140* (3), 465-477.

Honeywell. (2005). *Operating instructions: searchpoint optima plus IR gas detectors,* Sunrise, FL: Honeywell Analytics Distribution, Inc.

Ito, I. (1970). Studies on the spray with single hole cylindrical nozzles. *Bulletin of Japanese Society of Mechanical Engineers*, *36*, 759-772.

Ivings, M.J., Jagger, S.F., Lea, C.J., & Webber, D.M. (2007). Evaluating vapor dispersion models for safety analysis of LNG facilities. HSL Report No MSU/2007/04, Quincy, MA: Fire Protection Research Foundation.

Martinsen, W.E., & Muhenkamp, S.P. (1977). Disperse LNG vapors with water. *Hydrocarbon Processing*, *56* (7), 261-266.

Mary Kay O'Connor Process Safety Center (MKOPSC). (2008). LNG pool fire modeling. White Paper by Mary Kay O'Connor Process Safety Center, Texas A&M University, College Station.

McQuaid, J. (1977). The design of water spray barriers for chemical plants. In 2nd International Loss Prevention Symposium, Heidelberg, Germany.

McQuaid, J., & Fitzpatrick, R.D. (1981). The uses and limitations of water-spray barriers. In the Containment and Dispersion of Gases by Water Sprays, 1.1-1.13, North Western Branch Papers, Manchester, UK: Institution of Chemical Engineers.

McQuaid, J., & Fitzpatrick, R.D. (1983). Air entrainment by water sprays: strategies for application to the dispersion of gas plumes. *Journal of Occupational Accidents*, *5*, 121-133.

Moodie, K. (1985). The use of water spray barriers to disperse spill in the event of heavy gases – the performance characteristics of full-scale water spray barriers when dispersing spills of heavy gases. *Plant Operation Progress*, *4*, 234-241.

Moore, P.A.C., & Rees, W.D. (1981). Forced dispersion of gases by water and steam. In the Containment and Dispersion of Gases by Water Sprays, 4.1-4.14, North Western Branch Papers, Manchester, UK: Institution of Chemical Engineers.

Nakakuki, A. (1973). Properties of sprays injected into compressed atmospheres. In Annual Meeting of American Society of Mechanical Engineers, Paper No 73-WA/FE-18, New York.

Palazzi, E., Curro, F., Pastorino, R., & Fabiano, B. (2004). Liquid spray curtains design to contain and mitigate toxic and flammable jets and releases. In Proceedings of 11th International Loss Prevention Symposium, Loss Prevention and Safety Promotion in the Process Industries, 3127-3136, Praha, Czech Republic.

Prugh, R.W. (1985). Mitigation of vapor cloud hazards: part I. *Plant Operation Progress, 4* (2), 95-103.

Prugh, R.W. (1986). Mitigation of vapor cloud hazards: part II. *Plant Operation Progress, 5* (3), 169-174.

Prugh, R.W. (1987). Guidelines for vapor release mitigation. *Plant Operation Progress, 6* (3), 171-174.

Prugh, R.W., & Johnson, R.W. (1988). *Guidelines for vapor release mitigation*. Center for Chemical Process Safety (CCPS). AIChE, New York.

Qiao, Y., West, H.H., & Mannan, M.S. (2005). Assessment of the effects of release variables on the consequences of LNG spillage onto water using FERC models. *Journal of Hazardous Materials, 130*, 155-162.

Rabash, D.J., & Stark, G.W.V. (1962). Some aerodynamic properties of sprays. *The Chemical Engineer, 40*, 0.A.83.

Raj, P.K. (2007). LNG fires: a review of experimental results, models, and hazard prediction challenges. *Journal of Hazardous Materials, 140* (3), 444-464.

Rana, M. A., Cormier, B. R., Suardin, J. A., Zhang, Y., & Mannan, M. S. (2008). Experimental study of effective water spray curtain application in dispersing liquefied natural gas vapor clouds. *Process Safety Progress, 27* (4), 345-353.

Rana, M. A., Guo, Y., & Mannan, M. S. (2009). Use of water spray curtain to disperse LNG vapor clouds. *Journal of Loss Prevention in the Process Industries*, *22*, 707-718.

Rojey, A., Jaffret, C., & Marshall, N. (1997). *Natural gas: production, processing, transport*. 205-207, Paris, France: Editions TECHNIP.

Rothe, P. H., & Block, J.A. (1977). Aerodynamic behavior of liquid sprays. *International Journal of Multiphase Flow*, *3*, 263-270.

St-Georges, M., & Buchlin, J.M. (1995). Heat transfer in liquid curtains mitigating pollutant releases. *Loss Prevention and Safety Promotion in the Process Industries*, *2***,** 495-506.

Suardin, J. A. (2008). *The application of expansion foam on liquefied natural gas (LNG) to suppress LNG vapor and LNG pool fire thermal radiation*, PhD dissertation, Department of Chemical Engineering, Texas A&M University, College Station.

Texas Engineering Extension Service (TEEX). (2009). Brayton Fire Training Field, http: //www.teex.com., Accessed August 2009.

Uzanski, D.T., & Buchlin, J.M. (1998). Mitigation of industrial hazards by water spray curtains. In 5th Conference of the International Emergency Management Society (TIEMS). Washington, DC.

Van Doorn, M. (1981). *The control and dispersion of hazardous gas clouds with water sprays*, PhD Thesis, University of Delft, Holland.

Webber, D.M., Gant, S. E., Ivings, M.J., & Jagger, S. F. (2009). LNG source term models for hazard analysis: a review of the state-of-the-art and an approach to model assessment. HSL Report No MSU/2008/24, Quincy, MA: Fire Protection Research Foundation.

West, H.H., & Mannan, M.S. (2001). LNG safety practice & regulations: from the 1944 East Ohio tragedy to today's safety record. In Mary Kay O'Connor Process Safety Center Symposium, Houston, Texas.

Zinn, C.D. (2005). LNG codes and process safety. *Process Safety Progress*, *24* (3), 158-167.

VITA

Morshed Ali Rana was born in Dhaka, Bangladesh. He received his B.S. degree in chemical engineering from Bangladesh University of Engineering and Technology. He started his career as a young chemical engineer in Bangladesh and after several years he moved to the U.S. to pursue graduate studies. He received his M.S. in chemical engineering from the University of South Alabama in December 2004. He then entered the graduate program at Texas A&M University in August 2005 and received his PhD in chemical engineering in December 2009. His research interests include chemical process and process safety. He can be reached at 3132 Chemical Engineering Department, Mary Kay O'Connor Process Safety Center, Texas A&M University, College Station, TX 77843 and his email is morshedrana@gmail.com.